

Properties of Nano-Modified Fly Ash Concrete Cast and Cured Under Cyclic Low/Freezing Temperatures

By

ANIS ABAYOU

A Thesis submitted to the Faculty of Graduate Studies of
The University of Manitoba
in partial fulfillment of the requirements of the degree of

Master of Science

Department of Civil Engineering
Faculty of Engineering
University of Manitoba
Winnipeg

Copyright © 2019 by ANIS ABAYOU

ABSTRACT

Under lower temperatures, the hydration process of cement slows down significantly, and it completely stops when the temperature goes below 0°C. This hinders strength development and durability of concrete. The current practices for overcoming these challenges involve methods such as heating concrete ingredients and surroundings to provide favorable curing conditions for concrete. However, these practices are associated with significant costs and adverse environmental effects due to the requirements of enclosure materials, highly-skilled manpower for quality control, and considerable consumption of energy and significant amounts of greenhouse gas emissions.

Therefore, Phase I of this thesis focused on developing nano-modified concrete mixtures comprising cold weather admixture systems CWAS which were mixed, placed and cured at cyclic temperatures (-5 /5°C) targeting applications in early fall and late spring periods. This phase followed the design of experiments (DOEs) modeling approach to test 15 concrete mixtures. Three parameters were considered in the model: incorporation of fly ash (up to 25%) and nano-silica (up to 4%) as well as combination of two types of antifreeze admixtures (calcium nitrate and nitrite). The mixtures were assessed based on setting time (placement), compressive strengths (hardened properties) and absorption (infiltration of fluids). Moreover, microstructure analysis tests were conducted to characterize the microstructural features. The results showed that nano-silica, even with the inclusion of fly ash, significantly enhanced the overall performance and development of microstructure of concrete mixed, cast, and cured at cyclic freezing/low temperatures.

Phase II of this thesis targeted developing durable repair mixtures. The experimental program in this phase was composed of setting time, compressive strength, fluid absorption, bond strength, surface scaling, restrained shrinkage as well as mercury intrusion porosimetry tests. Seven mixtures incorporation of fly ash (up to 25%) and nano-silica (up to 4%) as well as CWAS

were selected to evaluate their potential use as cold weather repair materials for concrete infrastructure targeting late fall and early spring periods. The overall results of this phase showed that nano-modified concrete mixtures achieved a balance between early- and late-age properties and high compatibility with substrate concrete, thus a promising potential for their use as repair mixtures in cold regions.

To my Mother and Father,

To my beloved Fiancée,

To my three younger brothers,

And to my sincere friends who passed away defending our country,

Despite the distances that separated us, I hope that this work makes us
closer, and crowns our sacrifices.

Anis Abayou

ACKNOWLEDGEMENTS

All praise are due to Almighty Allah, I praise him, seek his assistance and forgiveness. I thank him for granting me the opportunity to seek knowledge and benefit mankind with this knowledge as he ordered me to do so. I thank my supervisor Dr. Mohamed T. Bassuoni, P.Eng. Professor, for his dedicated and continuous support throughout this program. Dr. Bassuoni showed a high level of dedication, patience and unremitting enlightening guidance at all times. Without his support, this accomplishment wouldn't have been possible.

I do most sincerely appreciate the support from Natural Sciences and Engineering Research Council of Canada and University of Manitoba, faculty of Graduate studies. The IKO Construction Materials Testing Facility at the University of Manitoba in which these experiments were conducted has been instrumental to this research. Moreover, my sincere thanks go to Mr. Chad Klowak, P.Eng., W.R. McQuade Heavy Structures Laboratory Manager, Samuel Abraha, and Syed Abdullah Mohit the structures laboratory technical staff at University of Manitoba for their technical support and valuable guidance. In addition, I would like to thank my colleagues, especially Ahmed Soliman for his tireless help during the experimental and technical analysis.

Finally, the highest gratitude goes to my mother for her never-ending love, care and support both in my ups and downs. Without my Mother & father and their encouragement and prayers, I wouldn't be able to come this far. Also, I sincerely thank my beloved fiancée, for her companionship through the times of ease and hardships, I do sincerely thank her for her patience and compassionate love. I thank my younger brother Abdulsalam, Abdulhakim, and Omar and I encourage them to go out there and make our parents proud.

Table of Contents

ABSTRACT	ii
ACKNOWLEDGEMENTS.....	v
List of Tables	x
List of Figures.....	xi
Abbreviation/Nomenclature	xiii
1. Introduction.....	1
1.1. Overview	1
1.2. Cold Weather Concreting.....	2
1.3. Need for Research.....	5
1.4. Objectives.....	6
1.5. Scope of work.....	7
1.5.1. Phase I: Properties of nano-modified concrete cast and cured under cyclic freezing/low temperatures.....	7
1.5.2. Phase II: Nano-modified concrete as a repair material under freezing/low temperatures.....	8
1.6. Thesis structure.....	9
2. Literature Review.....	10
2.1. Introduction	10
2.2. The Mechanism of the Hydration Process	11

2.3.	Effects of Below-Freezing Temperature on Concrete	13
2.4.	Air Entrainment	14
2.5.	Codes Provisions.....	15
2.5.1.	Guide to cold Weather ACI 306R-16	16
2.5.2.	Test methods and standards practices for concrete, CSA A23.1-14/A23.2-14	16
2.6.	Conventional Cold Weather Concreting Practices	17
2.6.1.	Heated Enclosures.....	17
2.6.2.	Protective Covers and Insulation	18
2.6.3.	Heating of Concrete Ingredients	18
2.7.	Cold Weather Admixture System	19
2.8.	Effect of Antifreeze Admixtures on Concrete	20
2.8.1.	Workability.....	21
2.8.2.	Compressive Strength	22
2.8.3.	Setting Time	23
2.8.4.	Tensile Strength	24
2.8.5.	Freeze-Thaw Resistance.....	24
2.8.6.	Corrosion of Embedded Steel.....	25
2.9.	Nano Materials in Cold Weather Concreting	27
2.10.	Design of experiments and Statistical Analysis Models	29
2.11.	Closure	32

3.	Experimental Program.....	35
3.1.	STATISTICAL MODELS	35
3.2.	MATERIALS AND MIXTURES	37
3.2.1.	Phase I: nano-modified concrete cast cured under cyclic freezing/low temperatures 37	
3.2.2.	Phase II. Nano-modified concrete as a repair material under freezing/low temperatures	40
3.3.	PROCEDURES	41
3.4.	TESTING METHODS.....	44
3.4.1.	Phase I Testing Methods	44
3.4.2.	Phase II Testing Methods.....	49
4.	Results and Discussion of Phase I.....	55
4.1.	DERIVED STATISTICAL MODELS	55
4.2.	SETTING TIME.....	57
4.3.	COMPRESSIVE STRENGTH.....	60
4.4.	FLUID ABSORPTION	63
4.5.	MERCURY INTRUSION POROSIMETRY (MIP)	65
4.6.	THERMAL ANALYSIS	67
4.7.	SCANNING ELECTRON MICROSCOPY.....	70
4.8.	NUMERICAL OPTIMIZATION	72

5. Results and Discussion of Phase II	77
5.1. SETTING TIME AND INTERNAL HEAT	77
5.2. STRENGTH DEVELOPMENT	81
5.3. FLUID ABSORPTION	84
5.4. SURFACE SCALING	86
5.5. RESTRAINED SHRINKAGE	89
5.6. BOND STRENGTH	91
5.7. MERCURY INTRUSION POROSIMETRY.....	93
6. Summary, Conclusions and Recommendations	96
6.1. Summary	96
6.2. Conclusions for Phase I.....	98
6.3. Conclusions for phase II.....	99
6.4. Recommendations for future research work.....	101
7. References.....	102
Appendix A: Statistical model tests for various responses.	112
Appendix B: Detailed ANOVA and Model coefficient tables.....	118

List of Tables

TABLE 2.1 Types of Anti-freeze admixtures (Courtesy Korhonen et al, 1990).....	20
TABLE 2.2 Effects of antifreeze admixtures on steel corrosion.....	26
TABLE 3.1 Coded and absolute values of investigated parameters.....	36
TABLE 3.2 Chemical composition and physical properties of binder components.....	38
TABLE 3.3 Properties of CNA and CNI.....	38
TABLE 3.4 Proportions of phase I mixtures per cubic meter.....	39
TABLE 3.5 Proportions of phase II mixtures per cubic meter.....	40
TABLE 4.1 Average results from the bulk tests.....	56
TABLE 4.2 Derived coefficients for the models and their significance based on ANOVA.....	57
TABLE 4.3 Summary of MIP test results.....	66
TABLE 4.4 Numerical optimization criteria, goals, and results.....	74
TABLE 5.1 Average results of compressive strength (MPa).....	83
TABLE 5.2 Summary of MIP results for repair mixtures.....	95
TABLE B1 IST detailed ANOVA results.....	119
TABLE B2 IST model coefficients.....	119
TABLE B3 FST detailed ANOVA results.....	120
TABLE B4 FST model coefficients.....	120
TABLE B5 3-days compressive strength detailed ANOVA results.....	121
TABLE B6 3-days compressive strength model coefficients.....	121
TABLE B7 28-days compressive strength detailed ANOVA results.....	122
TABLE B8 28- days compressive strength model coefficients.....	122
TABLE B9 Fluid absorption detailed ANOVA results.....	123
TABLE B10 Fluid absorption model coefficients.	123

List of Figures

Figure 2.1 Methods of RSM design techniques.....	31
Figure 3.1 Components of FCCD Design Block.	35
Figure 3.2 Phase diagrams of: (a) CNA, and (b) CNAI.....	40
Figure 3.3 Late Fall temperature history for City of Winnipeg (October to November).....	42
Figure 3.4 Early spring temperature history for City of Winnipeg (March to April).....	42
Figure 3.5 Solutions used to prepare mixtures.....	43
Figure 3.6 Flowchart of phase I experimental program.....	44
Figure 3.7 ACME penetrometer setting time apparatus.....	45
Figure 3.8 Mercury Intrusion Porosimetry (MIP) apparatus.....	46
Figure 3.9 Differential Scanning Calorimetry (DSC) apparatus.....	47
Figure 3.10 Scanning Electron Microscopy apparatus.....	48
Figure 3.11 Flowchart of phase II experimental program.....	49
Figure 3.12 Visual rating of concrete surface scaling.....	51
Figure 3.13 Pull-off test configuration.....	52
Figure 3.14 Shrinkage test specimen configuration.....	54
Figure 4.1 Isoresponse curves of IST.....	60
Figure 4.2 Isoresponse curves of FST.....	60
Figure 4.3 Isoresponse curves of 3-day compressive strength.....	63

Figure 4.4	Isoresponse curves of 28-day compressive strength.....	63
Figure 4.5	Isoresponse curves of fluid absorption.....	65
Figure 4.6	Thermogravimetry results for the portlandite contents at early-age up to 7 days.....	69
Figure 4.7	Thermogravimetry results for the portlandite contents up to 120 days.....	70
Figure 4.8	BSEM micrographs for thin sections from different mixtures.....	72
Figure 4.9	Contour Plots of the Desirability Function for various applications.....	75
Figure 5.1	Initial and Final Setting time.....	78
Figure 5.2	Internal Heat of Concrete.....	80
Figure 5.3	Results of fluid absorption test.....	85
Figure 5.4	Cumulative mass loss of concrete slabs.....	87
Figure 5.5	examples of visual rating after 50 F/T cycles.....	88
Figure 5.6	Restrained shrinkage of the repair layer in concrete slabs.....	90
Figure 5.7	Bond Strength test results.....	93
Figure A1	Log (IST) model statistical tests.....	113
Figure A2	Log (FST) statistical model tests.....	114
Figure A3	(1/fc ³) statistical model tests.....	115
Figure A4	fc 28 statistical model tests.....	116
Figure A5	Absorption statistical model tests.....	117

Abbreviation/Nomenclature

GU – General use cement
C₂S - Dicalcium silicate (belite), $2CaO \cdot SiO_2$
C₃A - Tricalcium aluminate, $3CaO \cdot Al_2O_3$
C₃S - Tricalcium silicate (alite), $3CaO \cdot SiO_2$
C₄AF - Tetracalcium aluminoferrite, $4CaO \cdot Al_2O_3 \cdot Fe_2O_3$
CH - Calcium hydroxide
C-S-H - Calcium silicate hydrate
DSC - Differential Scanning Calorimetry
FA - Fly ash
NA - Nano-alumina
NS - Nano-silica
SCMs - Supplementary cementitious materials
SEM - Scanning Electron Microscopy
XRD - X-ray Diffraction
CWAS - Cold weather admixture system
DOEs - Design of Experiments
RSM - Response Surface Method
FCCD - Face-centered Composite Design
CCD - Central Composite Design
ITZ - interfacial transitional zone
AE - Air Entrainment
HRWRA - High Range Water Reducer Admixture
CNI - Calcium nitrite
CNA- Calcium nitrate
CNAI - Calcium nitrate: Calcium nitrite (1:1)
CNAAI- Calcium nitrate: Calcium nitrite (2:1)
ANOVA- Analysis of Variance
COW- City of Winnipeg
SEM - Scanning Electron Microscopy
IST - Initial Setting Time
FST- Final Setting Time
TGA - Thermogravimetry Analysis

1. Introduction

1.1. Overview

Concrete is a porous material that is produced from mixing cement, water and aggregates together. The reaction by the virtue of which concrete gains its strength due to a process that is known as hydration. It occurs when cement components come in contact with water, which enables cement to hydrate and form a binding agent for aggregates. This binding agent or gel is known as calcium-silicate-hydrate (C-S-H), its rate of production is highly affected by temperature and relative humidity. As temperature drops, hydration proceeds in a slow rate and eventually stops when temperature drops below 0°C due to the freezing of mixing water (Korhonen et al, 1992; Ratinov et al, 1996). The stoppage of cement hydration results in producing concrete that lacks adequate physical and mechanical properties needed by concrete to serve for the desired service life. Moreover, the low temperature causes ice formation that is associated with volumetric expansion that exerts internal stresses and ultimately disturbs the microstructure of concrete leading to irreparable strength and durability damages (Powers et al, 1953). In cold regions, these durability issues were averted by avoiding casting concrete in the colder seasons of the year and limiting construction to only few warmer months (usually between May and September).

Several conventional heating practices were recommended (ACI 306R, 2016) to overcome the adverse effects of low temperatures on concrete such as heating the concrete ingredients and/or using heating enclosures. However, these methods come at high cost, require highly skilled manpower, and produce greenhouse gasses emissions. Hence, providing a more viable option that

uses innovative materials for cold weather concreting remains unresolved, which warrants further research.

1.2. Cold Weather Concreting

Temperature is a key factor affecting the hydration of cement paste in concrete. As the temperature drops, the hydration process of concrete proceeds at a slower rate and completely stops when the temperature drops below 0°C with approximately 95% of the mixing water turning into ice (Karagol et al, 2015; Ratinov et al, 1996), resulting in a heterogenous matrix with coarse microstructure. Moreover, when mixing water turns into ice, it experiences a volume expansion of about 9% inducing hydraulic and osmotic pressures on the walls of concrete pores causing micro-cracks and rapid deterioration (Powers et al, 1953; Prado et al, 1998). The optimum temperature and relative humidity for hydration of cement are 10 to 22°C and more than 85%, respectively (Karagol et al, 2015). Under freezing conditions, concrete may lose approximately one-half or more of its design strength when compared with concrete cast and cured under normal temperatures (Korhonen et al, 1992).

Cold weather, according to ACI 306R-16 (ACI 306R, 2016): Guide to Cold Weather Concreting, and CSA A23.1-14 (CSA A23.1, 2014): Concrete Materials and Methods of Concrete Construction, is defined as when the air temperature has fallen to or below 4°C and 5°C during concrete protection period, respectively. Therefore, both documents (ACI 306R, 2016; CSA A23.1, 2014) strongly advocate not to place concrete under cold weather conditions without extra precautions during the curing period of concrete to achieve desired physical and mechanical properties, allowing concrete to resist harsh conditions such as freezing-thawing cycles.

One option that has been introduced to mitigate the negative effects of low temperatures on concrete is cold weather admixture systems (CWAS). The incorporation of CWAS into concrete has two main functions: depressing the freezing point of the mixing water (antifreeze), and accelerating the rate of cement hydration and solidification (acceleration). Therefore, concrete can achieve adequate hardening and strength development rates (Polat, 2016; Karagol et al, 2013). CWAS such as calcium chloride, sodium chloride, potash, calcium nitrite, calcium nitrate, sodium nitrate, urea, and their combinations have been reported in the literature (Ratinov et al, 1996; Korhonen et al, 1997). However, chloride-based admixtures have been excluded due their ability to initiate rapid corrosion problems in steel reinforced concrete (Ratinov et al, 1996). In addition, sodium-based admixtures have provoked alkali aggregate reactivity (AAR) issues (Ratinov et al, 1996). Urea was found to retard the setting of concrete; thus, it has adverse effects on the early-age properties (Mwaluwinga et al, 1997). Furthermore, potash was reported to produce defective microstructure and inferior resistance to freezing and thawing cycles (Nami, 1998; Korhonen et al 1997; Korhonen et al 1990).

Comparatively, calcium nitrite and calcium nitrate were found to be effective in terms of enhancing the early-age properties of concrete by promoting superior strength gain and improving the hydration rates (Ratinov et al, 1996; Nami, 1998; Korhonen et al 1990). They increase the strength gain rate and ultimate strength of concrete cured at -5°C to comparable levels of normally cured concrete within 90 days (Karagol et al, 2015; Korhonen et al 1990). However, incorporating large amounts of more than 6% of CWAS (calcium nitrite and calcium nitrate) by mass of cement was reported to cause severe shrinkage cracking of concrete (Korhonen et al 1997). Moreover, the compressive strength and water absorption of concrete incorporating 6% calcium nitrate were negatively affected after being exposed to only 28 freezing and thawing cycles (Polat, 2016),

implicating coarse microstructure. Thus, while the use of CWAS may achieve satisfactory results in terms of hardening and strength rates, their effects on microstructure and durability of concrete are still uncertain.

The emerging innovations in nanotechnology have attracted much attention in the field of concrete research. Due to their high surface area and vigorous reactivity, nanoparticles enhance the physical and mechanical properties of concrete (Haruehansapong et al, 2014; Ghazy et al, 2016). Numerous studies (Said et al, 2012; Haruehansapong et al, 2014; Ghazy et al, 2016) have investigated the inclusion of nanoparticles such as nano-silica in cement-based systems mixed and cured under normal temperatures up to 30°C. The findings from these studies showed that nanoparticles contributed positively to concrete properties by speeding up the kinetics of cement hydration and refining the pore structure of hydrated cement paste, resulting in producing durable concrete to harsh exposures [Said et al, 2012; Haruehansapong et al, 2014; Ghazy et al, 2016]. A recent study at the University of Manitoba (Kazempour et al, 2014; Kazempour et al 2016) reported the ability of nano-silica to enhance the performance of masonry cement mortars (comprising 30% inert component), which were cast and cured at 5°C without any method of protection.

In addition, repair of concrete pavements and bridge decks is problematic during cold weather seasons. Depending on the situation, repairs are usually delayed until warmer temperatures are observed, leading to a jammed construction season. Repairs done in cold weather conditions experience premature failures, resulting in reducing the life-cycle of the concrete elements and significant socioeconomic losses (Al-Ostaz et al, 2010; Li et al, 2011). For such scenarios, competent rapid-setting repair mixtures with adequate durability properties are needed to overcome these repair issues. There is a large number of commercially available repair mixtures, but many of which only work under normal temperatures, vulnerable to cracking, have poor

bonding properties, do not provide adequate life-cycle, and/or incompatible with the existing parent concrete (Li et al, 2011; Soliman et al, 2014). Previous studies (Ghazy et al, 2016; Soliman et al, 2014) have showed concerns regarding the use of high-early strength concretes in pavements, as these materials can lead to internal stresses due to their thermal gradients, early age shrinkage and ultimately micro-cracks that propagates to macro-cracks and cause several durability problems.

Ghazy et al, 2015 have studied the potential of using blended binder nano-modified fly ash mixture as repair mixtures under normal temperatures. The findings of this study have showed that the synergistic effects of nanosilica and fly ash mixtures improved the early-age and long-term compressive, tensile, and bond strengths of concrete and improved the microstructural development, which ultimately shows the suitability of nano-modified fly ash mixtures for several repair applications.

1.3. Need for Research

During cold weather, ACI 306R-16 (ACI 306R, 2016) and CSA A23.1 (CSA A23.1, 2014) recommend conventional techniques such as heating concrete ingredients (water and aggregate), or installing heated enclosures to avert water from freezing and provide adequate curing conditions for concrete. These practices come at high costs and adverse environmental impacts (Barna et al, 2011). Thus, in cold regions, construction and maintenance season of concrete infrastructure is typically limited to three to five months (usually within May to September) leading to overwhelmingly busy construction periods, backlogged repair schedules and significant socioeconomic losses. Therefore, there is continual need for new and innovative options that permit concrete to be cast, finished, and cured at low temperatures. Consequently, the construction season may be extended within late fall (October to November) and early spring (March to April) periods without the shortcomings of conventional heating practices. Despite the positive advances

brought to cold weather concreting by the introduction CWAS, the behavior of most of these admixtures is still not well understood. Actually, some CWAS were found to initiate durability issues such as corrosion, alkali aggregate reactivity and defective microstructure (Nami, 1998; Ratinov et al, 1996).

Moreover, there is still dearth of information on nano-silica reactivity under sub-zero temperatures and its interaction with CWAS and other types of cements (e.g. ordinary cement, blended cements containing fly ash) to produce concrete mixtures at lower (e.g. freezing) temperatures. Therefore, in this thesis combinations of fly ash, nano-silica and CWAS were used to prepare concretes that were mixed, cast and cured under cyclic freezing/low temperatures (-5 and 5°C) representing the temperature range of late fall and early spring in cold regions including North America and Europe. The fresh, hardened and microstructural properties of these mixtures were assessed.

1.4. Objectives

The main objective of this research was to provide a viable option for cold weather concreting using innovative materials to produce mixtures that can withstand the severe environmental conditions caused by freezing/low temperatures on concrete. The specific objectives of this thesis were as follows:

- Develop innovative concrete mixtures using combinations of single or blended binders with CWAS and nano-silica, which can be cast and cured and under cyclic freezing/low temperatures without heating or protection practices.
- Evaluate the physico-mechanical durability properties of the developed mixtures and explore the compatibility between fly ash, nano-silica and CWAS under cold conditions.

- Study the fresh, hardened, and durability properties of these mixtures, build a statistical analysis model that is capable of predicting certain responses and exploring the optimum behavior for multiple construction scenarios.
- Assess the potential of using the developed mixtures in extending the construction season in cold weather regions to late fall and early spring and examine the compatibility of using them as repair mixtures.

1.5. Scope of work

To achieve the specific objectives of this work, this master's research was conducted over two phases as described below:

1.5.1. Phase I: Properties of nano-modified concrete cast and cured under cyclic freezing/low temperatures.

In this phase, 15 concrete mixtures involving key variables expected to have effects on concrete mixtures cast and cured under low temperatures were developed. Combinations of fly ash (up to 25%), nano-silica (up to 4%) and CWAS were used to prepare concretes that were mixed, cast and cured under cyclic freezing/low temperatures (-5 and 5°C) representing the temperature range of late fall and early spring in cold regions. Each of these variables was evaluated at three dosage levels: low, medium and high. Mixing and casting was done without any heating methods.

Design of Experiments (DOEs) was used to categorize the experimental variables and test their significance based on the Response Surface Method (RSM). This method enabled the reduction of the size matrix to 15 mixtures with high level of confidence. Based on DOEs, regression models were derived to predict the performance of the proposed mixtures under the aforementioned exposure regime. The models were trained using experimental laboratory data,

and the merit of the models lies in their ability to predict a number of responses that represent mixture's fresh, hardened, and durability properties. Moreover, numerical optimization was performed to identify optimum mixtures for different target applications.

1.5.2. Phase II: Nano-modified concrete as a repair material under freezing/low temperatures.

Based on the results of Phase I, a reduced matrix of mixtures was selected to evaluate their potential as cold weather repair materials for concrete infrastructure (e.g. pavements). Mixtures containing GU cement, Class F fly ash, CWAS represented by calcium nitrate and calcium nitrite, and nano-silica were used to prepare cold weather repair mixtures. Laboratory performance of the innovative nano-modified and nano-modified fly ash mixtures were evaluated on early-age and long-term basis as well as the compatibility between the repair mixtures and substrate (parent) concrete. To simulate the field conditions, the proposed mixtures were cast and cured under cyclic freezing/low conditions representing late fall and early spring in some regions in North America (e.g. Winnipeg City) and were exposed to Freezing/Thawing, and wetting/drying cycles to represent the alternation of seasons. The exposure involved wetting using the aggressive calcium chloride salt solution that is commonly used as de-icing salt in cold regions.

Seven mixtures of single and blended binders were developed with different dosages of fly ash and nano-silica and the optimum CWAS concluded from phase I. The assessment criteria were based on physico-mechanical properties including fresh properties represented by initial and final setting time, hardened properties represented by compressive strength development (up to 91 days), durability properties represented by fluid absorption, bonding strength, surface scaling, and restrained shrinkage. These tests shall serve to evaluate the early-age and long-term performance of the repair mixtures as well as their compatibility with the substrate parent concrete. Moreover,

a forensic analysis on the microstructure of the optimum mixtures was conducted using mercury intrusion porosimetry (MIP) was conducted to corroborate the trends acquired from the bulk tests.

1.6. Thesis structure

This thesis consists of six chapters, described as follows:

- CHAPTER 1 contains brief introduction, description of problem statement, objectives and scope of work.
- CHAPTER 2 provides comprehensive literature review on the effects of cold weather on concrete. Also, it describes the limitations of conventional methods to deal with cold weather issues, and possible innovative solutions.
- CHAPTER 3 describes the adopted methodology, materials and mixtures, exposure regime and comprehensive details of the macro- and micro- scale testing setups.
- CHAPTER 4 comprises presentation of results and discussion of Phase I. It includes experiments on fresh, hardened and durability properties of concrete cast and cured under cold weather laboratory simulated exposure regimes. This chapter also includes detailed discussion on the derived statistical models based on the laboratory experiments.
- CHAPTER 5 provides results and discussion of Phase II on utilizing nano-modified concrete mixtures as a repair material for concrete pavements to achieve balanced early-age and long-term performance under freezing/low cyclic temperatures.
- CHAPTER 6 provides a conclusive summary of the findings of both phases, list the major conclusions of the entire thesis and proposes recommendations for future research.

2. Literature Review

2.1. Introduction

Cold weather, according to ACI 306R-16 (ACI 306R, 2016): Guide to Cold Weather Concreting, and CSA A23.1-14 (CSA A23.1, 2014) Concrete Materials and Methods of Concrete Construction, is defined as when the air temperature has fallen to or below 4°C and 5°C during concrete protection period, respectively. Therefore, both documents (ACI 306R, 2016; CSA A23.1, 2014) strongly advocate not to place concrete under cold weather conditions without extra precautions during the curing period of concrete to achieve desired physical and mechanical properties, allowing concrete to resist harsh conditions such as freezing thawing cycles. In the United States of America, winter construction operations involving concrete performed in winter are governed by ACI 306R guidelines, which prescribes steps to ensure that concrete placed in cold weather does not freeze during its placing, finishing, and curing period. ACI recommends users to place a warm concrete mixture on surfaces above the freezing temperature. In addition, concrete must then be kept warm by placing insulating sheets covering the freshly placed concrete to conserve the internal heat developed within the concrete mixture resulting from the internal chemical reactions, or by providing heated enclosures. These methods of protection must be kept in place until concrete develops sufficient strength, be safe and perform as designed.

ACI (ACI 306R, 2016) suggests that the Protection period needed by concrete to achieve sufficient strength may be shortened by adding rapid-setting cement, commonly known as High Early strength type HE cement, or by adding accelerating admixtures. However, no other methods of protections against freezing is recommended by ACI (ACI 306R, 2016). These practices result in high heating costs in addition to the extra labor and materials that are needed to protect concrete from freezing.

Chemical admixtures are widely used in Russia, China, and the Scandinavian regions, such admixtures are added to concrete mixtures to depress the freezing point of mix water, they allow concrete to cure at below-freezing temperatures with adequate concrete properties. Large number of chemical compounds have been tested in the aforementioned regions and some of these provide an economical alternative to conventional cold weather concreting practices (Korhonen, 1990).

2.2. The Mechanism of the Hydration Process

Portland cement is a composite material that consists mainly of lime, silica, alumina and iron oxide. These chemical compounds interact with each other during manufacturing to form a more complex product until a state of chemical equilibrium is achieved. The final cement product has four major constituents, Tricalcium Silicate (C_3S), Dicalcium Silicate (C_2S), Tricalcium aluminate (C_3A), and tetracalcium aluminoferrite (C_4AF). The components of cement react with water and form hydrated products that are firm and hard in nature and act as the bonding agent in concrete. This chemical reaction is known as the hydration process.

The hydration of cement is known to be an exothermic reaction since the rate of heat is used to indicate the rate of cement hydration. Three heat peaks occur during the cement hydration, the first peak happens as soon as water touches the cement, this peak corresponds to the initial hydration at the surface of cement particles. The first heat peak is high and lasts for a very short period of time, less than an hour, and it heavily involves the reaction of C_3A . Concrete then reaches a stage that is known as the dormant period that lasts approximately one to two hours under normal conditions, during which the concrete is still workable. The heat of hydration increases at a slow rate until it reaches the second peak after approximately 6 to 10 hours. During this second stage the hydration products come into contact with one another, concrete gains strength and until final

setting occurs. At the age of 18 to 30 hours a third heat peak occurs which is also related to a renewed reaction of C₃A (Neville, 2012).

The aforementioned setting of concrete is a term that defines the stiffening of concrete. Setting occurs when concrete transforms from its fresh fluid state to its' rigid hardened state. Practically speaking, setting of concrete is divided to initial setting and final setting, which is the time that is needed by certain mixture to reach a certain strength as specified in ASTM C403,2016 (ASTM C403, 2016).

The hydration process is directly influenced by temperature, relative humidity, the optimum temperature and relative humidity are 20°C and 80%, respectively. However, as temperature drops, water freezes and the hydration process rate slows down and, in turn, decreases strength gain in concrete. When temperature reaches 4°C or below, concrete is not allowed to be placed without extra precautions as per ACI 306-16 (ACI 306R, 2016), as below this temperature the hydration theoretically stops and concrete will suffer from unrepeatable damages. Moreover, more than 95% of water turns to ice when the temperature reaches -5°C and hydration totally ceases at this stage. Thus, with only less than 5% of water remains unfrozen, fresh concrete can lose approximately one-half of its design strength (Korhonen et al, 1992).

When saturated fresh concrete has the majority of its pores filled with unreacted water experience a very low temperature, the water turns to ice. When turning into ice, water experiences a volume expansion of about 9%, therefore the volume of the pores will be able to accommodate this expansion. As a result, internal hydraulic stresses will be generated from the expanded water. These internal stresses, which act in a tensile manner, could reach up to 100 MPa, which is much

higher than the tensile capacity of concrete that is 10% of its compressive strength, about 6 MPa for high strength concrete (Karagöl et al, 2015; Prado et al, 1998; ACI 318, 2002).

In cold weather environments, the goal is to conserve the internal heat generated by the hydration process and maintain favorable conditions that are adequate to allow the continuation of the hydration process and the prevention of ice formation, thus gaining desired strength.

2.3. Effects of Below-Freezing Temperature on Concrete

Concrete is a composite material that is composed of cement, aggregate, and water. This composite material gains its strength by a chemical reaction between water and cement to form binding gel that hardens overtime and aggregates together. This chemical reaction, formally known as the hydration process, depends on temperature and humidity conditions. Optimum conditions for the hydration process include temperature that ranges from 10 to 20 °C and Relative Humidity (RH) of 80%.

Under freezing conditions, the hydration process gets affected by a number of factors including migration of moisture inside the mixture, the change of water phase from liquid phase (water) to solid phase (Ice), and the reduction of the reaction rate between cement and water. Some water molecules remain unfrozen, those unfrozen molecules allow cement to continue to hydrate at low temperatures in a slow rate, and however the hydration process completely stops when temperatures reach below -0°C. This happens as a result of two things, the concrete becomes dormant and freezing of the remaining of the water. Concrete may resume hydration if temperature rises and ice melts. However, if freshly placed concrete freezes before developing much strength, concrete would suffer permanent damage regardless of resuming the hydration process (Korhonen et al, 1990).

Migration of moisture and formation of ice inside concrete are directly influenced by cooling rates. Rapid cooling rate limit the movement ability of moisture inside concrete, thus moisture freezes in place. In turn, this forms a uniform distribution of small dispersed ice crystals, which causes approximately a 9% expansion of concrete at an early age. This expansion disrupts the weaker components of concrete such as cement paste. On the other hand, slow cooling rates allows water to move within the concrete mixture and freeze at colder temperatures. When water moves to colder areas where it freezes, the ice thickens and concrete can be damaged by ice crystals forms layers or lenses, this forces the aggregates and cement paste apart. In both cases, rapid and slow freezing rates, concrete can suffer irreparable damage and substantial strength losses (Korhonen et al, 1990).

2.4. Air Entrainment

The damaging mechanism of freezing and thawing happens due to the expansion of water upon freezing, thus if an extra space of air-filled voids is present in the concrete media, the damage will be reduced. The main principle of air entrainment is to provide air voids which allows excess water to escape to them and expand without causing internal stress in the concrete. Minimizing capillary pores is an essential part in making a successful air entrained concrete system because otherwise volume of excess water would exceed the volume of entrained air voids which in turn disrupt the system.

This, in other words, means a low water/binder ratio is required to provide such an adequate system. In addition, this ensures a stronger concrete which has a better ability to resist internal stresses induced by freezing. ACI 201-16 (ACI 201, 2016) directs users to use a maximum of water/binder ratio of not more than 0.50 for mild exposure and 0.45 for severe exposure, this is in addition to adequate curing that ensures concrete to reach a minimum of 25 MPa compressive

strength before being exposed to multiple freeze-thaw cycles. Neville, 2012 defines entrained air as “Air intentionally incorporated by means of a suitable agent”. Air entrained concrete is produced by using air-entraining admixture, air-entrained cement, or both. The size of air-entrained bubbles should be clearly distinguished from entrapped air, the air entrained has an average diameter of approximately 50 μm whereas entrapped air has much larger air voids (Neville, 2012).

The shape of the entrained air is nearly spherical and they are separate and randomly distributed throughout the concrete mixture. The air bubbles are formed in a manner so that no channels allowing water flow are created, thus concrete permeability is not affected. The main types of Air-entrain admixtures are salts or fatty acids, alkali salts from wood resins, and alkali salts of organic compounds, all of these admixtures are surfactants, that is as described by Neville, 2012 as “long-chain molecules which orient themselves so as to reduce the surface tension of water and direct the other end of the molecule toward the air”. As a result, the air bubbles formed during mixing of concrete are covered by a tight layer of air-entrain molecules that repels from one another which prevents merging of air bubbles and ensures uniform dispersion in the concrete media. The optimum spacing between air bubbles that maximize protection against frost damage ranges from 200 μm to 250 μm (Powers, 1954; ACI 201, 2016). The recommended air content for severe exposure is 7.5 and 6% for nominal maximum aggregate sizes of 9.5 and 19 mm, respectively. For moderate exposure 6 and 5.5% for nominal maximum aggregate sizes of 9.5 and 19 mm, respectively. In construction field these percentages are tolerated up to $\pm 1.5\%$ (ACI 201, 2016).

2.5. Codes Provisions

The objective of guides and codes in general is to provide guidance to contractors and sets requirements to ensure that concrete placed in cold weather develops sufficient strength and

durability to satisfy the intended service life. In this section a brief overview of American Concrete Institute (ACI) 306R-16 (ACI 306R, 2016): Guide to cold Weather Concrete and Canadian Standards Association (CSA) A23.1-14/A23.2-14 (CSA A23.1, 2014): Concrete materials and methods of concrete construction/Test methods and standards practices for concrete.

2.5.1. Guide to cold Weather ACI 306R-16

ACI 306R (ACI 306R, 2016) defines cold weather as when the air temperatures has fallen or expected to fall below a temperature of 4°C during the protection period, a period which freshly placed concrete needs to be protected against cold weather exposure until it gains certain strength. Concrete must not be exposed to a single freezing-thawing cycle until it attains a compressive strength of 3.5 MPa, at 10°C most well-proportioned concrete mixtures reach this strength within 48 hours. Moreover, the guide states that concrete should not be allowed to experience multiple freeze-thaw cycles before it attains a strength of 24 MPa. During the protection period concrete, conventional protection methods, which will be discussed in a separate section, such as heating enclosures shall be used. The protection period varies between 1 to 4 days for the accelerated set concrete, and from 2 to 6 days for normal-set concrete based on exposure and loading conditions. ACI 306 (ACI 306R, 2016) is written in a non-mandatory language which makes it a guide that recommends best practices to by practitioners.

2.5.2. Test methods and standards practices for concrete. CSA A23.1-14/A23.2-14

The Canadian code definition for cold weather is when there is a probability of the air temperature falling below 5°C within 24 hours of the concrete. If the temperature of concrete is to fall below 5°C, then protection is required to maintain the concrete temperature at a minimum of 10°C. The protection shall be used such as heated enclosures, insulation, among other. Under such condition, all snow and ice shall be removed from surfaces where concrete it to be placed, chlorides and other

de-icing salts be used as de-icing agents in the forms. Concrete temperature at placing shall not be lower than 10°C when the thickness of concrete sections is between 0.3 to 1 m, and not lower than 5°C when the thickness of concrete sections is between 1 to 2 m. However, these temperatures are tolerated up to -5°C when non-chloride, non-corrosive accelerators are used. CSA is written in a mandatory language which makes it a standard that must be followed by practitioners.

2.6. Conventional Cold Weather Concreting Practices

2.6.1. Heated Enclosures

Heated enclosures are used to protect concrete, they should be windproof and weatherproof so proper temperature can be maintained throughout the whole targeted area, they also should be able to withstand snow loads. Ventilated combustion heaters are used to heat the enclosures; however, heaters should not be allowed to directly heat or dry the concrete to avoid evaporation of mixing water (ACI 306R, 2016). Thus, at the time of placing, curing, and finishing concrete, concrete surfaces shall be protected from direct exposure by formwork, impermeable membrane, or other suitable measures.

When fresh concrete gets exposed to carbon dioxide, generated from heaters exhaust, damage by carbonation of concrete may occur. Carbonation causes softening and crazing of concrete surfaces based on the concentration of the exhaust gasses, concrete temperature, and relative humidity. Some other disadvantages are associated with using heated enclosures including hazardous effects to workers due to high levels of carbon dioxide, negative environmental impacts because of the exhaust gasses, and fire hazardous that may occur due to overheating enclosures. Removing the heated enclosures should be incremental to avoid thermal cracking of concrete.

2.6.2. Protective Covers and Insulation

Several types of protective covers and insulations are commonly used to protect fresh concrete from cold weather exposure. The hydration of cement is an exothermic reaction that generates heat especially during the first 3 days, thus, in some cases, external heating may not be needed to prevent freshly placed concrete from freezing. Protective and insulation covers are utilized to retain the heat generated by the hydration of cement, so that concrete continues to maintain sufficient strength development. The insulation cover should be kept in close contact with the protected concrete surface to minimize heat loss, the amount of insulation needed is determined based on the expected temperature during the protection period, moisture imperviousness, wind chill, size and shape of the concrete structure, and thermal resistance (R-value) of the used insulating material.

The commonly used insulating materials include, but not limited to, polystyrene foam sheets, Urethane foam, insulation blankets, straw (not recommended), and polyethylene sheets. It is essential to avoid sudden temperature change that may cause serious damage to concrete. Thus, upon finishing the protection period, the protection covers shall not be completely removed until concrete has cooled to an acceptable temperature that is determined based on the thickness of the protected member as specified by ACI 306R (ACI 306R, 2016) and CSA A23.1 (CSA A23, 2014).

2.6.3. Heating of Concrete Ingredients

Heating of mixing water and aggregates (both coarse and fine) is another conventional practice that is used to overcome the negative effects of cold weather on concrete. ACI 306R (ACI 306R, 2016) specifies minimum temperatures of concrete at mixing, based on air temperature and concrete thickness. It should be noted that premature contact of very hot water with bulk quantities of cement causes flash set and cement balls in mixers. Water with temperature as high as the

boiling point may be used, however, special precautions may be taken to avoid the pre-mentioned negative effects.

In addition to flash setting and cement balls formation, using very hot mixing water was reported to cause air-entraining admixtures to lose their effectiveness, thus it compromises the freeze-thaw resistance of concrete (ACI 306R, 2016). Heating aggregates is usually needed when air temperature drops below -4°C . However, on an average scale, heating aggregates to a temperature higher than 15°C is rarely needed.

2.7. Cold Weather Admixture System

Antifreeze admixtures have been used in the former Union of Soviet Socialist Republics (U.S.S.R) as early as the 1950's. Chlorides such as Calcium chloride and Sodium Chloride have been used on a wide scale in low temperature concreting. However, chlorides were discovered later to cause major corrosion problems. The interest in developing admixtures that are capable of making concrete mixtures withstanding the cold environments has dramatically increased on an international scale since its first use in the Soviet Union (Korhonen et al, 1990; Mironov et al. 1976).

Cold weather admixtures include anti freezing admixture, which are used to depress the freezing point of the mixing water. And accelerators, which are used to accelerate the hydration process of cement. The main objectives of using these practices are to eliminate concrete damage that happens due to freezing at plastic stage, ensure that there is enough strength before removing any forms, and ensure that the concrete is durable enough for its intended service life (Nmai, 1998). Several antifreeze admixtures were used and listed in **Table 2.1**. Among the list of antifreezes in the table the chloride admixtures "Calcium chloride and sodium chloride" were used and

investigated extensively. However, they were found to greatly increase corrosion problems in steel reinforced concrete structures. This issue related to chloride anti-freezing admixtures led to the development of other anti-freezing admixtures. The key anti-freezing admixtures, as listed in the table below, were used at range from 5% to 14% by cement weight as reported by (Korhonen et al, 1990).

TABLE 2.1 Types of Anti-freeze admixtures (Courtesy Korhonen et al, 1990).

Admixture Type	Percent By Cement Weight	Strength* (%)	Temperature (°C)
NaNO ₂	6	70	-5
	8	57	-10
	10	36	-20
Ca(NO ₂) ₂ +CO(NH ₂) ₂	9.5	55	-10
	11	35	-15
Ca(NO ₃) ₂ +CO(NH ₂) ₂	8.8	29	-10
	9	34	-20
Ca(NO ₃) ₂ +Na ₂ SO ₄	6.6	56	-10
K ₂ CO ₃	6	75	
	8	70	-5
	10	65	-10
	10	47	-15
	12	55	-20
NaNO ₂ + Na ₂ SO ₄	9	62	-10
NH ₄ OH	5.2	93	-20

* Percent strength of control sample cured at room temperature for 28 days.

2.8. Effect of Antifreeze Admixtures on Concrete

Properties of concrete are affected by any additives that may be added to it, these additives may influence concrete's fresh, harden, and durability properties. This section focuses on discussing some properties that are affected by anti-freezing admixtures.

2.8.1. Workability

Workability is a term that is determined by the means of ease of placement, handling, finishing, and ability to resist to segregation. It is a vital property of concrete; workable concrete is achieved by reducing the friction between the individual particle in the concrete and between concrete and other surfaces. ASTM C125-18 (ASTM C125, 2018) defines workability as “property determining the effort required to manipulate a freshly mixed quantity of concrete with minimum loss of homogeneity”, ACI 116R-00 (ACI 116R, 2000) defines it as “that property of freshly mixed concrete that determines the ease with which it can be mixed, placed, consolidated, and finished to a homogenous condition”.

Sufficient compaction by ramming or vibrating the concrete is essential to eliminate entrapped air until adequate workability is achieved, insufficient workability may cause reduction in compressive strength and durability problems. For cold weather concreting ACI (ACI 306R, 2016) directs uses to use low slump values to reduce possibility of water bleeding, as it leads to lower strength, frost damages, and thus less durable concrete It was found that for every 11 °C drop in temperature, concrete loses 2 cm of its slump (ACI 306, 2016; Evan, 2008).

Karagol et al, 2015 have investigated the effect of calcium nitrate, urea, and a combination of both additives with dosages of 9% calcium nitrate, 9% urea, 4.5% urea and 4.5% calcium nitrate by weight of cement. Comparing them to the control mix which had a slump of 4 cm, the slump was 6, 12, and 22 cm for calcium nitrate, urea, and a combination of calcium nitrate and urea, respectively.

2.8.2. Compressive Strength

Compressive strength is a common indicator of hardened concrete quality, it has been widely used and proven to be economical, safe, and easy to verify. ACI 306R (ACI 306R, 2016) specifies that concrete must not be exposed to a single freezing-thawing cycle until it attains a compressive strength of 3.5 MPa. The strength before freezing of normal concrete in Russia is 5 MPa according to (Krylov et al 1979). Formwork is essential and must be in place until concrete has enough strength to support itself and any imposed loads. Moreover, concrete must achieve a compressive strength of 24 MPa before it can be exposed to multiple freeze-thaw cycles. Thus, the anti-freeze admixtures have a direct and crucial effect on concrete because it influences the rate of strength gain and the ultimate strength of concrete.

As indicated in the **Table 2.1**, concrete develops its strength at a much slower rate when it is under low-temperature environment when compared to similar concrete mixture under room temperature. This lag in strength gain varies based on the temperature and the type of antifreeze admixture added to the concrete. Commonly, the design strength of concrete is the 28-day compressive strength, however, concrete continues to gain strength after this period. Concrete in room temperature gains strength in a slower rate in the post 28-day period due to the consumption of water in the system, while antifreeze concrete under low temperature continues to gain strength after 28-days based on the type of antifreeze admixture and the amount of the unconsumed water in the system. It was reported that some antifreeze combinations enables the concrete to reach 100% of the 28-day control design strength after 90 days of low-temperature curing.

Korhonen et al (1992) has reported that the lag in strength gain in early age for antifreeze concrete cured under early age can be compensated if concrete is cured at room temperature for an additional period. It has been shown an that there is an improvement in compressive strength gain

after antifreeze concrete was cured initially in low-temperature then followed by curing at 20 °C. This may be attributed to the melting of frozen ice which reacts with unhydrated cement to form binding gel which is responsible for the strength gain. On the practical scale, this implicates that concrete placed in the winter can be expected to gain strength during the following spring and summer seasons as temperature rises.

Korhonen et al, 1997 have studied several antifreeze admixtures cured at a temperature of -5 °C, compression cylinders were tested at 7, 14, and 28 days. The admixtures investigated in this project were K_2CO_2 + lignosulfonate (6.0, 1.5%), $Ca(NO_2)_2$ + $NaNO_2$ (3.0, 3.0%), $NANO_3$ + Na_2SO_4 (6.0, 2.0%), $Ca(NO_2)_2$ + water reducer (4.0, 0.7%), among other non-disclosed admixtures. All dosages were by percent weight of cement, the water/cement ratio was kept constant at 0.48 in all mixtures. The results have showed at a curing temperature of -5 °C, all of the investigated admixtures have reached a strength ranged between the values of control specimens cured at 20 °C and 5 °C. The 28-days strength have ranged from 27 to 34 MPa. However, when the curing temperature was lowered to -10 °C, only $NANO_3$ + Na_2SO_4 have developed strength higher than that of control specimens cured at 5 °C up to 14 days then the strength fell right below this value to 24 MPa.

2.8.3. Setting Time

Setting time is a term that is used to describe the stiffing of cement paste, setting refers to the rate of change of a cement paste from fluid to a rigid stage. During setting, cement paste develops some strength, however, setting is clearly distinguished in the literature from hardening, which represents the strength gain in the paste (Neville, 2012). Practically speaking, setting is divided into two arbitrarily stages, which are initial set and final set of paste that can be measured as specified in ASTM C403 (ASTM C403, 2016).

Setting time of cement is directly influenced by temperature and relative humidity, thus rate of setting decrease or increase depending on these factors. At low temperature setting is retarded due to the slower rate of hydration kinetics, in contrast, rise in temperature decreases the setting time. In conventional cold weather concreting practices where heating of concrete ingredients, premature contact of very hot water with cement causes flash-setting (premature stiffening of cement within few minutes), thus not enough time to place, finish, and cure the concrete properly. In cold weather regions, lengthy setting time causes delays in opening newly constructed projects, accelerating admixtures are used to counteract this by reducing setting time.

2.8.4. Tensile Strength

Tensile strength is an important design parameter especially when it comes to designing pavements. Higher tensile capacity results in high flexure strength which in turn contributes to decreasing thickness. Moreover, tensile strength contributes to concrete ability to resist frost. Concrete with high tensile strength are advantageous in resisting expansive stresses that occur as a result of expanding water molecules when it forms ice. It was reported that tensile strength of concrete was affected by potash (K_2CO_3), a decrease in a dynamic modulus of elasticity, an increase in the coefficient of expansion, and a decrease in the split-tensile strength were measured in concrete specimens with potash (Grapp et al, 1975).

2.8.5. Freeze-Thaw Resistance

In cold regions, the ability to resist freeze-thaw cycles is a critical factor when it comes to measuring durability of concrete. Adding antifreeze admixtures positively contribute to the concrete ability in terms of resisting freeze-thaw cycles by depressing the freezing point of water so it remains in a liquid phase for longer periods. A number of studies were conducted on antifreeze concrete to test its freeze-thaw resistance. Goncharova et al, 1975 have studied concrete specimens

containing antifreeze admixtures and compared them to non-air-entrained specimens. The antifreeze admixtures investigated in this study were Sodium Nitrite (10%), Potash (10%), Calcium Chloride + Sodium Chloride (8.5%), Calcium Nitrate + Urea (9%) and Calcium Chloride + Sodium Nitrite (9%) by weight of cement. The ingredients used to cast the antifreeze concrete specimens were cooled to -5 °C, then cured at -20 °C for 28 days followed by curing for an additional 28 days at room temperature, the specimens were subjected to cycles of freezing in air and thawing in water. While on the other hand the non-air-entrained specimens were cured at standard room temperature and were subjected to the same freeze-thaw cycles. The results from this study shows that all antifreeze admixtures, other than potash, have increased freeze-thaw resistance when compared to control specimens.

Non-air-entrained concrete along with potash specimens have showed a strength reduction by the 200th freeze-thaw cycle, considering that durable concrete should withstand 300 cycles and remain relatively unaffected. Similarly, Grapp et al, 1975 have investigated freeze-thaw durability but under freezing temperature of -20 °C and -60 °C. Ultrasonic waves and flexure strength tests were conducted to monitor durability of concrete specimens. The findings of this study were similar to that of Goncharova et al, 1975 which concluded that all investigated antifreeze admixtures improved freeze-thaw resistance, while only potash have reduced it.

2.8.6. Corrosion of Embedded Steel

Cement provides an alkaline environment that protects steel from corrosion. Any additives that may neutralize this alkalinity environment may cause steel to corrode when moisture and oxygen are present (Korhonen et al, 1990). Chlorides and carbon dioxide are commonly known to cause corrosion of embedded steel. Several antifreeze admixtures were found to have effects on steel corrosion. Antifreeze admixtures that contain chlorides such as calcium chloride and sodium

chloride were identified to cause corrosion problems. Sodium nitrite, sodium hydroxide, and calcium nitrite are found to be corrosion inhibitors according to (Kuzmin, 1976; Sheikin et al, 1980; Ovcharov, 1972). The following table, **Table 2.2**, summarize the effects of some antifreeze admixture on embedded steel.

TABLE 2.2 Effects of antifreeze admixtures on steel corrosion.

Type of Antifreeze	Corrosion Effects	Reference
NaNO ₃	No corrosion	Mironov et al, 1979
NH ₄ OH	No corrosion	Kuzmin et al, 1976
Ca(NO ₃) ₂	No corrosion	Kuzmin, 1976
K ₂ CO ₃	No corrosion	Kuzmin, 1976
NaSO ₄	No corrosion	Kuzmin, 1976
Ca(NO ₃) ₂ + CO(NH ₂) ₂	No corrosion	Kuzmin, 1976
Ca(NO ₂) ₂	inhibitor	Kuzmin, 1976
NaNO ₂	inhibitor	Kuzmin, 1976; Sheikin et al, 1980
NaOH	inhibitor	Ovcharov, 1972
NaCl	Causes corrosion	Kuzmin, 1976
CaCl ₂	Causes corrosion	Kuzmin, 1976

Chlorides are the primarily responsible for corrosion of steel reinforcement, which lead to damaging the surrounding concrete. A tight adhering protective passivity layer is formed on steel as soon as the hydration of cement begins. This oxide layer protects the steel and keeps it intact. However, the presence of chloride ions disrupts this system by destroying the protective layer. And when moisture and oxygen are present, steel corrosion occurs. Chlorides can be present in concrete media by the means of contaminated aggregates, sea water, de-icing salts, or admixtures containing chlorides.

Despite their wide use in early stages of developing antifreeze admixtures in 1950s, none of the chloride base antifreeze admixtures should be permitted to be used with steel reinforced

concrete. Standards and codes worldwide have imposed strict limits on the chloride content in concrete. For instance, European Standard (BS EN 206-1, 2000) limits the total chloride-ion content to 0.40 percent by mass of cement in reinforced concrete. ACI 318 (ACI 318, 2002) limits the water-soluble chloride ions to 0.15 percent by mass of cement. These two values are very different considering that water-soluble chlorides are a part of the total chloride content. These limits are conservative and should ensure no chloride-induced corrosion occurs, thus the addition of chloride-based antifreeze admixtures that causes chloride content to rise above the mentioned limits is not advised in steel reinforced concrete. (Neville, 2012).

2.9. Nano Materials in Cold Weather Concreting

Nano materials is a new innovation that has recently attracted researchers in many fields. Using a material with ultrafine nature in concrete has the potential to provide superior concrete properties. Nanoparticles react with the cementitious materials in an enhanced manner due to their high surface area, which provide enhanced mechanical properties (Abd.El.Aleem et al, 2014; Haruehansapong et al 2014). Several studies have investigated the inclusion of nanoparticles in concrete mixtures mixed and cured under normal temperatures (22 ± 2 °C), the findings show that nanoparticles have contributed positively to concrete properties by refining and densifying the pore structure of hydrated cement paste.

The addition of nano-silica (NS) and nano-alumina (NA) were specifically found to add significant beneficial properties to cement-based materials. They shorten the setting time of freshly placed concrete by accelerating the hydration process, improve compressive and flexure strength, densify the Interfacial Transition zone (IT zone), reduce CO₂ emissions, and enhance the production of binding gel (calcium silicate hydrate CSH). (Belkowitz et al 2015; senff et al, 2010; Jo et al, 2007).

Studies on the effects nanoparticles on concrete under low temperatures are very little, many questions regarding the behavior of nanoparticles with cementitious systems are yet to be answered. Kazempour et al, 2015 have investigated the effects of NS and NA on masonry mortar mixed and cured at a temperature of 5 ± 1 °C, with dosages of 2, 4, and 6% by weight of cement. The findings of this study show that both high dosages of NA and NS increase the overall air content of the mixtures, accelerate the hydrations reactions, decreased setting time and shortened the dormant period. All dosages of NS have significantly improved the early age (1, 3 days) and later age (28, 75 days) compressive strength. the researches have attributed the improvement in compressive strength in early age was due to physical filler effect, and was due to the latent pozzolanic effect in later ages.

Behfarnia et al, 2013 have investigated the frost resistance of normal concrete incorporating NS with dosages of 3, 5, 7% and NA with dosages of 1, 2, and 3% by weight of cement. The specimens in this research were casted and cured under room temperature of 20 ± 2 °C. Results have showed that concrete specimens containing 5% NS and 3% NA have performed the best, with a strength loss of 16.2% and 18.2% after 300 freeze-thaw cycles for 5%NS and 3%NA, respectively. While shrinkage wise, the same mixture have given lowest shrinkage with shrinkage of 1.4% and 3.8% for 5%NS and 3% NA, respectively. Moreover, the lowest mass loss was 4.3% for 5% NS and 11.47% for 3% NS after 300 freeze-thaw cycles. The researchers have found that the incorporated nano materials promotes the pozzolanic reaction and act as a filler that improves the pore structure of concrete and densify the microstructure of cement paste. Gonzalez et al, 2016 have confirmed these results, resistance to freeze-thaw test was done according to ASTM C666 (ASTM C666, 2015) on concrete specimens with NS with dosages of 1 and 2%.

Improvements to compressive strength and aggregate-paste were noticed, reduced deterioration for specimens with NS even in the presence of de-icers.

Nano Calcium carbonate (nano CaCO_3) was also investigated using dosages of 0.5, 1 and 2% of nano CaCO_3 with 7% of fly ash, 10% of slag by wt. of cement and 1.5% of calcium nitrate by wt. of cementitious materials. The study focused on the compressive strength of high strength concrete cured in both standard temperature ($21\pm 1^\circ\text{C}$) and low temperature ($6.5\pm 1^\circ\text{C}$). The findings have showed that nano CaCO_3 have improved the workability of the high strength concrete due to the enhancement of the micro-aggregate through the ball affect. The dosage of 0.5% of nano CaCO_3 was found to inhibit the effect of calcium nitrite as an accelerator, thus reduction in compressive strength occurred, especially under low temperature conditions. However, with higher dosages of 1 and 2% improvements to compressive strength was noted in both standard and low curing temperatures (Xu et al, 2012).

2.10. Design of experiments and Statistical Analysis Models

Experiments are generally run to discover new information about a system or to verify a previous experience or theory to confirm or deny it accuracy. Forensic series of experiments are often run where the input variables are purposefully changed in order to identify reasons or trends that may be observed in the outputs (Montgomery, 2017). Experimental design is crucial in the scientific and the engineering fields in terms of optimizing products/materials and ensuring best practices of innovative materials.

The applications of the experimental design in the engineering field includes; evaluation and comparison of design configurations, assessing material alternatives, selection and evaluation of design parameters, in order to ensure that the product/material functions under a wide range of field exposure conditions, deciding the main design parameters that effects the product

performance, and creating new products (Montgomery, 2017). In addition, design of experiments can be utilized to enhance the field performance and reliability and facilitates easier manufacturing process. Moreover, the objective of conducting these types of experiments is typically assessed by several statistical calculations to achieve high confidence limits and minimal systematic and random errors (Cox et al. 2000).

Factorial designs are often used when designing an experiment that involves several parameters on multiple levels. A complete factorial experiment consists of the total number of possibilities of all possible combinations of all investigated parameters at all levels. For instance, studying the effects of water-to-binder ratio (w/b), fly ash content, and air content on the compressive of concrete assuming three levels of each parameter (e.g. 4, 5, and 6% air content), results in $3 \times 3 \times 3 = 27$ possible mixtures. Despite the fact the complete factorial design gives highly reliable results, it tends in some instances to have an extremely large matrix that requires significant amounts funds, time and material. Thus, some methods such as response surface method were developed to avoid the overzealous matrix size. It is strongly recommended to have a well-planned experimental program, to ensure accuracy and simplicity of the analysis (Montgomery, 2017).

Several statistical experimental design problems could arise, which can substantially affect the results and lead to inconclusive or misleading results. The potential problems that can occur when statistical considerations are not incorporated in the design can include, but not limited to, the following: experimental variation masks factor effects, uncontrolled factors effecting the results, false principles that leads to inconclusive results, (Mason et al. 2003). Analyzing Multifactor experiments for data obtained from randomized designs is commonly done through an analytic technique called Analysis-of-Variance (ANOVA). In multifactor experiments, this

technique is used to separate the observed variation in the responses into two fractions; variations due to assigned factors (known controlled factors) or due to random causes. Statistical models can be derived and tested based on the ANOVA techniques. ANOVA models contains conferences for the investigated parameters and their interactions (Mason et al. 2003; Montgomery, 2017).

There are various types of models were used for the optimization process of concrete mixtures such as Factorial design, fractional factorial design and response surface method (RSM). RSM is a collection of statistical and mathematical techniques to develop and optimize responses on investigated parameters. The main objective of RSM to determine factors optimum conditions to reach a target response. Central composite design (CCD) and face-centered composite design (FCCD) are the most used RSM design techniques which were applied in different civil engineering fields (Kang et al. 2010, Bayramov et al. 2004). Both methods uses multiple points out of a factorial set that can represent accurate information about the response space (Montgomery, 2017). These methods divides the experimental space into three components: the factorial (2^n , where n = number of factors) axial, and central parts as shown in **Figure 2.1**.

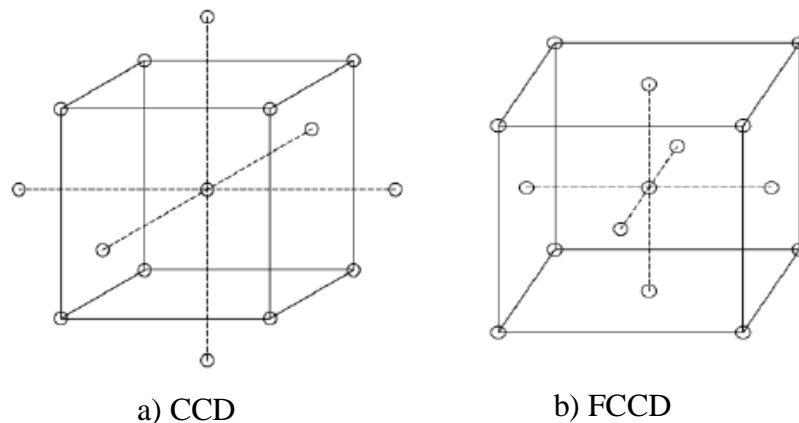


Figure 2.1 Methods of RSM design techniques.

A number of studies (Sonebi et al. 2013; Al-Alaily et al. 2016) used statistical analysis models to study concrete behavior from different aspects and to optimize concrete mixtures. However, there is dearth of information when it comes to the behavior and optimization of concrete under freezing/low temperature using statistical modeling approach. Damle et al. 2009 conducted a study to optimize the proportions of three different commercial admixture to be suitable for cold weather concreting using (RSM) to derive statistical analysis models. The models were used to predict the optimized dosages of the admixtures based on a desirability function. Moreover, Arslan et al. 2011 studied the effect of using 3 different antifreeze admixtures (calcium nitrate, hydroxyl ethoxy amin, and Polyhydroxy amine) at different dosages (4 levels) on concrete compressive strength after being cured for 2 days under low temperatures as low as -20°C . This study used ANOVA along with regression analysis to determine the significance of these studies and their interactions.

2.11. Closure

There is a renewed interest regarding the cold weather concreting; research on this area has started and evolved since 1950s (Korhonen, 1997). Since then, a great amount of resources has been designated by authorities in cold regions to develop suitable cold weather concreting practices and to mitigate its problems. This literature review provided a conclusive summary of the current research efforts that have been carried out to mitigate the durability issues of cold weather concreting. It discussed several cold weather admixtures and various curing methods that have been tried as solutions for concrete cast under low temperatures. Moreover, related code provisions in North America and Europe have been discussed. These codes and guides direct concrete practitioners to use conventional techniques such as heating concrete ingredients (water, sand and coarse aggregate), and using enclosures to heat up the surrounding environment to prevent water

from freezing and provide favorable curing conditions for concrete, to maintain the concrete temperature at a minimum of 10°C. These practices are associated with significant costs and adverse environmental effects due to the requirements of enclosure materials, highly-skilled manpower for quality control, and considerable consumption of energy and carbon gas emissions.

Thus, in cold climate countries, construction and maintenance seasons of concrete infrastructure are typically limited to three to five months (within May to September) leading to overwhelmingly busy construction periods, backlogged repair schedules and significant socioeconomic losses. Therefore, there is a serious need to extend construction periods in cold regions, by allowing concrete to be cast, finished, and cured at lower temperatures considering novel strategies that may minimize/eliminate shortcomings of the aforementioned conventional practices and to direct research towards finding new methods for cold weather concreting.

CWAS have been introduced to mitigate challenges of cold weather concreting. They depress the freezing point of the mixing water (antifreeze), accelerate the rate of cement hydration (accelerator) (Polat et al, 2016). However, some CWAS led to losses in strength, reduced resistance to freeze-thaw and adversely affected the microstructure of the concrete (Karagol et al, 2015; Demirboğa et al 2014). Chloride-based admixtures were the first to be tried; however, using these admixtures led to corrosion problems of steel reinforcement (Ratinov et al, 1996). Sodium-based antifreeze admixtures have led to durability issues such as alkali aggregate reaction (Ratinov et al, 1996). Moreover, potash was reported to impair concrete's microstructure and resistance to freezing and thawing cycles (Korhonen et al, 1997).

On the other hand, calcium nitrite and calcium nitrate were proved to bring about the most favorable effects on the properties of concrete (Nami, 1998). With the incorporation of calcium nitrite and calcium nitrate, concrete cast and cured under low temperatures could reach the same

compressive strength as normal concrete cured in lime saturated water (Karagol et al, 2015). Furthermore, using nano materials generally proved to be beneficial for concrete mechanical and physical properties. They can accelerate hydration kinetics, enhance mechanical properties of concrete (Abd.El.Aleem et al, 2014; Haruehansapong et al, 2014), refine the pore structure and densify the cement matrix (Jo et al, 2007; Li et al, 2004). However, most previous studies on the effect of nano-silica on cement-based systems have been done at normal casting and curing temperatures up to 30°C (Ghazy et al, 2016; Said et al, 2012), and there is still dearth of information on its action under sub-zero temperature.

Up to date, the behavior of concrete incorporating a combination of CWAS and nanomaterials at low temperatures is still unknown and has not been investigated. Thus, this thesis is dedicated to investigate and to better understand the effects of using these materials and the combination between them on the properties of concrete cast and cured under freezing/low temperatures. This combination has promising expectations to enhance concrete's microstructure and strength development without the need to use the conventional cold weather concreting methods, which ultimately can save money, time and energy, and lead to producing a durable speciality concrete for cold regions.

3. Experimental Program

3.1. STATISTICAL MODELS

Design of Experiments (DOEs) was used to categorize the experimental variables and test their significance based on the Response Surface Method (RSM). This method uses multiple points out of a factorial set that can represent accurate information about the response space (Montgomery, 2017). Face-centered Composite Design (FCCD), which is an RSM statistical approach, was adopted to evaluate three key parameters (i.e. $n = 3$) that are expected to have marked effect on the performance of concrete mixed, cast, and cured under freezing/low temperatures. FCCD divides the experimental space into three components: the factorial (2^n , where $n =$ number of influential factors, i.e. the number of factorial points in this study was $2^3 = 8$ points), axial, and central parts. The total number of points for this method were fifteen points divided as follows; 8 factorial points, 6 axial points (2 for each factor), and 1 central point as shown in **Figure 3.1**. Moreover, the central point was replicated three times to estimate experimental error to reach high level of confidence and improve the reliability of the derived models (Montgomery, 2017).

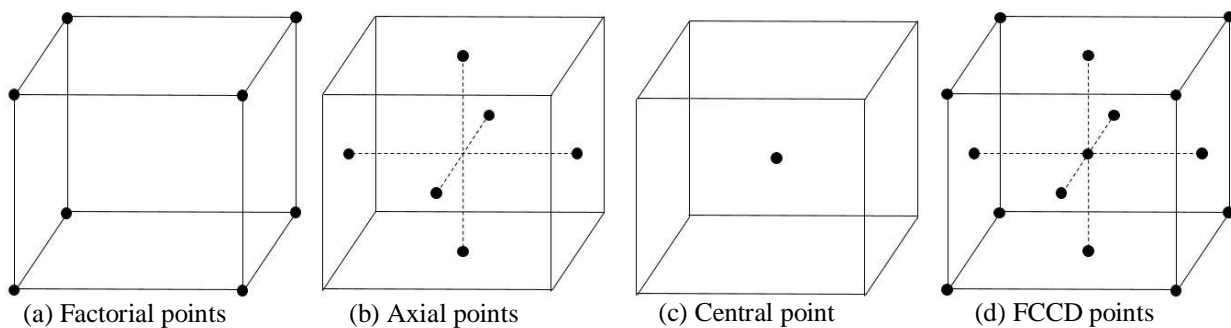


Figure 3.1 Components of FCCD Design Block.

The three parameters investigated were: fly ash and nano-silica dosages, as well as the type of the antifreeze admixture. Each factor was evaluated at three different levels and coded as follows: maximum (+1), minimum (-1), and central (0). This model is valid for mixtures with

water-to-binder ratio (w/b) of 0.32 mixed, cast, and cured under cyclic freezing/low temperatures and made with fly ash contents of 0 to 25%, nano-silica contents of 0 to 4% and a combination of calcium nitrite (CNI) and calcium nitrate (CNA) admixtures as shown in **Table 3.1**. The selected ranges for each of the variables were chosen based on practical considerations and literature to cover a wide range of mixture proportions. Experimental laboratory data was used to train the models and they were represented by five responses: initial and final setting times, compressive strengths at 3 and 28 days, and fluid absorption to assess the fresh, hardened and durability properties, respectively.

TABLE 3.1 Coded and absolute values of investigated parameters.

Parameter	Coding Values		
	-1	0	+1
Fly ash content, kg/m ³	0	50	100
Nano-silica content, kg/m ³	0	16	32
Antifreeze ratio (CNA:CNI)	1:0	2:1	1:1

Notes: The components of antifreeze for levels -1, 0 and +1 were 100% CNA, 67% CNA + 33% CNI and 50% CNA + 50% CNI, respectively.

Statistical Software (Design expert, 2018) was used to derive the equations for each model, which have the capability of predicting the response based on given inputs. In other words, given the fly ash content, nano-silica dosage, and the type of antifreeze (within the previously mentioned ranges), the models produce the expected initial and final setting times, compressive strength at 3 and 28 days, and the amount of fluid absorption. Multi-linear regression analysis with an assumption that the data are normally distributed was used to determine the models' coefficients. Analysis of Variance (ANOVA) was used to test the different factors and their interactions to identify insignificant variables and secondary interactions, which were subsequently eliminated from the derived modeling equations. The significance of each coefficient was based on the probability value (p -value), which was limited in all models to 5% (i.e. 95% confidence limit).

3.2. MATERIALS AND MIXTURES

3.2.1. Phase I: nano-modified concrete cast cured under cyclic freezing/low temperatures

In this phase, general use (GU) Portland cement, and Class F fly ash, meeting the requirements of the CAN/CSA-A3001-13 (Cementitious Materials for Use in Concrete) (CAN/CSA-A3001, 2013), were used as the main components of the binder. In addition, a commercial nano-silica solution with mean particle size of 35 nm, 50% solid content of SiO₂ dispersed in an aqueous solution was incorporated in some binders. The chemical analysis and physical properties of GU cement, fly ash and nano-silica are listed in **Table 3.2**. A high-range water reducing admixture (HRWRA) based on polycarboxylic acid complying with ASTM C494; Standard Specification for Chemical Admixtures for Concrete, (ASTM C494, 2015), Type F, was used to control the consistency of fresh concrete. Variable dosages (0.20 to 1.8 liters per 100 kg binder) of HRWRA was added to the mixtures in order to maintain a slump range of 150 to 200 mm.

In addition, an air-entraining (AE) admixture complying with ASTM C260/C260M; Standard Specification for Air-Entraining Admixtures for Concrete, (ASTM C260, 2016) was used to obtain a fresh air content of 6±1%. Natural gravel (max. size of 9.5 mm) were used as coarse aggregate; its specific gravity and absorption were 2.65 and 2%, respectively. The fine aggregate was well-graded river sand with a specific gravity, absorption and fineness modulus of 2.53, 1.5% and 2.9, respectively. Calcium nitrate (CNA) and combination of calcium nitrate and calcium nitrite (CNI) were used as antifreeze admixtures. The CNA product used in this study comes in solid form with 70% active content soluble in water, while the CNI used was aqueous solution with 30% solid content. These admixtures have proven to achieve efficient performance as anti-freeze and accelerating admixtures [3, 14]. The properties of CNA and CNI are given in **Table 3.3**.

TABLE 3.2 Chemical composition and physical properties of binder components.

Composition/Property	GU Cement	Fly Ash	Nano-silica
<u>Chemical composition</u>			
SiO ₂ (%)	19.21	55.2	99.17
Al ₂ O ₃ (%)	5.01	23.13	0.39
Fe ₂ O ₃ (%)	2.33	3.62	0.02
CaO (%)	63.22	10.81	--
MgO (%)	3.31	1.11	0.21
SO ₃ (%)	3.01	0.22	--
Na ₂ O _{eq.} (%)	0.12	3.21	0.20
<u>Physical properties</u>			
Specific gravity	3.15	2.12	1.40
Mean particle size, μm	13.15	16.56	35 × 10 ⁻³
Fineness, m ² /kg	390 ^a	290 ^a	80,000 ^b

^aBlaine fineness.^bFineness was determined by titration with sodium hydroxide.**TABLE 3.3** Properties of CNA and CNI.

Parameter	CNA	CNI
Density, g/ml	1.86	2.26
Sulfate, %	0.01% max.	--
Chloride, %	0.01% max.	--
Molecular weight, g/mol	236.15	132.09
Solubility in water, g/l	1470 (0°C)	freely soluble in water
pH	5.0 to 9.0	8 to 12

Fifteen concrete mixtures were prepared to investigate the three parameters adopted (**Table 3.4**), which were expected to have significant effects on the properties of concrete: fly ash content, nano-silica dosage, and type of anti-freeze admixture. Each mixture ID starts with a number that stands for the percentage of the subsequent letter and then the type of antifreeze admixture. The letters in the mixture ID are defined as follows: general use cement (GU), fly ash (F), nano-silica (N), level -1 of antifreeze (CNA), level 0 (CNAAI) and level 1 (CNAI).

The total binder (single or blended) content in all mixtures and the *w/b* were kept constant at 400 kg/m³ and 0.32, respectively. This *w/b* was selected to advantageously affect the properties

of concrete similar to the ratios used in high-performance concrete cast and cured under normal temperatures (Neville, 2011; Mindess et al, 2003). Fly ash was used to prepare blended binders with GU cement without or with nano-silica, at dosages of 12.5% and 25% by the total binder content (50 and 100 kg/m³, respectively). The nano-silica was incorporated at dosages of 2% and 4% by the total binder content (solid content of 8 and 16 kg/m³, respectively), as a replacement of the total binder by mass. These dosages of fly ash and nano-silica yielded improved fresh and hardened properties of concrete cast and cured at normal temperatures (Haruehansapong et al, 2014; Ghazy et al, 2016; Said et al, 2012).

TABLE 3.4 Proportions of phase I mixtures per cubic meter.

Mix ID	Coding Notation	Fly Ash (kg)	Nano-Silica (kg)	CNA ^a +CNI (kg)	Cement (kg)	Water ^b (kg)	Fine Aggregate (kg)	Coarse Aggregate (kg)
4N25FCNAI	1, 1, 1	100	32	14+32	284	90	608	1130
4N25FCNA	1, 1, -1	100	32	27+0	284	112	603	1120
4N CNAI	-1, 1, 1	0	32	14+32	384	90	621	1152
4NCNA	-1, 1, -1	0	32	27+0	384	112	616	1143
25FCNAI	1, -1, 1	100	0	14+32	300	106	610	1132
25FCNA	1, -1, -1	100	0	27+0	300	128	605	1123
GUCNAI	-1, -1, 1	0	0	14+32	400	106	622	1156
GUCNA	-1, -1, -1	0	0	27+0	400	128	617	1147
12.5FCNAAI	0, -1, 0	50	0	18+21	350	113	614	1141
4N12.5FCNAAI	0, 1, 0	50	32	18+21	334	97	613	1138
2N25FCNAAI	1, 0, 0	100	16	18+21	292	100	607	1128
2NCNAAI	-1, 0, 0	0	16	18+21	392	105	620	1151
2N12.5FCNAI	0, 0, 1	50	16	14+32	342	98	615	1142
2N12.5FCNA	0, 0, -1	50	16	27+0	342	120	610	1133
2N12.5FCNAAI	0, 0, 0	50	16	18+21	342	105	613	1139

^aThe CNA admixture was in a solid form with 70% active ingredient.

^b Adjusted amount of water considering the water content of nano-silica (aqueous solution with 50% solid content of SiO₂) and the CNI (aqueous solution with 30% solid content).

The dosage of antifreeze admixtures was kept constant at 15% by mass of mixing water.

This concentration had been selected conservatively according to the phase diagrams for these

admixtures, **Figure 3.2**, to depress the freezing point of mixing water down to the target casting temperature (-5°C) and account for temperature uncertainties in the field.

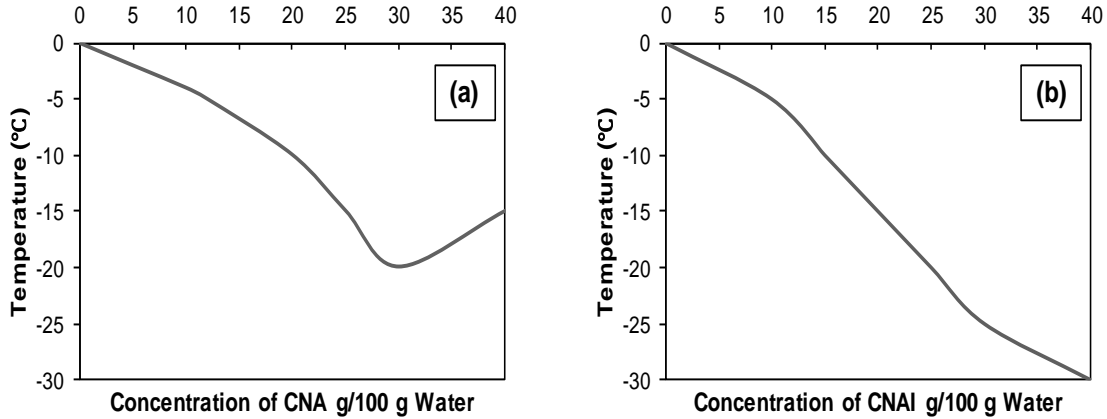


Figure 3.2 Phase diagrams of: (a) calcium nitrate (CNA), and (b) calcium nitrate-nitrite (CNAI).

3.2.2. Phase II. Nano-modified concrete as a repair material under freezing/low temperatures

The materials used in this phase are similar to that used in phase I (refer to section 3.2.1). Optimum mixtures we selected for this phase to evaluate their suitability as repair mixtures. Based on results from Phase I, seven mixtures were prepared to evaluate the suitability of nano-modified concrete mixtures as cold weather repair materials (**Table 3.5**).

TABLE 3.5 Proportions of phase II mixtures per cubic meter.

Mix ID	Fly Ash (kg)	Nano-Silica (kg)	CNA ^a +CNI (kg)	Cement (kg)	Water ^b (kg)	Fine Aggregate (kg)	Coarse Aggregate (kg)
GUCNAI	0	0	14+32	400	106	622	1156
4NCNAI	0	32	14+32	384	90	621	1152
2NCNAI	0	16	14+32	392	98	621	1154
4N15FCNAI	60	32	14+32	324	90	613	1138
2N15FCNAI	60	16	14+32	332	97	614	1140
4N25FCNAI	100	32	14+32	284	90	608	1130
2N25FCNAI	100	16	14+32	292	98	608	1130

^a The CNA admixture was in a solid form with 70% active ingredient.

^b Adjusted amount of water considering the water content of nano-silica (aqueous solution with 50% solid content of SiO₂) and the CNI (aqueous solution with 30% solid content).

Similar to Phase I, These mixtures incorporated fly ash (up to 25%) and nano-silica (up to 4%) with CNAI as CWAS. phase I, the total binder (single or blended) content in all mixtures and the w/b were kept constant at 400 kg/m³ and 0.32, respectively.

3.3. PROCEDURES

In both phases, the mixing and casting operations were done at temperature of $-5\pm 1^{\circ}\text{C}$, and the curing was done under cyclic freezing/low ($5\pm 1^{\circ}\text{C}$) temperatures until testing. These cycles were designed based on the temperature data extracted from the City of Winnipeg weather data for the last 10 years **Figures 3.3 and 3.4**. The data represents weather in late fall (October and November) and early spring (March and April), where approximately 67% of the occurrences yielded an average of -5°C and 33% reached an average of 5°C (Environment and climate change Canada, 2018). Thus, an environmentally controlled chamber was utilized to mimic these cycles. The temperature of the chamber was calibrated before casting at $-5\pm 1^{\circ}\text{C}$ for 16 hours, 0.5 hour for ramping up to $+5\pm 1^{\circ}\text{C}$ for 7 hours and then 0.5 hour for ramping down to $-5\pm 1^{\circ}\text{C}$. To ensure homogeneous air temperature throughout the controlled area and to simulate wind effect, the chamber was equipped with a fan that circulated the air at an average speed of 25 km/h.

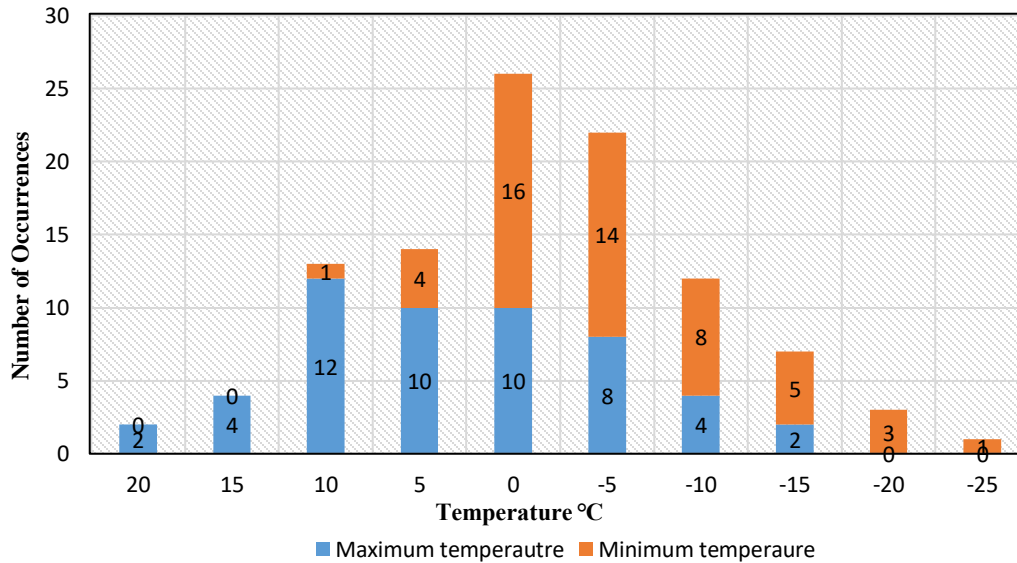


Figure 3.3 Late Fall temperature history for City of Winnipeg (October to November). (Environment and climate change Canada, 2018).

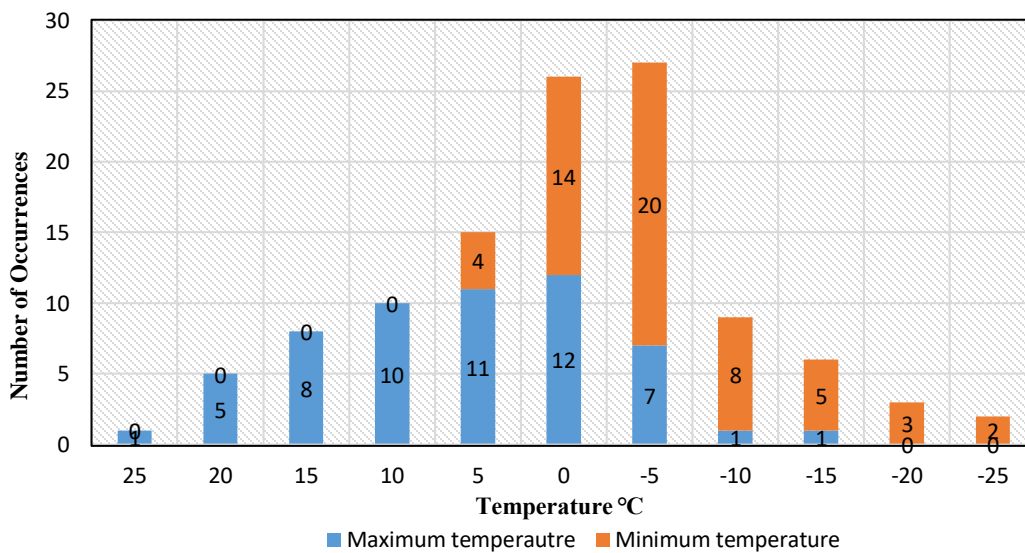


Figure 3.4 Early spring temperature history for City of Winnipeg (March to April). (Environment and climate change Canada, 2018).

To attain homogenous dispersion of components, a specific sequence of mixing was adopted based on trial batches. The nano-silica and the admixtures (AE, HRWRA) were added to two thirds of the mixing water (solution A) while the antifreeze admixtures (CNA and CNI) were added to the remaining one third of the mixing water (solution B) as shown in **Figure 3.5**. First, both solutions A and B were stirred vigorously for 45 seconds until complete dissolution of the

additives. Approximately one half of solution A was added to the aggregate and mixed for 30 seconds. The cement and fly ash were then added to the aggregate and mixed together for 30 seconds. The remaining amount of solution A was then added to the mixture and mixed for another 30 seconds. Finally, solution B was added to the mixture and mixed continuously for 3 minutes. After mixing and casting the concrete, a vibrating table (60 Hz) was used to ensure adequate compaction of specimens. All specimens were demolded after 24 hours and covered with polyethylene sheets for 3 days; subsequently, they were left uncovered in the environmental chamber until testing.

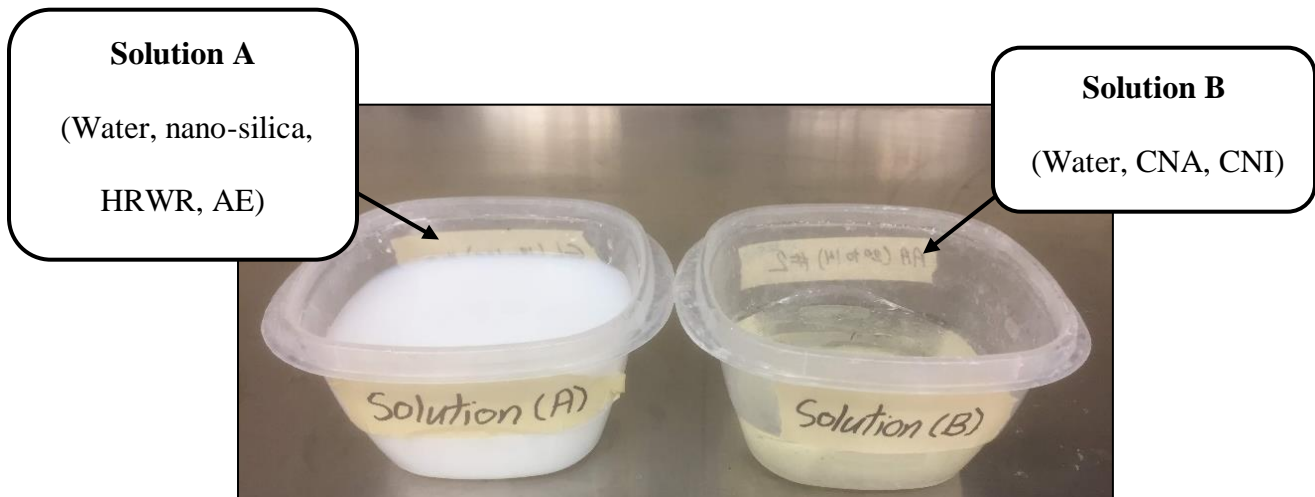


Figure 3.5 Solutions used to prepare mixtures.

3.4. TESTING METHODS

3.4.1. Phase I Testing Methods

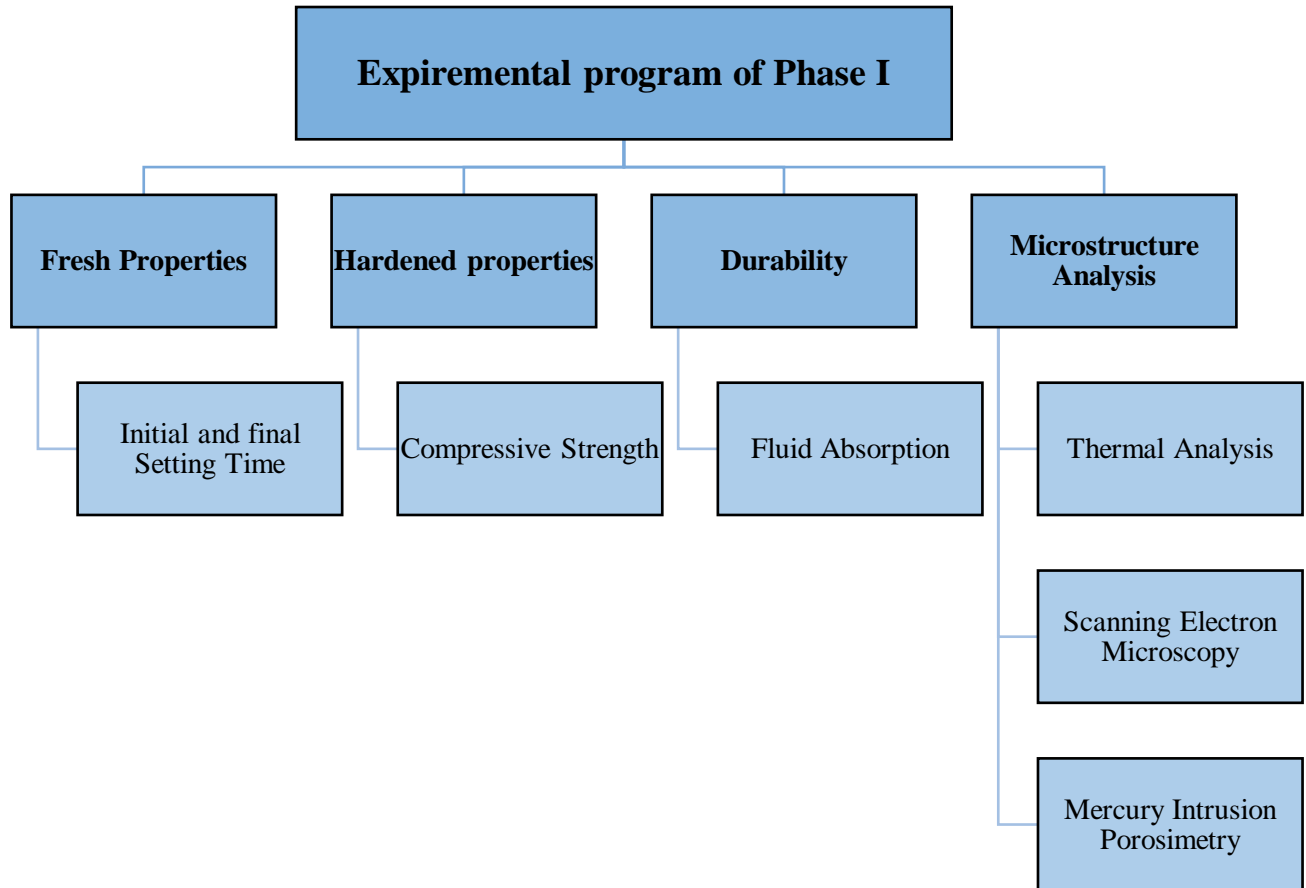


Figure 3.6 Flowchart of phase I experimental program.

The initial and final setting times were characterized based on the penetration resistance of the mortar part of each mixture according to ASTM C403 (ASTM C403, 2016) using ACME penetrometer. Mortar specimens were cast under a temperature of -5°C in molds with lateral dimension of 150 mm and height of 150 mm. Both initial (IST) and final (FST) setting times were using standard penetration needles. The measurement was recorded at different intervals until a pressure of 3.5 and 27.6 MPa representing IST and FST, respectively, is reached.

A total of six needles with bearing area of 645, 323, 161, 65, 32 and 16 mm² were used to measure the setting time. The first reading was recorded by penetrating the largest needle, which provides the lowest penetration resistance. The following readings were progressively measured by smaller needles until final setting time occurs. The loading device as shown in **Figure 3.7** measures the penetration force up to 600 N with an accuracy of ± 10 N. A minimum of eight penetration readings were recorded for each mixture, the penetration of the needles was done at a distance of at least 25 mm. the readings displayed on the ACME Penetrometer gauge represents a load in N, each reading was divided by the bearing area of the used needle to calculate the penetration resistance.



Figure 3.7 ACME penetrometer setting time apparatus.

In addition, triplicates 100×200 mm concrete cylinders were tested for compressive strength according to ASTM C39 (ASTM C39, 2018) at early- (3 days) and later- (28 days) ages. The fluid absorption of concrete was evaluated based on a test protocol developed by Tiznobaik and Bassuoni (Tiznobaik and Bassuoni, 2018) on concrete discs (75×50 mm). After 28 days of curing in the environmental chamber at the stated cyclic temperatures, the concrete discs were placed in an oven at $50\pm 2^{\circ}\text{C}$ and 40% RH until reaching a constant mass. They were then put in a

sealed desiccator under vacuum pressure (~ 85 KPa) for 6 hours. Subsequently, each specimen was freely immersed in 4% calcium chloride (CaCl_2) solution for up to 360 min, and the amounts of absorption were recorded after 1, 5, 10, 20, 40, 80, 160 and 360 minutes to the nearest 0.01 g.

Furthermore, mercury intrusion porosimetry (MIP) was conducted on concrete samples to examine the characteristics of their pore structure after 28 days of curing under the cyclic freezing/low temperatures (**Figure 3.8**). Small chunks with the size of 4–7 mm were extracted from concrete cylinders for the MIP test. Thereafter, they were oven dried at 45°C until reaching a constant mass. This drying method was adopted to avoid decomposition of the hydration products and to reduce the potential of drying shrinkage that leads to development of micro-cracks when exposed to higher temperatures. The surface tension and contact angle of mercury were taken as 485 dynes/cm and 130° , respectively (Tiznobaik and Bassuoni, 2018)

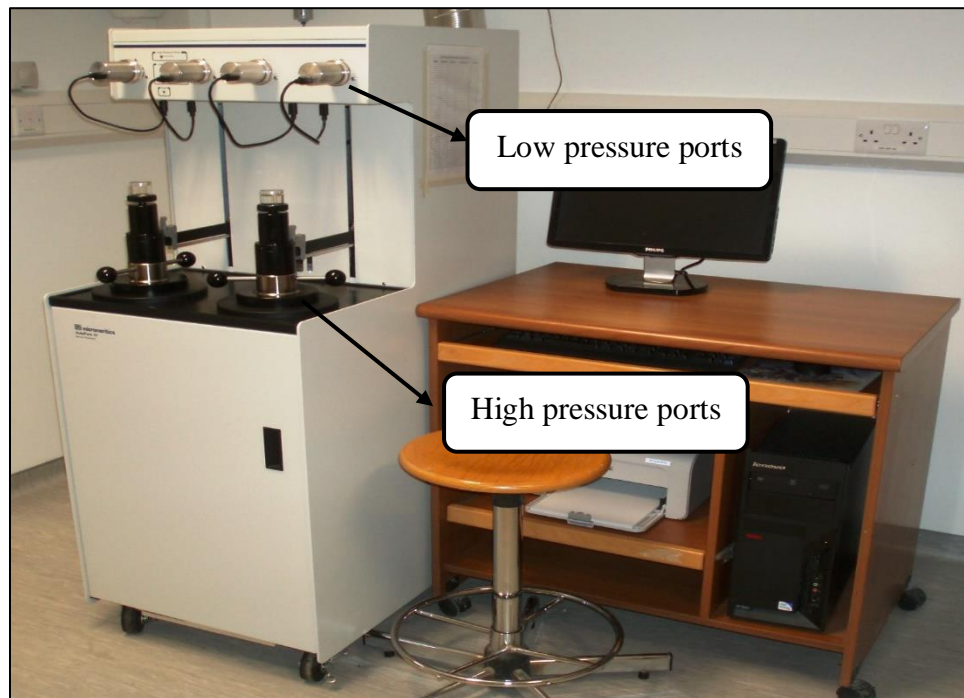


Figure 3.8 Mercury Intrusion Porosimetry (MIP) apparatus.

Upon the completion of the drying period, approximately 3.0 ± 0.1 g of the pre-prepared pea-sized chunks were inserted into a penetrometer that in turn is placed in the low pressure port,

subsequently, into the high pressure port. The apparatus has a pressure that ranges from sub-ambient to 228 MPa. This pressure intrudes all capillary pores in concrete (larger than 5nm). The apparatus produces a number of results, however, for the purposes of this study, Apparent total porosity, threshold pore diameter, and proportion of micro-pores ($< 0.1\mu\text{m}$) are thoroughly discuss.

In addition, thermal analysis and microscopy studies were conducted to corroborate the trends acquired from the bulk tests. Differential scanning calorimetry (DSC) apparatus (**Figure 3.9**) was used for thermal analysis on powder samples which were extracted from the concrete mixtures. The powder was prepared by extracting pieces (excluding coarse aggregate pieces) from the cores of concrete specimens, then ground using a mechanical grinder that produces a fine powder passing through sieve #200 (opening of 75 μm) . Thermogravimetry (TG) was conducted at a constant heating rate of 10°C/min to assess the portlandite content (CH), which was calculated by determining the percentage drop of an ignited mass of the TG curves at a temperature range of 400 to 450°C and multiplying it by 4.11 (ratio of the molecular mass of CH to that of water).



Figure 3.9 Differential Scanning Calorimetry (DSC) apparatus.

Backscattered scanning electron microscopy (BSEM) with elemental dispersive X-ray (EDX) analysis was applied on polished thin sections from different mixtures. Slices were cut out from specimens after 28 days of curing under the aforementioned cyclic freezing/low temperature. The thin sections were then dried and impregnated by a low-viscosity epoxy resin under vacuum pressure and polished by consecutive diamond surface-grinding to a thickness of 30 to 50 μm . A layer of carbon coating was applied on the thin sections to enhance the conductivity for the BSEM analysis.



Figure 3.10 Scanning Electron Microscopy apparatus.

3.4.2. Phase II Testing Methods

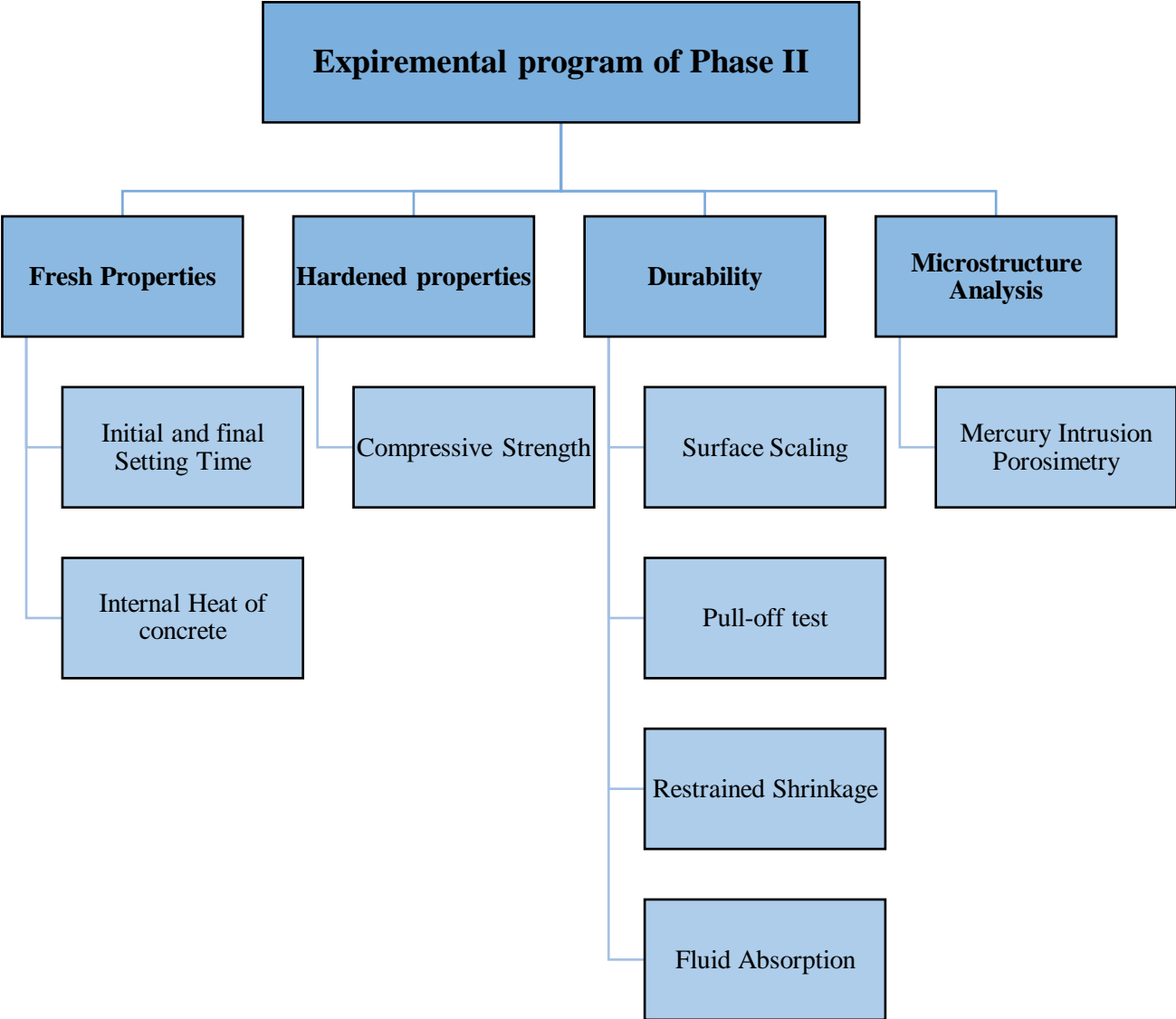


Figure 3.11 Flowchart of phase II experimental program.

The fresh properties in the phase were evaluated by determining the setting time of the mortar fraction (portion passing sieve #4 (4.75 mm)) of each mixture. The test was conducted inside an environmental chamber according to ASTM C403 (ASTM C403, 2016). The hardened properties were assessed by triplicate 100×200 mm concrete cylinders tested for compressive strength according to ASTM C39 (ASTM C39, 2018). In this phase, compressive strength test was conducted on cylinders at 1, 3, 7, 14, 28, 56 and 90 days to evaluate the early-age and long-term effects of fly ash and nano-silica. Moreover, the fluid absorption test was done on 50 mm discs after 28 days of curing under cyclic freezing/low conditions. The details of the setting time, compressive strength and absorption testing procedures are illustrated in previous Section 3.4.1.

Resistance to scaling of a horizontal concrete surface exposed to freezing and thawing cycles in the presence of de-icing chemicals was determined according to ASTM C672 (ASTM C672, 2014). This test is used to evaluate the surface resistance by visual examination and mass loss. The standard specifies a numerical rating from 0 to 5, where 0 represents no scaling and 5 represents severe scaling, as shown in **Figure 3.12**. For each mixture, two concrete slabs with dimensions of 250×250×90 mm were cast and cured for 28 days under the aforementioned cyclic freezing/low temperature. Then, the surface of each specimen was covered with approximately 6 mm of a solution of 4% calcium chloride, a salt that is considered one of the most aggressive de-icing salts. The specimens were exposed to 50 freeze-thaw cycles. Each cycle consists of 16 to 18 h of freezing at $-18\pm 2.0^{\circ}\text{C}$, then 6 to 8 h of thawing at $23\pm 2.0^{\circ}\text{C}$ and a relative humidity of 45 to 55 % under laboratory conditions. At the end of every fifth cycle, solution was flushed off the surface thoroughly and replaced by freshly made solution. Visual examination and mass loss was monitored over the same increments.



Figure 3.12 Visual rating of concrete surface scaling.

Pull-off test was conducted according to CSA A23.2-6B (CSA A23.2 6B, 2014) to evaluate the bond between the repair mixtures and the existing substrate concrete on two exposure conditions. Concrete slabs of 250×250 mm surface area and a depth of 130 mm were used as substrate concrete. The substrate concrete slabs were cast under normal room temperature, cured in curing room with relative humidity of more than 90%, and then left under normal laboratory conditions for approximately one year. The mixture design for the substrate slabs was adopted from a commonly used mixture design that is used for concrete pavements (350 kg/m³ GU cement, 15% type F fly ash, 0.4 *w/b*). The top repair layer, which has a thickness of 70 mm was cast on the top of the substrate concrete and cured under the adopted cyclic freezing/low temperatures (-5 and 5°C) for 28 days. A total of fourteen pull-off concrete slabs were prepared as aforementioned. The slabs were partially cored to a depth of 100 mm (30 mm into the underlying concrete) using a coring disk with a 50 mm diameter at distance of 50 mm from the edge of the slab as shown in **Figure 3.13**. The surface of each slab was smoothed and flattened using a grinder to clear any impurities in the surface and to avoid any loading eccentricity that might compromise the results. Metal fastening devices were mounted to center of the cored disks using adhesive epoxy and were

left to cure for approximately 48 hours to reach sufficient strength. The device shown in **Figure 3.13** was used to apply a tensile load at a rate of 50 ± 20 N/s with extra attention paid to the perpendicularity of loading device to axis of the fastening device until failure occurs.

The slabs were divided into two groups; the first group consisted of 7 slabs (one slab representing each mixture) that were tested after 28 days of curing inside the chamber under cyclic freezing/low temperatures (-5 and 5°C). The second group consisted of 7 slabs (one slab representing each mixture) was evaluated after consecutive Freezing/Thawing (F/T) and Wetting/Drying (W/D) following the 28 days of curing under adopted cyclic freezing/low temperatures. A total of 50 F/T according to ASTM C672 (ASTM C672, 2014) followed by 50 W/D cycles in presence of water were applied. Each W/D cycle consisted of 16 hours at a temperature of $22\pm 2^{\circ}\text{C}$ followed by drying at $40\pm 2^{\circ}\text{C}$ and $40\pm 5\%$ RH. This customized exposure regime mimics the climate conditions of alternating winter and summer seasons, which correlates the in-service conditions.

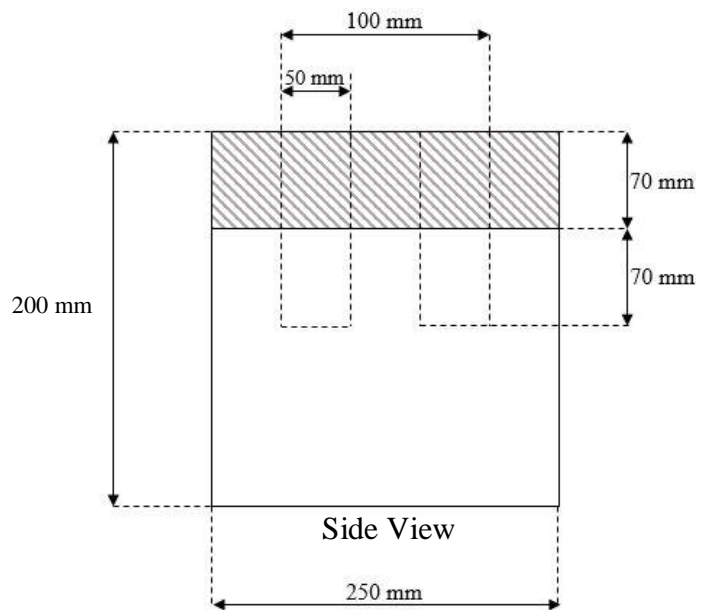


Figure 3.13 Pull-off test configuration.

The restrained Shrinkage test was performed in accordance with (Ghazy et al, 2017) to evaluate the compatibility between the selected cold weather mixture (**Table 3.5**) and the existing substrate concrete. This test focuses on evaluating and understanding the shrinkage behavior of nano-modified and nano-modified fly ash cold weather repair mixtures. It is vital to understand the shrinkage behavior of nanoparticle due to their rapid rate of hydration and pozzolanic reactions especially at early age, even when cast and cured under low temperatures. Differential shrinkage rates between the substrate concrete and the new repair material may create stresses that lead to extensive cracking and ultimately compromises the durability of concrete.

Repair materials in concrete pavements are restrained by the substrate concrete either at the interface and/or the edges in the case of confined patches. This configuration promotes multiple cracks both at the surface and at the restraint end of concrete (Ghazy et al, 2017). In this study, fourteen concrete slabs with surface area of 250×250 mm and a depth of 130 mm were cast in normal laboratory conditions using a typical mixture design used for concrete pavements (350 kg/m³ GU cement, 15% type F fly ash, 0.4 *w/b*). The slabs were demolded one day after casted, cured in a curing room for 7 days and then kept under normal laboratory conditions (23±2°C and 55±5 % RH). After approximately one year, the top surface of substrate concrete was roughened with a saw and then was wire brushed and dust cleared to minimize any impurities.

The slabs were moved to an environmental chamber under the adopted cyclic freezing/low temperatures (-5 and 5°C). The surface of the substrate slabs was slightly wetted with water solution containing 10% CNAI to avoid ice formation at the interface layer. Simultaneously, the investigated repair mixtures cast under the same regime (-5°C) and immediately placed on the top surface with a thickness of 70 m. the slabs were demolded after 24 hours, then six pairs of Demec points were attached to the surface and sides of each slab at a distance of 200 mm as shown in

Figure 3.14. The slabs were covered with polyethylene sheets for three days to simulate field conditions, then left to cure inside the environmental chamber. The early-age shrinkage was evaluated during the first 28 days while inside the chamber every 5 days by recording the length change between each pair of the Demec points using dial gauge extensometer. Subsequently, the slabs were exposed to hot-dry conditions ($40\pm 2^{\circ}\text{C}$ and $35\pm 5\%$ RH) for another 28 days and the length change was recorded in a similar manner.

The fluid absorption, thermal analysis and MIP were also conducted as previously explained in section (3.4.1).

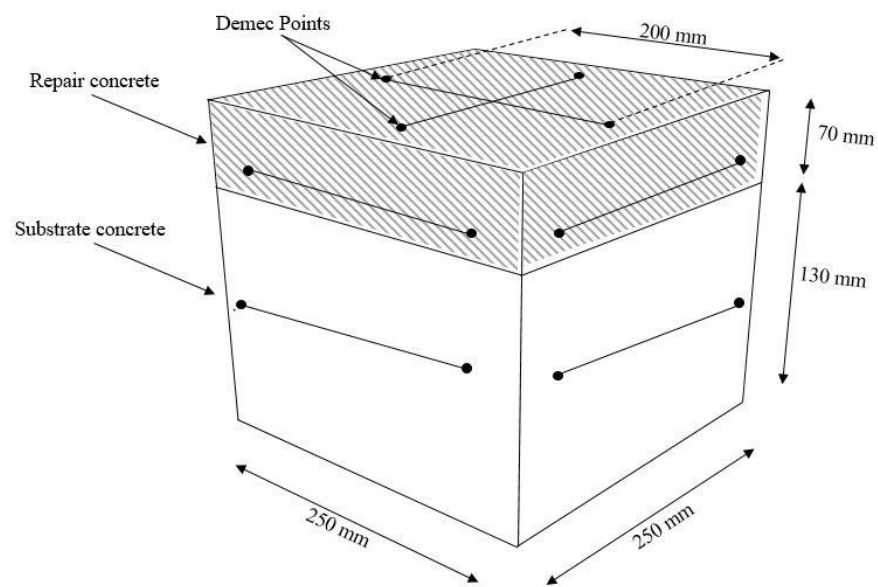


Figure 3.14 Shrinkage test specimen configuration.

4. Results and Discussion of Phase I

4.1. DERIVED STATISTICAL MODELS

The experimental results of five responses that represent fresh (initial and final setting times), hardened (compressive strength at 3 and 28 days), and durability (fluid absorption) properties are summarized in **Table 4.1**. Statistical models were derived to evaluate the three independent variables (fly ash, nano-silica, antifreeze admixture) at three levels (high, medium and low). The general model is expressed by:

$$y = \alpha_0 + \sum \alpha_i X_i + \sum \alpha_{ij} X_i X_j + \sum \alpha_{ii} X_i^2 + \epsilon \quad (1)$$

where, y is the response, X_i is the independent variable, α_0 is a constant (intercept), while α_i ($i = 1, 2, 3$), α_{ij} ($i = 1, 2, 3; j = 2, 3; j > i$) and α_{ii} ($i = 1, 2, 3$) represents the linear, interaction, and quadratic regression coefficients of each variable, respectively and ϵ is the random error term representing the effects of uncontrolled variables.

Models' coefficients were determined using multi-linear regression analysis with an assumption that the data are normally distributed. Moreover, Analysis of Variance (ANOVA) was used to test the different factors and their interactions to identify insignificant variables and secondary interactions, which were subsequently eliminated from the derived modeling equations. The probability value (*P-value*), which determines the statistical significance of each term in the models was limited to 5%; thus, there is less than 5% chance (or 95% confidence limit) that a tested response exceeds the value of the specified coefficient. Large *P-values* (>0.05) is an indication that the term is insignificant, and thus it did not have an effect on the measured response.

TABLE 4.1 Average results from the bulk tests.

Mix ID	Model Code	Initial Setting Time (min)	Final Setting Time (min)	f'_c 3d (MPa)	f'_c 28d (MPa)	Absorption (%)
4N25FCNAI	1, 1, 1	60	335	16.0	33.3	2.9%
4N25FCNA	1, 1, -1	145	570	14.8	34.8	3.2%
4NCNAI	-1, 1, 1	30	220	24.4	50.2	2.0%
4NCNA	-1, 1, -1	100	290	21.2	49.9	2.4%
25F CNAI	1, -1, 1	80	430	13.0	24.1	3.2%
25FCNA	1, -1, -1	240	930	11.7	25.2	3.8%
GUCNAI	-1, -1, 1	35	275	19.9	42.4	2.3%
GUCNA	-1, -1, -1	130	500	17.1	39.9	3.2%
12.5FCNAAI	0, -1, 0	110	500	14.8	34.9	2.7%
4N12.5FCNAAI	0, 1, 0	65	375	22.6	41.6	2.5%
2N25FCNAAI	1, 0, 0	90	460	17.5	33.8	2.8%
2NCNAAI	-1, 0, 0	65	315	26.9	48.4	2.2%
2N12.5FCNAI	0, 0, 1	65	310	22.8	41.3	2.5%
2N12.5FCNA	0, 0, -1	125	615	19.2	37.7	2.7%
2N12.5FCNAAI	0, 0, 0	85	415	21.4	41.9	2.6%

The coefficients of determination (R^2) of all the derived statistical models were $\geq 94\%$ with the experimental results, and the statistical software (Design Expert, 2018) validated the assumption that the residual terms are normally distributed. This indicates a high confidence level in the models. The results of the models as well as their correlation coefficients and the relative significance of variables according to ANOVA are listed in **Table 4.2**. The best fit responses of the models for initial and final setting times, 3 and 28 days compressive strengths and absorption are given in **Eqs (2)-(6)**.

$$\text{Log}_{10}[\text{IST}](\text{min}) = 0.12 * F - 0.08 * N - 0.22 * A + 1.92 \quad (R^2 = 0.94) \quad (2)$$

$$\text{Log}_{10}[\text{FST}](\text{min}) = 0.11 * F - 0.08 * N - 0.12 * A + 0.03 * NA + 2.61 \quad (R^2 = 0.97) \quad (3)$$

$$\frac{1}{(f'_c 3d)} (MPa) = 0.01 * F - 0.008 * N - 0.004 * A + 0.01 * N^2 + 0.05 \quad (R^2 = 0.98) \quad (4)$$

$$f'_c 28d (MPa) = -7.96 * F + 4.33 * N - 2.54 * N^2 + 40.99 \quad (R^2 = 0.97) \quad (5)$$

$$Absorption (\%) = 0.38 * F - 0.22 * N - 0.23 * A + 2.54 \quad (R^2 = 0.95) \quad (6)$$

Where, F , N and A represent fly ash, nano-silica and antifreeze (CNA:CNI), respectively. These equations are in terms of coded factors and can be used to make predictions for a response at given levels of each factor. Each coefficient indicates an expected change in a response per unit change in the factor value. Coded equations are useful for identifying the relative impact of the factors by comparing factors coefficients. The validity of the models is bounded by the high level factor (+1) and the low level factor (-1).

TABLE 4.2 Derived coefficients for the models and their significance based on ANOVA.

Multiplied by	Log(IST)	log(FST)	$1/f'_c 3d$	$f'_c 28d$	Absorption
F	0.12	0.11	0.012	-7.96	0.38
N	-0.08	-0.08	-0.008	4.33	-0.22
A	-0.22	-0.12	-0.004	0.39	-0.23
FN	-	0.002	-0.001	0.12	0.02
NA	-	0.03	0.001	-0.33	0.07
FA	-	-0.02	0.000	-0.67	0.05
F^2	-	-	0.002	0.29	0.03
N^2	-	-	0.011	-2.54	0.16
A^2	-	-	0.003	-1.31	0.16
Constant	1.920	2.61	0.046	40.99	2.54
R^2	0.94	0.97	0.98	0.97	0.95

Note: bold factors and interactions are significant.

4.2. SETTING TIME

The experimental results of the initial setting time (IST) and final setting time (FST) widely varied between 0.5 to 3.95 h and 3.7 to 15.5 h, respectively. Thus, the hardening process of all mixtures took place during the first freezing time interval at -5°C . The corresponding statistical models

presented by **Eqs. 2 and 3** indicated that the IST and FST were significantly influenced by the fly ash content and antifreeze admixtures. The antifreeze admixture had a dominant effect on the IST relative to the fly ash content (-0.22 vs. 0.12). However, the effect of the antifreeze admixtures and fly ash content was comparable in the case of FST. The nano-silica content had a significant effect on the IST and FST models, but its coefficients were less than that of the fly ash content and antifreeze admixtures.

The isoresponse curves, generated from the derived models in **Eqs. 2 and 3**, graphically show these trends. For instance, **Figs. 4.1 and 4.2** show that the IST and FST were extended with increasing the fly ash dosage, whereas they were shortened with increasing the nano-silica dosage, irrespective of the type of antifreeze admixture. Also, at any fixed fly ash and nano-silica contents, the IST and FST were markedly shortened with the use of a mixed CWAS such as CNAI, as depicted by **Figs. 4.1 (b) and 3(b)** in comparison to **Figs.4.2 (a) and 3(a)**. This can be ascribed to the incorporation of CNI, which acts as a stronger accelerator compared to CNA (Ratinov et al, 1996), thus speeding the setting process of concrete under the freezing/low temperature.

The effect of high dosages of fly ash in delaying the setting time of concrete cast and cured at normal temperatures is well-documented in the literature (Neville, 2011; Wesche, 2014). In this study, increasing the fly ash content up to 25% markedly prolonged the setting time under the freezing temperature, even with the incorporation of CWAS, especially in the case of CNA alone. For example, incorporating 25% fly ash in mixture GUCNA to produce mixture 25FCNA resulted in 85% (4 h) and 86% (15.5 h) increase of IST and FST, respectively. This can be attributed to the dilution of cement with less reactive SCM, resulting in slowing down the kinetics of the hydration and hardening processes. While the incorporation of fly ash in concrete is not recommended for cold weather applications (ACI 306R, 2016; CW3310, 2015), it is needed to produce concrete with

improved long-term performance/durability. Thus, such early-age technical limitations should be mitigated.

Nano-silica decreased the setting time of nano-modified and nano-modified fly ash mixtures. For the GU mixtures (single binders), the decrease for the nano-modified mixtures ranged between 5 to 30 min and 55 to 210 min for IST and FST, respectively. Compared to the fly ash mixtures (blended binders), the nano-modified fly ash mixtures showed more pronounced reductions in the IST and FST, which ranged between 20 to 95 min and 95 to 360 min, respectively. This alluded to synergistic effects of nano-silica and fly ash on accelerating the reactivity of produced mixture, as will be discussed in the TG section. For instance, adding 4% nano-silica to mixture 25FCNA to produce mixture 4N25FCNA resulted in decreasing the IST and FST by 40% (2.4 h) and 39% (9.5 h), respectively.

Indeed, the setting times of all nano-modified and nano-modified fly ash mixtures were further shortened with the incorporation of mixed CWAS (e.g. CNAI), suggesting efficient placement and finishing operations in cold weather within a reasonable time frame (4 to 8 h). Previous studies (Haruehansapong et al, 2014; Ghazy et al, 2016; Senff et al 2009) reported the ability of nano-silica to accelerate the hydration process of cementitious binders at early-age under normal temperatures. In this study, the functionality of nano-silica was still maintained under the freezing/low temperature. The high surface area of nano-silica (80,000 m²/g) might act as nucleation sites for the hydration products to precipitate, which led to faster dissolution of calcium silicate phases (C₃S and C₂S) and in turn increasing the production of calcium hydroxide (CH). These trends are highlighted in the thermal analysis section.

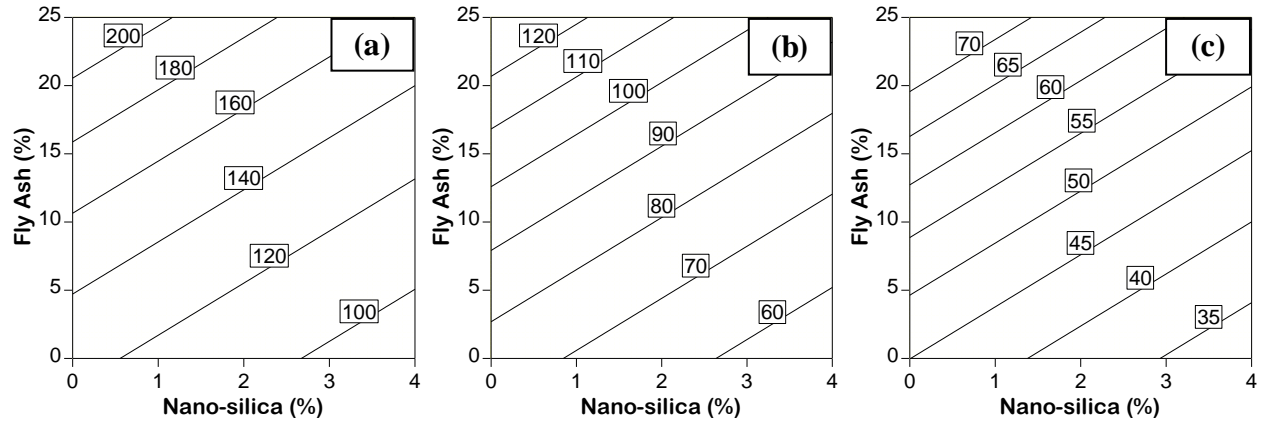


Figure 4.1 Isoresponse curves of IST (min): (a) CNA, (b) CNAAI, and (c) CNAI.

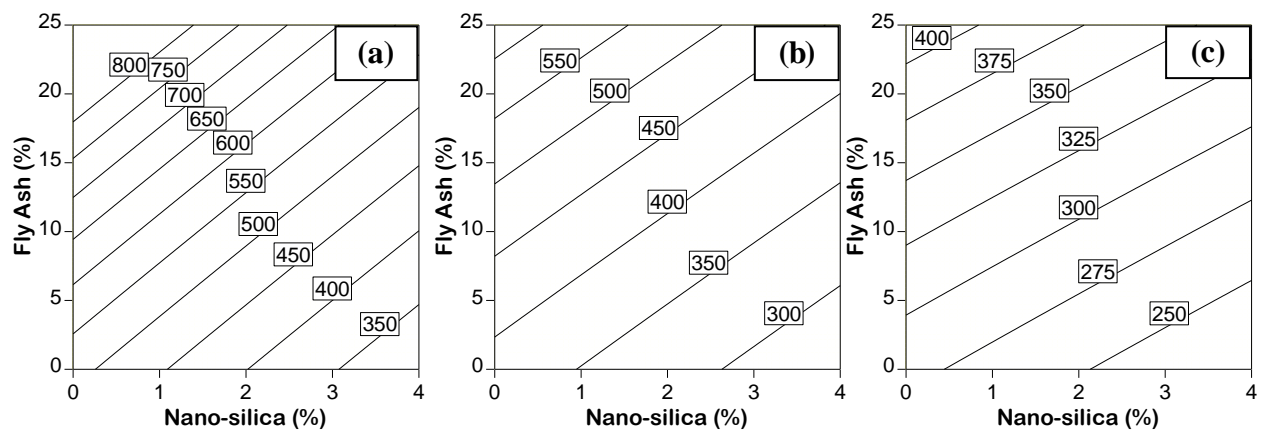


Figure 4.2 Isoresponse curves of FST (min): (a) CNA, (b) CNAAI, and (c) CNAI.

4.3. COMPRESSIVE STRENGTH

The experimental results of compressive strengths at 3 and 28 days varied from 11.7 to 26.9 MPa and 24.1 to 50.2 MPa, respectively. Generally, mixtures with blended binders incorporating high dosages of fly ash (25%) showed lower compressive strength, while nano-modified mixtures showed higher compressive strengths. These trends were depicted by the contour plots shown in **Figs. 4.3 and 4.4**. **Equation 4** indicates that the 3 day compressive strength was affected by the fly ash content, nano-silica content and antifreeze admixtures ratio. The fly ash content had the most significant effect (0.012) on the 3 days compressive strength when compared to nano-silica and antifreeze admixtures which had coefficients of -0.008 and -0.004, respectively. Similarly, the

28 days compressive strength was significantly influenced by the fly ash content followed by nano-silica content (-7.96 vs. 4.33) as shown by **Eq. 5**. However, in contrast to the 3 day compressive strength, the effect of the antifreeze admixtures was insignificant on the 28 compressive strength (**Table 4.2**). This indicates that the type of antifreeze was important in accelerating the hardening process (setting time) and strength development of concrete at early-age. Subsequently, the development of strength of concrete curing under the cyclic freezing/low temperatures up to 28 days was governed by the reactivity of fly ash and nano-silica, irrespective of the type of antifreeze admixtures.

Increasing the fly ash content up to 25% resulted in decreasing the compressive strength at a constant nano-silica dosage. For instance, incorporating 25% fly ash in mixture GUCNA to produce mixture 25FCNA led to 32% (11.7 MPa) and 37% (25.2 MPa) reduction of compressive strength at 3 and 28 days, respectively. The incorporation of high dosages of fly ash in cold weather concrete mixtures is not recommended by ACI 306R (ACI 306R, 2016). Slowly reactive SCMs such as fly ash and slag delay the strength development of concrete at early-age; thus, they may prevent concrete from developing adequate resistance to cold weather conditions such as freezing and thawing, especially at early-age. However, adequate dosages of fly ash in concrete is needed to achieve long-term durability. At 28 days, all the mixtures tested in this study achieved compressive strength higher than 24.5 MPa, which is required by ACI 306R (ACI 306R, 2016) for concrete to resist multiple cycles of freezing and thawing, even with the replacement of GU cement with 25% fly ash. It seems that the developed mixture designs herein with low w/b of 0.32, binder content of 400 kg/m³ and incorporation of 15% antifreeze admixtures were efficient at maintaining adequate levels of hydration and strength development under these freezing/low temperatures curing conditions.

Generally, the incorporation of nano-silica to produce nano-modified and nano-modified fly ash concrete mixtures significantly improved strength values. For the GU mixtures (single binders), the increase for nano-modified mixtures was approximately 4.5 and 9 MPa at 3 days and 28 days compressive strength, respectively. Nano-modified mixtures with GU cement showed the highest compressive strength. For instance, mixture 4NCNAI had 24.4 and 50.2 MPa compressive strength at 3 and 28 days, respectively. Compared to the fly ash mixtures (blended binders), the nano-modified fly ash mixtures showed increase in the 3 and 28 days compressive strengths, which was approximately 3 and 9.5 MPa, respectively. For instance, adding 4% nano-silica to mixture 25FCNAI to produce mixture 4N25FCNAI resulted in increasing the 3 and 28 days compressive strengths by 27% (16 MPa) and 38% (33.3 MPa), respectively. This role was captured in **Eqs. 4 and 5** by the appearance of two terms for the nano-silica content (non-squared and squared).

The effect of nano-silica on enhancing the compressive strength of concrete at normal temperatures has been reported in previous studies (Haruehansapong et al, 2014; Ghazy et al, 2016). It was reported that nano-silica has various effects on hardened properties of concrete through enhancing hydration reactions, pozzolanic and filler effects and reducing the apparent w/b in cementitious systems by absorbing water into its ultrafine surface (Haruehansapong et al, 2014; Ghazy et al, 2016; Senff et al 2009). Complying with the fresh properties behavior of nano-modified mixtures, the results herein indicated that nano-silica maintained its functionality under the freezing/low temperatures with the coexistence of antifreeze systems. Nano-silica led to fast rate of strength gain, high degree of hydration and dense matrix as will be discussed in the MIP, thermal and microscopy sections. The compressive strength values (30 to 50 MPa) of nano-modified concrete mixtures, cast and cured under cyclic freezing/low temperatures, qualify them

for various infrastructural applications, including concrete pavements and bridges (MacGregor et al, 1997).

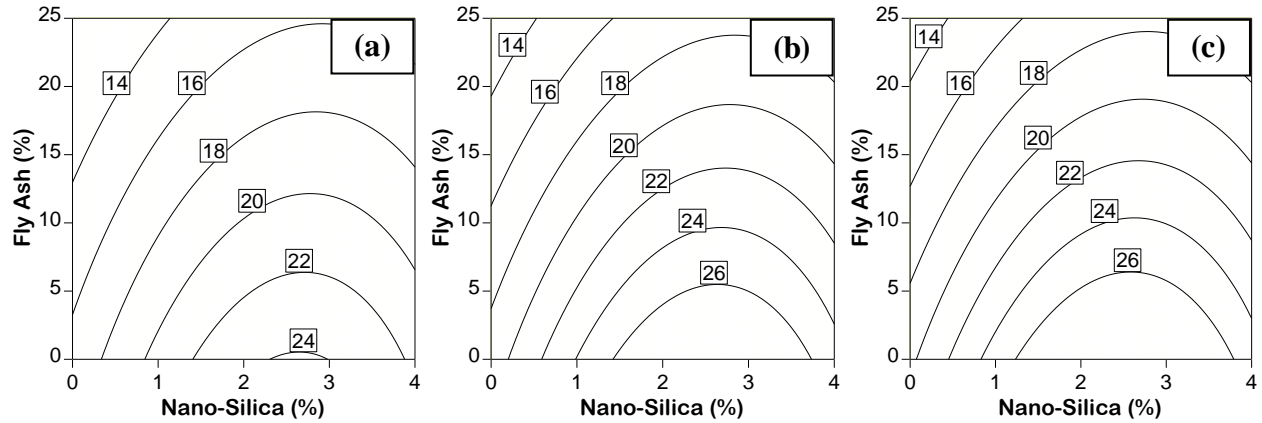


Figure 4.3 Isoresponse curves of 3-day compressive strength (MPa): (a) CNA, (b) CNAAI, and (c) CNAI.

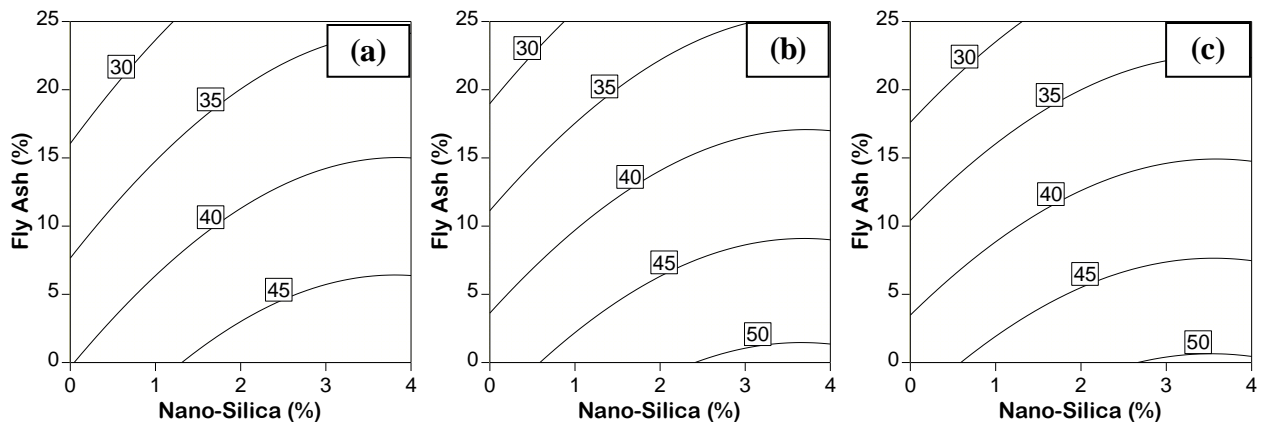


Figure 4.4 Isoresponse curves of 28-day compressive strength (MPa): (a) CNA, (b) CNAAI, and (c) CNAI.

4.4. FLUID ABSORPTION

Penetrability of the different concrete mixtures was assessed based on a fluid absorption test results after 28 days of curing under the adopted curing regime. The results ranged from 2.0 to 3.8% (Table 4.1). The derived model, represented by Eq. 6, indicates that the fly ash and nano-silica contents as well as antifreeze admixtures are all significant factors controlling the mass transport properties. The fly ash content had a predominant effect on absorption with a coefficient of 0.38,

followed by nano-silica content and antifreeze admixtures which had comparable coefficients of 0.22 and -0.23.

Complying with the compressive strength results, the absorption of concrete yielded marked accretion (up to 3.8%) with increasing the fly ash dosage, when holding other variables constant. This trend is depicted in the isoresponse curves in **Fig. 4.5**. For instance, incorporating 25% fly ash in mixture GUCNAI to produce mixture 25FCNAI led to increasing the fluid absorption by 28% (3.2%). As previously discussed, this can be ascribed to the dilution of cement with a slower reactivity SCM which deaccelerated the kinetics of the hydration processes, subsequently less degree of hydration was reached at the time of testing, especially under the curing regime adopted. Thus, the microstructure produced comprised higher proportion of accessible capillary pores, as will be discussed in the subsequent section, which facilitated fluid penetration.

Contrary to the effect of fly ash, the increase of nano-silica and CNI dosages had a positive effect on reducing the amount of fluid absorbed by concrete. For the nano-modified mixtures (single binders), the fluid absorption ranged from 2.0 to 2.4%, whereas the nano-modified fly ash mixtures (blended binders) had absorption values which ranged from 2.5 to 3.2%. For instance, the incorporation of 4% nano-silica in mixtures GUCNA and 25FCNA to produce mixtures 4NCNA and 4N25FCNA resulted in decreasing the absorption by 25% and 16%, respectively.

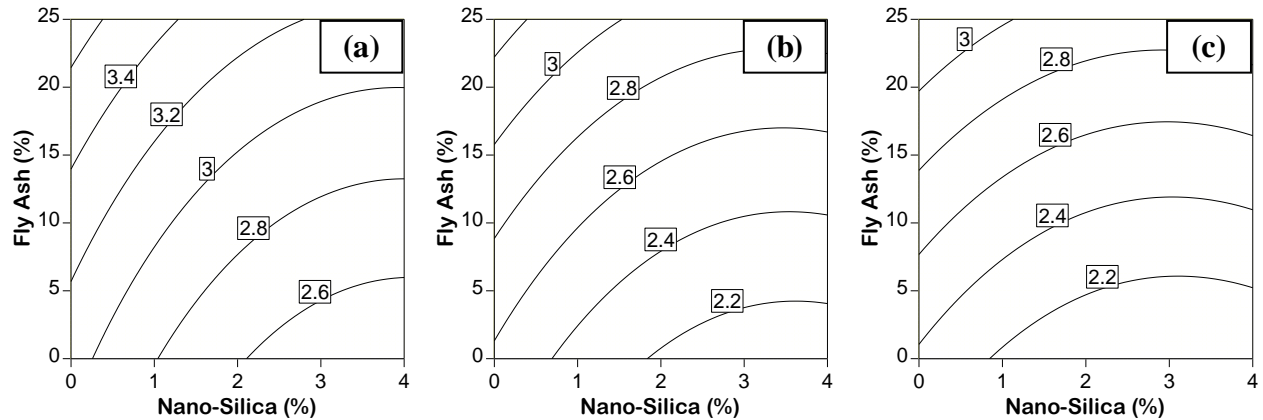


Figure 4.5 Isoresponse curves of fluid absorption (%): (a) CNA, (b) CNAAI, and (c) CNAI.

The synergistic effect of nano-silica and fly ash on the development of concrete microstructure, which was cast and cured at normal temperatures has been reported in the literature (Ghazy et al, 2016). In this study, the effect of nano-silica on improving the resistance of concrete to infiltration of fluids was still maintained under the cold curing regime (-5 and 5°C). This can be attributed to the previously discussed physical and chemical actions of nano-silica, which significantly densified the microstructure of concrete. In addition, further reduction of absorption was achieved with the inclusion of mixed CWAS. **Figures 4.5 (a)-(c)** indicate adding CNAAI and CNAI to concrete led to lower absorption in comparison to CNA. This can be attributed to the incorporation of CNI that sped up the hydration process of concrete, as shown earlier by the setting times trends and substantiated later in the microstructural analysis sections.

4.5. MERCURY INTRUSION POROSIMETRY (MIP)

After 28 days, the MIP test was performed on specimens extracted from eight mixtures (the factorial component of the model), which were selected to capture the effect of the variables tested on the concrete pore structure and corroborate the trends obtained from the bulk tests. The MIP results are listed in **Table 4.3**.

TABLE 4.3 Summary of MIP test results.

Mixture ID	Apparent Total Porosity (%)	Threshold Pore Diameter (μm)	Proportion of Micro-pores [$<0.1 \mu\text{m}$] (%)
GUCNA	15.6	0.5	51
25FCNA	18.6	0.80	45
4NCNA	14.8	0.16	61
4N25FCNA	16.1	0.35	50
GUCNAI	14.2	0.25	59
25FCNAI	17.9	0.75	48
4NCNAI	12.1	0.07	68
4N25FCNAI	15.4	0.25	55

Generally, the MIP trends complied with that of the macro-scale tests. The use of mixed antifreeze admixtures improved the microstructural features of concrete. For instance, mixture GUCNAI had 9% and 50% lower porosity and threshold pore diameter, respectively as well as 16% higher proportions of micro-pores compared to that of mixture GUCNA. The increase in the CNI (strong accelerator) dosage in the CNAI system led to improving the degree of hydration of the cement paste under this cold curing regime, and consequently enhanced the pore structure of the different concrete mixtures. This explains the relatively lower fluid absorption values of mixtures incorporating CNAI [Figure 4.5(c)], relative to corresponding mixtures comprising CNA and CNAAI [Figures 4.5 (a)-(b)].

Generally, mixtures incorporating fly ash showed higher porosity and threshold pore diameter as well as lower proportions of micro-pores. For instance, mixture 25FCNAI showed 26% and 200% higher total porosity and threshold pore diameter, respectively as well as 19% increase in the proportion of macro-pores compared with mixture GUCNAI. The coarser pore structure of mixtures incorporating fly ash explains the reduction in strength and increase in fluid absorption of concrete. Accordingly, mixtures 25FCNAI and 25FCNA, comprising 25% fly ash,

had the highest porosity, lowest compressive strength (at 3 and 28 days) and highest absorption among all mixtures.

The MIP results of nano-modified and nano-modified fly ash mixtures substantiated the positive effects of nano-silica on densifying the pore structure of concrete mixtures cast and cured under freezing/low temperature cycles. For instance, incorporating 4% nano-silica in mixture GUCNAI to produce mixture 4NCNAI decreased the porosity and threshold pore diameter by 15% and 72%, respectively as well as increasing the proportion of micro-pores by 15%. Similarly, addition of nano-silica refined the coarse microstructure of fly ash mixtures. For example, adding 4% nano-silica to mixture 25FCNAI to produce mixture 4N25FCNAI resulted in decreasing the porosity by 14% and threshold pore diameter by 67%; correspondingly, the proportion of micro-pores increased by 15%. These trends implicated the increased resistance to saturation of nano-modified mixtures due to their refined pore structure, which corresponds to their relatively lower absorption and improved compressive strength.

4.6. THERMAL ANALYSIS

The portlandite production and consumption in eight concrete mixtures (factorial component), which were cured under the adopted curing regime, were determined using TG at different ages: 12 h and 1, 3, 7, 14, 28, 56 and 120 days (**Figs. 4.6 and 4.7**). As depicted in **Fig. 4.6**, the CH content in the factorial mixtures at very early-age (12 hr), complied with the setting time results. Generally, the mixtures with high dosages of fly ash (25FCNA and 25FCNAI) produced the smallest amounts of CH due to the dilution of cement component and slow reactivity of fly ash at early-age (Neville, 2011; Wesche, 2014), which led to decelerating the hydration and hardening rates of these mixtures, especially at this freezing temperature (-5°C) during the first 16 h. Comparatively, the incorporation of nano-silica in concrete led to producing higher CH contents

at early-age compared with counterpart mixtures without nano-silica. For instance, at 1 and 3 days, the normalized CH contents of the nano-silica mixtures relative to their corresponding mixtures without nano-silica ranged from 1.9 to 2.1 and 1.17 to 1.27, respectively, which conformed to the noticeable improvement in early-age hardening rate and compressive strength of the nano-modified mixtures (**Table 4.1**). This substantiated the role of nano-silica in accelerating the kinetics of hydration reactions with the coexistence CWAS, under freezing/low temperatures, through its nucleation effect by creating additional nucleation sites for the precipitation of hydration products at early-age (Ghazy et al, 2016; Senff et al, 2009). Complying with the setting time results, the incorporation of CNAI produced higher amounts of CH in the mixtures compared to CNA which explains the relatively faster hardening and reactivity rates of CNAI mixtures compared with corresponding mixtures incorporating CNA. This can be ascribed to the relatively stronger accelerating effect of CNI on speeding up hydration of cement.

At later ages (**Fig. 4.7**), the previously described trends continued in the case of mixtures without nano-silica up to 120 days under the adopted curing regime. Conforming to the strength results, the CH contents in these mixtures steadily increased at different rates depending on the type of binder and CWAS. After 56 days, a slight reduction in CH content was observed in the fly ash mixtures without nano-silica which alluded to very slow and delayed pozzolanic reactivity because of the freezing/low temperatures; typically, concrete comprising fly ash show the commencement of pozzolanic reactivity after 28 at normal curing temperatures (Neville, 2011; Wesche, 2014). Comparatively, after 7 days, all the nano-modified concrete mixtures showed consumption of the CH contents up to 120 days, which was indicated by the significant decrease in the normalized CH contents (**Fig. 4.7**). For example, the average normalized CH contents in mixture 4NCNA relative to mixture GUCNA at 28 and 120 days were 0.63 and 0.41, respectively.

These trends can be attributed to the pozzolanic effect of nano-silica by reacting with CH to produce secondary C-S-H gel, which was reported to have high stiffness (Ghazy et al, 2016; Said et al, 2012; Senff et al 2009), and thus densifying the pore structure of concrete. This explains the superior performance of nano-modified concrete mixtures in terms of higher strength and lower absorption capacity. The latent behavior of nano-silica was also reported in the previous study at the University of Manitoba, which showed that the pozzolanic effect of nano-silica commenced after 28 days in masonry mortar that were cast and cured at +5°C, but without CWAS (Kazempour et al, 2016; Kazempour et al 2014). Under normal conditions, nano-silica starts its pozzolanic activity in cementitious systems within 1 to 3 days depending on the other binder components (Ghazy et al, 2016; Hou et al, 2013).

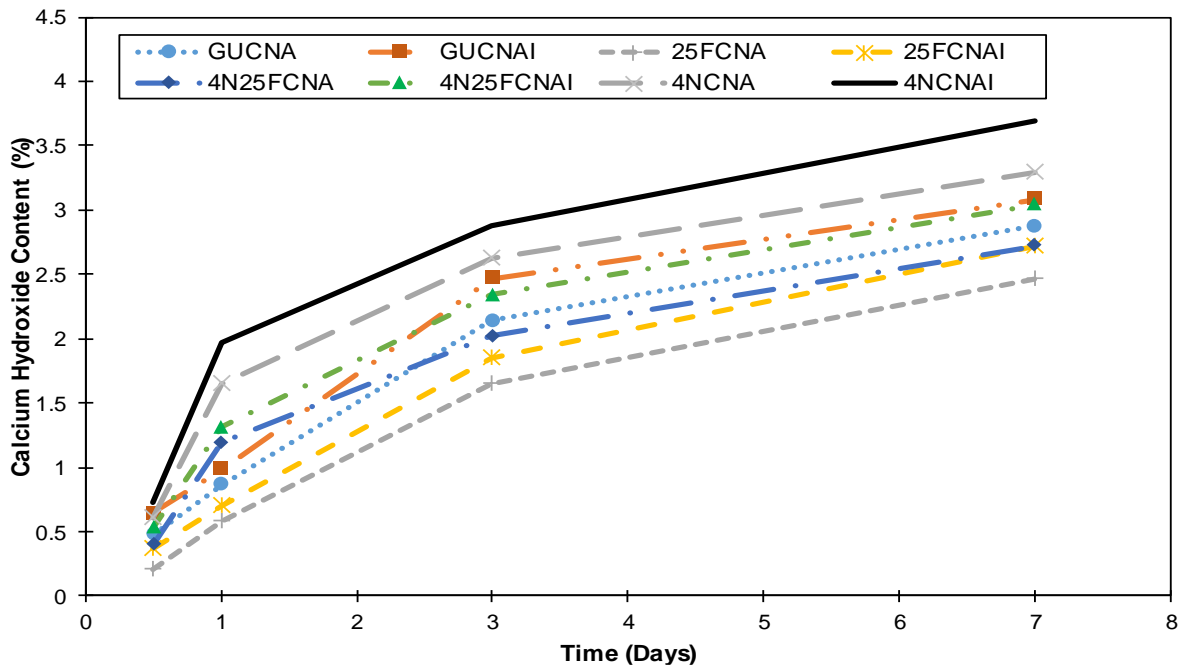


Figure 4.6 Thermogravimetry results for the portlandite contents at early-age up to 7 days.

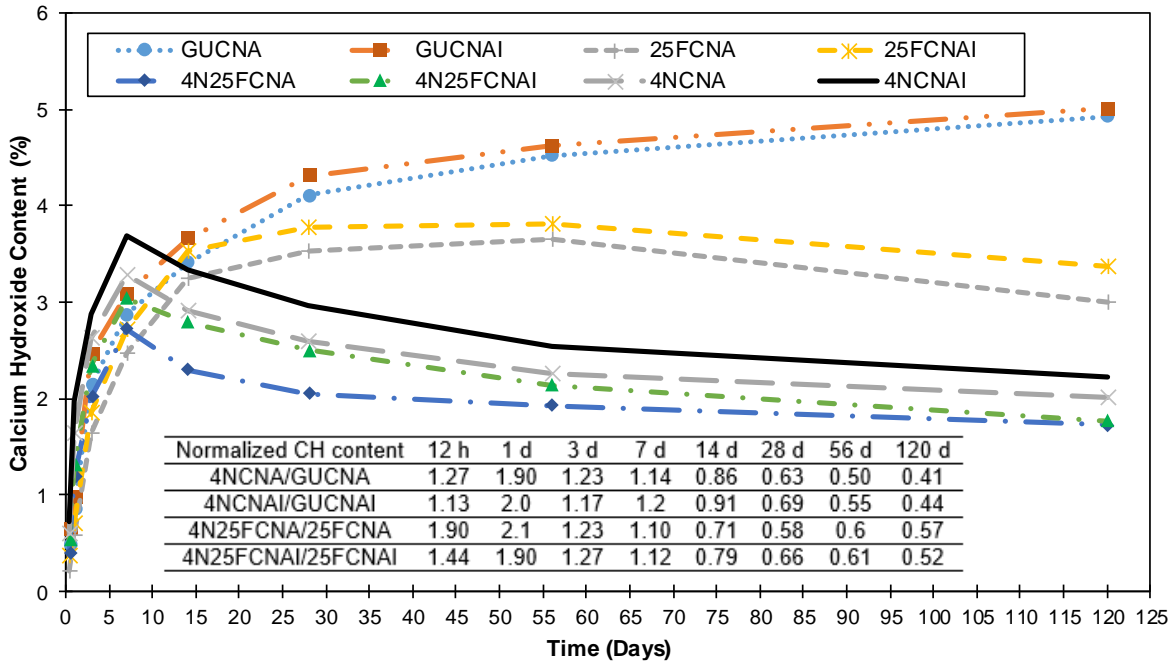


Figure 4.7 Thermogravimetry results for the portlandite contents up to 120 days.

As discussed earlier, the incorporation of CNAI in concrete catalyzed the hydration reactions and led to higher amounts of CH in the matrix compared to CNA. It nucleated the early precipitation of CH, which in turn led to better/earlier development in the microstructure, especially with the coexistence of nano-silica which requires CH to start its pozzolanic reactivity. Together with the filler effect of nano-silica, this led to densifying the pore structure and reducing the absorption of CNAI concrete mixtures compared to that of corresponding CNA mixtures. Thus, the combination of CNAI and nano-silica may present a viable option for low temperature construction, as it produces concrete with mutual balance of early-age and durability properties.

4.7. SCANNING ELECTRON MICROSCOPY

Based on the superior performance of CNAI compared to CNA, BSEM on thin sections prepared from four CNAI mixtures (half of the factorial part) was performed to augment the findings drawn from the previous tests, with respect to fly ash and nano-silica. In addition, EDX analysis was performed on several points within the interfacial transitional zone (ITZ) between hardened paste

and aggregates to calculate the calcium-to-silicate ratio (C/S) of calcium silicate hydrate (C-S-H). It was reported that the C/S of secondary/pozzolanic and conventional C-S-H are approximately 1.1 and 1.7, respectively (Detwiler et al, 1996).

Generally, there was dissimilarity between the microstructure of the different CNAI mixtures as shown in **Figs. 4.8 (a)-(d)**, depending on the inclusion of fly ash and/or nano-silica. Generally, antifreeze admixtures such as calcium nitrite, that contain similar cations as β -C₂S and C₃S in cement, may accelerate the hydration process due to the nucleation action of these ions leading to intensification of the hydrate precipitation processes and improvement in concrete microstructure and strength at the very early-age (Ratinov et al, 1996). However, the replacement of cement with either fly ash and/or nano-silica significantly affected the morphology of concrete microstructure. For instance, mixture GUCNAI had an intermediate microstructure in the ITZ, where the C/S varied between 1.65 and 2.1 with an average of 1.9 [**Fig. 4.8 (a)**].

The incorporation of 25% fly ash to produce mixture 25FCNAI produced coarser microstructure comprising interconnected micro-cracks in the ITZ, where the C/S varied from 1.8 up to 2.4 with an average of 2.1 [**Fig. 4.8 (c)**]. These features indicate less degree of hydration conforming the previously described trends of strength, absorption and pore structure of mixtures containing fly ash, without nano-silica.

Comparatively, the incorporation of nano-silica in mixture GUCNAI to develop mixture 4NCNAI produced the most homogenous matrix and refined microstructure with the lowest C/S in the ITZ of 1.1 [**Fig. 4.8 (b)**], which indicated efficient pozzolanic activity and densification of ITZ by deposition of secondary C-S-H. In addition, when comparing the fly ash mixtures 25FCNAI, to the nano-modified fly ash mixture 4N25FCNAI, noticeable improvement was achieved in the degree of hydration and refinement in the ITZ and hydrated paste due to the

synergistic effects of nano-silica and fly ash [Fig. 4.8 (d)]; correspondingly, the average C/S in the nano-modified fly ash mixture was around 1.4. Again, this substantiates the superior performance of nano-modified mixtures with the coexistence of antifreeze admixtures, and highlights the promising potential of these mixtures for construction applications at freezing/low temperatures.

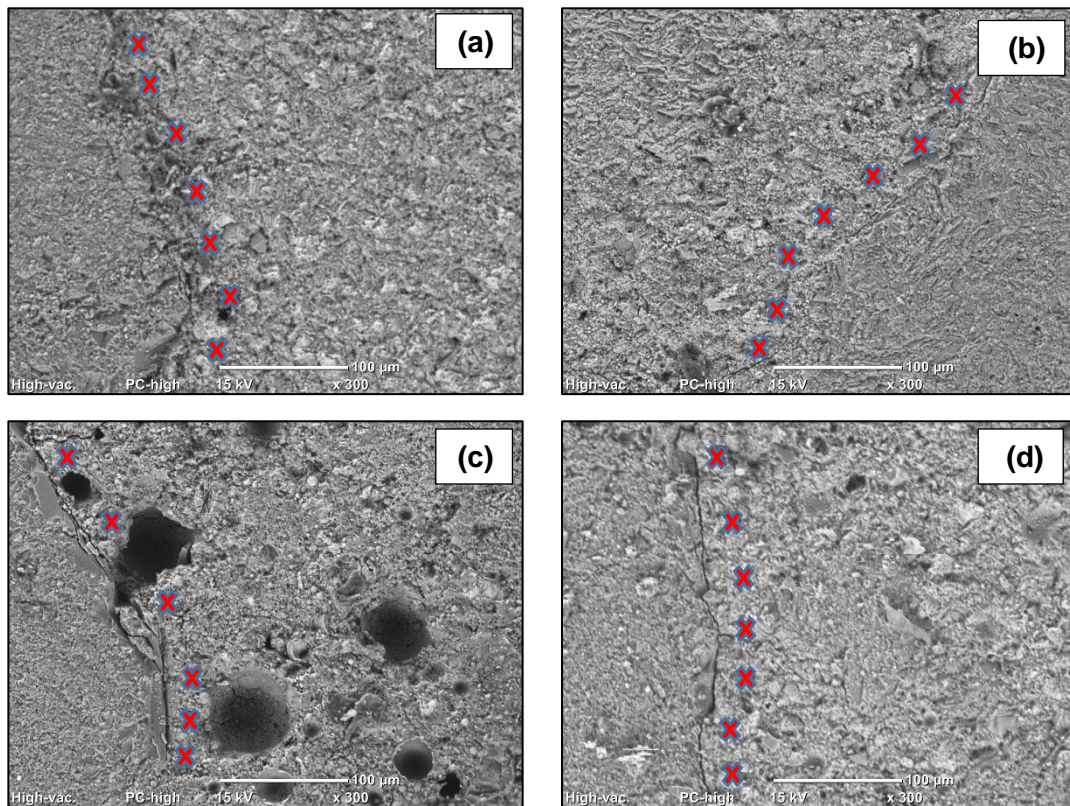


Figure 4.8 BSEM micrographs for thin sections from mixtures: (a) GUCNAI, (b) 4NCNAI, (c) 25FCNAI, (d) 4N25FCNAI.

4.8. NUMERICAL OPTIMIZATION

This section shows the practicality and inwardness of this model to numerical optimize different concrete mixtures suitable for different cold weather applications. The optimization was conducted for a combination of factors at multiple levels, in a manner such that the outcome would satisfy the desired requirements for the target application. The response simultaneous optimization has

upper and lower values which were assigned for each goal. All responses were assigned different goals which were one of the following choices: none, maximum, minimum, target, or within a specific range. All the responses were evaluated simultaneously and were bounded by upper and lower limits based on the design range and the experimental data or as minimum/maximum desired goal. Subsequently, each goal was given a weight on a scale from one to five that reflects the degree of importance with one being least important and five being most important. All factors considered in the optimization process can be maximized, minimized, within range or target value. Once the goals were set, they were all combined into a conclusive desirability function, which reflects the advisability of this function to obtain a compromised solution that satisfy all factors and Responses target goals.

For each response, the desirable range is from one to zero. Multiple trials were run, using a statistical software (Design Expert, 2018), from which the highest desirability function was obtained by the inauguration with a random point and moving forward to the steepest slope to a maximum value. It worth noting that, two or more maxima can be defined due to the curvature of the response surfaces and their combination into the desirability function. The desirability ranges from zero to one, with one being the best case scenario and zero indicates that one or more responses fall outside the desirable boundaries.

To clarify the optimization theory, two cold weather concrete applications were targeted; non-structural and structural applications, based on the City of Winnipeg (COW) Portland cement concrete pavement specifications and requirements CW3310 (CW3310, 2015). Moreover, a third scenario was exercised where all responses were set to give their best potential result in terms of fresh, hardened and durability properties weighted equally (importance factor of 5). The isoresponse of the desirability function may change if different criteria is selected in the

optimization process. The target criteria for the three adopted scenarios and their optimum results are listed in **Table 4.4**. For non-structural applications such as curbs and sidewalks, the COW specifications stipulate only a target compressive strength of 30 MPa after 28 days. While for structural applications such as reinforced concrete pavements, the criteria aims to achieve a balance between strength (32 MPa) and durability (best performance). Whereas, the optimum mixture, which was not obligated to reach any target value for either factor, it was constrained to achieve minimum final setting time and fluid absorption and maximum late age strength.

TABLE 4.4 Numerical optimization criteria, goals, and results.

Criteria	Goal	Weight	Result
<u>non-structural Applications</u>			
Fly Ash	Within range from 0 to 25%	-	10.5%
Nano-Silica	Within range from 0 to 4%	-	0%
CAN:CNI	Within Range	-	CNAI
IST	Minimize	1	56 minutes
FST	Minimize	2	331 minutes
f'_c 3d	None	-	16.6 MPa
f'_c 28d	Within range 30 to 35 MPa	5	35 MPa
Absorption	Minimize	2	2.7%
<u>structural Applications</u>			
Fly Ash	Within range from 0 to 25%	-	10%
Nano-silica	Within range from 0 to 4%	-	0.50%
CAN:CNI	Within Range	-	CNAI
IST	Minimize	4	54 minutes
FST	Minimize	4	322 minutes
f'_c 3d	Maximize	1	18.3 MPa
f'_c 28d	Within range from 32 to 37 MPa	5	37 MPa
absorption	Minimize	5	2.6%
<u>Optimum mixture</u>			
Fly Ash	Within range from 0 to 25%	-	0%
Nano-silica	Within range from 0 to 4%	-	3.50%
CAN:CNI	Within Range	-	CNAI
IST	Minimize	4	32 minutes
FST	Minimize	4	230 minutes
f'_c 3d	Maximize	3	27 MPa
f'_c 28d	Maximize	5	50.5 MPa
absorption	Minimize	5	2.0%

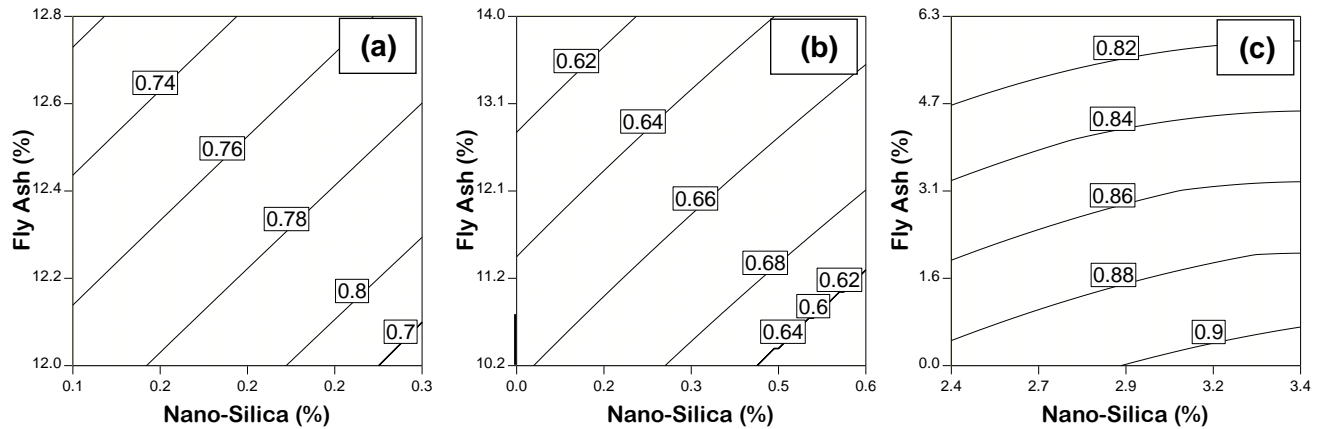


Figure 4.9 Contour Plots of The Desirability Function For: (a) Non-Structural Applications, (b) Structural Applications, (c) Optimum Mixture.

The obtained results showed a desirability of 0.81, 0.70 and 0.91 for the non-structural, structural applications, and the optimized mixture, respectively as shown in **Fig. 4.9**. The contour plots in **Fig. 4.9** graphically show the desirability functions of both applications obtained from the optimization process of the criteria given in **Table 4.4**. The contour plots showed that desirability function increased with decreasing the fly ash dosage, and it increased with increasing the nano-silica dosage. The highest desirability function for non-structural applications was achieved with approximately 10.5% fly ash, 0% nano-silica, and CNAI. This finding does not conform to the CW3310 (CW3310, 2015), which restricts the incorporation of fly ash in concrete with dosages more than 15%. Moreover, the specification does not permit the use of fly ash between October 1 and May 15 (which represent the cold period in Winnipeg, Manitoba, Canada).

The optimum desirability function for structural applications was obtained with 10% fly ash, 0.50% nano-silica, and CNAI, with high degree of importance mechanical strength and durability. The suggested mixture is capable of achieving 37 MPa compressive strength after 28 days and absorption of 2.6%. Finally, the optimum mixture was optimized by using 0 % fly ash, 3.50% nano-silica, and CNAI as CWAS. The results from these three scenarios confirm the

aforementioned trends regarding the effects of fly ash and nano-silica on concrete mixtures under cyclic low temperatures.

The optimum mixture showed an extra ordinary high compressive strength of 50.5 MPa and a relatively low absorption of 2.0 % when compared to the other two scenarios and this clearly shows the effect of reducing the dosage of fly ash to 0% and the incorporation of high dosages of nano-silica.

Thus, the findings of this optimization exercises suggest that appropriate combinations of fly ash, nano-silica, and CWAS can produce various concrete mixtures, which can be cast cured under the aforementioned cyclic freezing to low temperatures, that meet difference specifications for multiple applications.

5. Results and Discussion of Phase II

5.1. SETTING TIME AND INTERNAL HEAT

The properties of fresh concrete different mixtures were evaluated by assessing the initial (IST) and final (FST) setting times as shown in **Figure 5.1**. As expected, mixtures incorporating fly ash generally showed longer setting time than fly ash free mixtures, especially with higher dosages of fly ash (25%). The longest hardening rate was observed in 25F2N mixture with an IST and FST of 145 and 630 minutes, respectively. The trends noticed herein show a significant influence on the setting time of concrete caused by the fly ash content. The effect of higher dosages of fly ash on prolonging the setting time of concrete under normal temperatures is well-documented in the literature (Neville, 2011; Wesche, 2014). Even under the freezing and cyclic temperature curing regime adopted in this study, the effect of increasing the fly ash content notably retarded the setting time, which was previously proved in Phase I of this study. For instance, mixture 25F2N exhibited IST and FST of 35 and 120 minutes longer than mixture 15F2N as a result of increasing the fly ash content by 10%, respectively. Fly ash is known to be less reactive material with latent pozzolanic material due to the lower lime content compared to Portland cement. Thus, the skeletal rigidity rate was slow due to the dilution effect of cement, consequently slower kinetics of the hardening processes and retarding the setting time of concrete (Neville, 2011; Wesche, 2014).

Contrary, the nano-modified mixtures hardening rate were inevitably shortened due to the incorporation of high surface area nano-particles when compared to other reference mixtures. For instance, adding 4% nano-silica to GU mixture to produce mixture 4N resulted in decreasing both IST and FST by 20% and 23%, respectively. Similar trends were noticed regarding nano-modified fly ash mixtures (GU and fly ash). For example, adding extra 2% of nano-silica to mixture 25F2N

to create mixture 25F4N resulted in decreasing the IST and FST by 15 and 100 minutes, respectively. This remarkable effect on setting times can be attributed to the ultrafine nature of nano-silica particles which accelerate the hydration kinetics through nucleation effect by providing the hydration products with surface to precipitate on at very early age (Ghazy et al, 2016; Senff et al, 2009) which explains the trends observed in this section. It is worth noting that, the incorporation of CNAI, which acts as anti-freeze and setting accelerator admixture, preserved the vigorous reactivity of nano-silica compared to other studies conducted same nano-particles under normal temperatures.

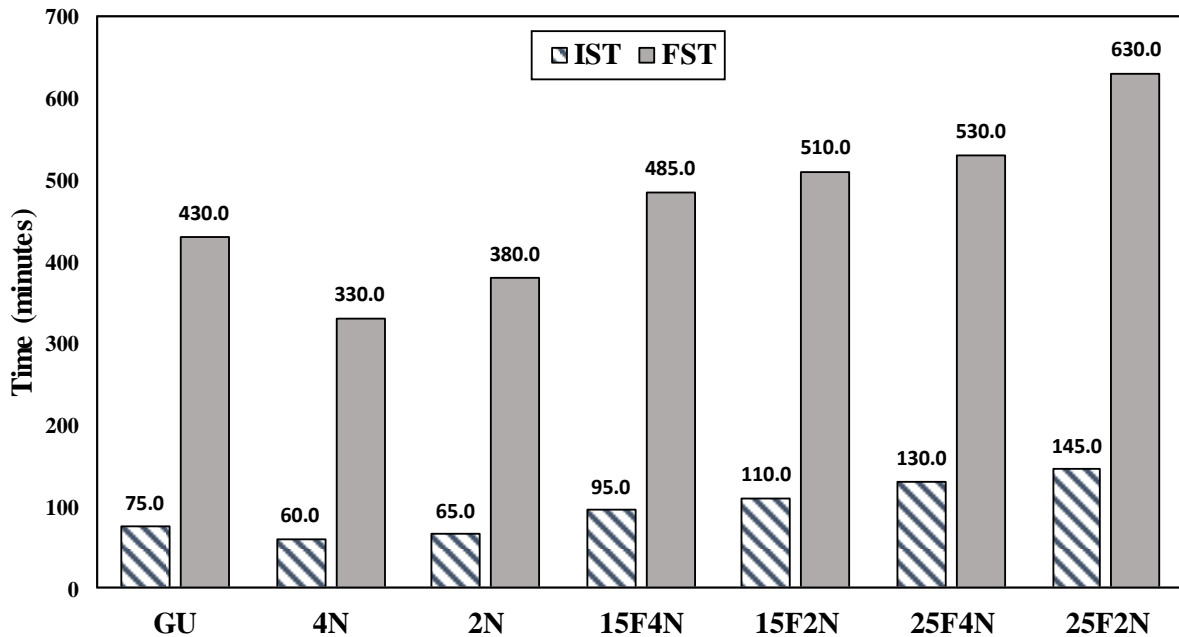


Figure 5.1 Initial and Final Setting time.

The internal heat of each mixture was simultaneously measured using thermocouples, which were embedded to be in the middle of concrete cubes representing different mixtures, along with the setting time. **Figure 5.2** shows the internal heat development of the different mixtures up to 40h. The initial temperature was measured instantly after casting the concrete. The mixing and casting and curing operations were done under the cyclic freezing/low temperatures regime. Mixing and casting were done at the beginning of the freezing cycle. At the beginning of the first

16 h period which represent the freezing period, as shown in **Figure 5.2**, all mixtures experienced relatively high initial temperature which can be ascribed to the heat induction caused by initial contact between mixing water and the cementitious materials (Neville, 2011; Mindess et al, 2003). Thereafter, all mixtures experienced a drop in internal temperature which can be attributed to the loss of temperature, even with the production and emission of heat due to hydration development, to the freezing surrounded environment (-5°C). Thereafter, there was a significant rise in the internal temperature of the all mixtures. This rise in temperature occurred due to the increase in the environment temperature to $+5\pm 1^{\circ}\text{C}$, the peak of the curve occurred toward the end of $+5\pm 1^{\circ}\text{C}$ curing temperature period roughly after 24 hours. Complying with the hardening rate results, nano-modified single binder mixtures maintained higher internal temperature when compared to other mixtures. It is worth mentioning that the final setting time for all mixtures happened during the freezing period at $-5\pm 1^{\circ}\text{C}$, the latest FST happened for 25F2N after 10.5 hours of mixing.

Generally, Mixtures incorporating fly ash showed a steep drop in temperature during the first 4 hours after mixing, the internal temperature gradually continued to decrease during the freezing period. In agreement with the trends of the setting time which showed the retarding effect of higher fly ash content, it can be noticed herein that there is a delay in hydration, lower internal temperature, of mixtures containing 25% and 15% fly ash. The internal heat of these mixtures were considerably lower than the corresponding single binder mixtures. The peak of the internal temperature of 25F4N and 25F2N were 34% and 35% lower than the corresponding single binder mixtures (4N and 2N), respectively. This can be attributed to the previously mentioned effect of dilution of cement with low reactive material such as class F fly ash consequently longer setting times.

In contrast, despite being subjected to a freezing temperature of $-5\pm 1^\circ\text{C}$, nano-modified mixtures were capable of maintaining the internal temperature above 10°C during the first 16 hours. Nano-modified mixtures showed higher magnitude of internal temperature when compared to the reference mixture (without nano-silica), which proves the vigorous reactivity of silica nanoparticles at the very early age. For instance, the peak temperature of 4N and 2N were 20% and 12.5% higher than the peak temperature of GU mixture, respectively. This higher internal temperature ensures the continuation of the hydration process, and it confirms the previously discussed trends of nano-silica in decreasing the setting time. This higher magnitude in internal temperature is likely due to speeding up the hydration kinetics that is caused by ultrafine silica particles, as it has been observed in previous studies (Ghazy et al, 2016; Said et al 2012) under normal temperatures. Speeding the hydration kinetics enabled nano-modified mixtures to maintain relatively higher temperatures, despite the freezing exposure conditions, subsequently faster hardening rate of the cementitious matrices.

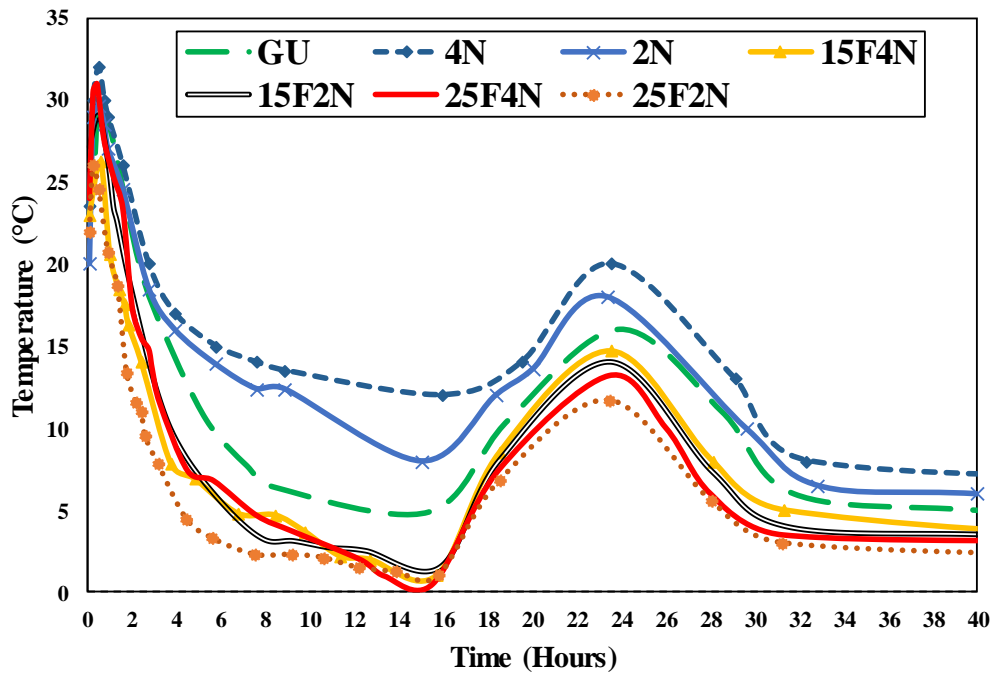


Figure 5.2 Internal Heat of Concrete.

5.2. STRENGTH DEVELOPMENT

The compressive strength of the different mixtures were assessed for both early (1, 3 and 7 days) and late (14, 28, 56 and 91 days) ages as shown in **Table 5.1**. ACI 306R (ACI 306R, 2016) stipulates 3.5 and 24.5 MPa concrete compressive strength grade before being exposed to one cycle and multiple cycles of freezing and thawing, respectively. Generally, most of the studied mixtures, which were cast and cured under the cyclic curing regime, surpassed the required compressive strength stipulated by ACI 306R (ACI 306R, 2016) after 1 and 3 days, respectively. In addition, all mixtures have achieved a high strength values (between 33.6 and 43.6 MPa) after 28 days only, even under the adopted low temperatures curing conditions, which qualifies them for various structural applications such as buildings, bridges and concrete pavements, which require concrete with strength grade of 20 to 40 MPa.

For early age, the average results of compressive strength after 1, 3 and 7 days varied between 3.4 to 10.7, 20.9 to 32.5 and 26.9 to 43.5 MPa, respectively. Generally, incorporating fly ash in concrete, at constant nano-silica dosages, markedly decreased the strength at early age. For instance, incorporating extra 10% fly ash to mixture 15F2N to produce mixture 25F2N led to compressive strength reduction of 30%, 14% and 14% after 1,3 and 7 days, respectively. This can be attributed to the slow reactivity nature of class F fly ash which replaced the GU cement which has higher reactivity leading to deceleration in the kinetics of hydration and delay in strength development. On contrary, the incorporation of nano-silica in concrete significantly improved the strength gain rate at early age. For example, the incorporation of 4% nano-silica in mixture GU to produce mixture 4N increased the compressive strength by 215%, 27% and 19% after 1, 3 and 7 days, respectively. It worth noting that the compressive strength of all nano-modified mixtures, even with the coexistence of 25% fly ash, exceeds the GU mixture strength value at 1 day. This

superior performance can be attributed to the filler and nucleation effects of nano-silica, as well as reducing the apparent w/b due to the absorption of water into their ultra-high nano porosity (Senff et al, 2009; Ghazy et al, 2016; Haruehansapong et al 2014).

On the other side, the late age compressive strength of the different mixtures varied between 30.5 to 39.8, 33.6 to 43.6, 37.6 to 44.6 and 39.6 to 46.4 after 14, 28, 56 and 91 days, respectively. Again, increasing the percentage of fly ash from 15% to 25% led to a notable decrease in strength. For instance, increasing the fly ash percentage from 10% in mixture 15F4N to produce mixture 25F4N reduced concrete compressive strength by 19%, 15% , 8% and 13% after 14, 28, 56 and 91 days, respectively. This can be attributed to the previously mentioned effect of dilution of cement with slower reactive material.

However, increasing silica nano-particles dosage in concrete significantly improved late age strength. For instance, the incorporation of 4% nano-silica in mixture GU to produce mixture 4N improved the late age strength by 17%, 25%, 29% and 27% after 14, 28, 56 and 91 days, respectively. This can be ascribed to the previously mentioned filler effect as well as the pozzolanic effect of nano-silica, by producing secondary high stiff C-S-H gel.

It is worth noting that nano-modified mixtures maintained a continuous steady and significant improvement in strength up to 56 days then a plateau appeared up to 91 days which indicates reaching sufficient pozzolanic reactivity to reach high degree of hydration after 56 days only. However, the fly ash mixtures showed a significant increase in strength up to 91 days. This can be ascribed to the long term performance effect of SCM such as fly ash which needs more than 56 to start its pozzolanic activity (Neville, 2011; Wesche, 2014). Hence, Codes such as CSA A23.1 (CSA A23.1, 2014) stipulates fly ash concrete properties to be examined at 56 or 91 days.

Incorporating nano-silica in different mixtures even with the presence of high dosages of fly ash led to producing concrete with higher and comparable strength to single binder nano-free mixture (GU). This can be imputed to the synergistic effects of the combination of nano-silica and fly ash on the performance and development of concrete microstructure at the adopted curing regime (Ghazy et al 2016). Several Codes and guides such as ACI306R (ACI 306R, 2016) does not recommend high dosages of slowly reactive material such as fly ash due to the expected delay of strength development at early age. However, the results presented herein indicate that the short coming of slow rate strength development for fly ash mixtures can be mitigated by incorporating nano-silica.

TABLE 5.1 Average results of compressive strength (MPa).

Mixture ID	1 day	3 days	7 days	14 days	28 days	56 days	91 days
GU	3.4 (0.1)	25.6 (0.9)	36.6 (0.2)	39.8 (0.4)	43.6 (0.3)	44.6 (0.2)	46.4 (0.3)
4N	10.7 (0.2)	32.5 (0.2)	43.5 (0.3)	48.2 (0.3)	54.6 (0.3)	57.7 (0.1)	59.1 (0.1)
2N	7.5 (0.1)	30.1 (0.1)	39.1 (1)	42.9 (0.8)	50.6 (0.8)	55.3 (0.2)	56.5 (0.4)
15F4N	7.2 (0.1)	26.4 (0.4)	33.6 (0.2)	39.2 (0.1)	44.7 (0.2)	46.3 (0.1)	49.7 (0.1)
15F2N	6.4 (0.1)	24.2 (0.1)	31.2 (1.1)	37.2 (1.5)	40.8 (0.2)	45.2 (0.1)	47.2 (0.6)
25F4N	6.2 (0.3)	22.6 (0.3)	29.4 (0.6)	31.8 (0.1)	37.8 (0.6)	41.2 (0.1)	43.3 (0.2)
25F2N	4.5 (0.3)	20.9 (0.2)	26.9 (0.1)	30.5 (0.3)	33.6 (0.3)	37.6 (0.1)	39.6 (0.1)

Notes: The values between the parentheses represent the standard error.

5.3. FLUID ABSORPTION

The fluid penetrability of the proposed repair concrete mixtures was assessed by fluid absorption test which was developed by Tiznobik and Bassuoni (Tiznobik and Bassuoni, 2018) to evaluate the mass transport properties of concrete after 28 days of curing at the cyclic freezing/low exposure regime. The fluid absorption of the different mixtures varied between 1.8% and 3.1%, as shown in **Figure 5.3**. Complying with the strength results, increasing the percentage of fly ash affected negatively on concrete by markedly reducing the penetration resistance of the cementitious matrix. For instance, at constant nano-silica dosage, adding 25% fly ash to mixtures 4N and 2N to produce mixtures 25F4N and 25F2N resulted in increasing the fluid absorption by 56% and 55%, respectively. It is worth noting that, the highest absorption rate of 3.1% occurred in mixture 25F2N, complying with its lowest compressive strength of 33.6 MPa at this age (28 days), when compared to the other mixtures. This again highlights the noxious effects of replacing cement with slower reactivate material such as fly ash which requires more than 56 days to initiate its pozzolanic reaction. Hence, the fly ash modified concrete suffered from coarse and inferior pore structure after 28 days, as will be seen in the MIP section, consequently a decrease in concrete resistance to fluid penetration leading to various durability issues.

In contrary, the effect of incorporating nano-silica in concrete was complete antithesis to the addition of fly ash. Considerable reduction in absorbed fluids was noticed with the addition of the ultra-fine silica particles. Single binder nano-modified repair mixtures showed the lowest absorption values among all mixtures. For instance, adding 4% and 2% nano-silica to mixture GU to produce 4N and 2N mixtures drove the absorption values down by 22% and 13 %, respectively. The low absorption values of nano-modified mixtures (1.8% and 2%) indicates the improvement and densification in concrete microstructure as well as the strength of pore structure that led to

minimizing the ingress of fluids through the concrete, as will be proved in the MIP section. Nano-silica particles have augmented the resistance of concrete against fluids infiltration through its early pozzolanic reaction by producing secondary high stiff C-S-H gel, as well as its filler effect by precipitating in and filling pore voids (Said et al 2012; Haruehansapong et al 2014). Hence, the silica nano-particles notably blocked concrete pores and prominently mitigated the ingress of fluids inside the concrete.

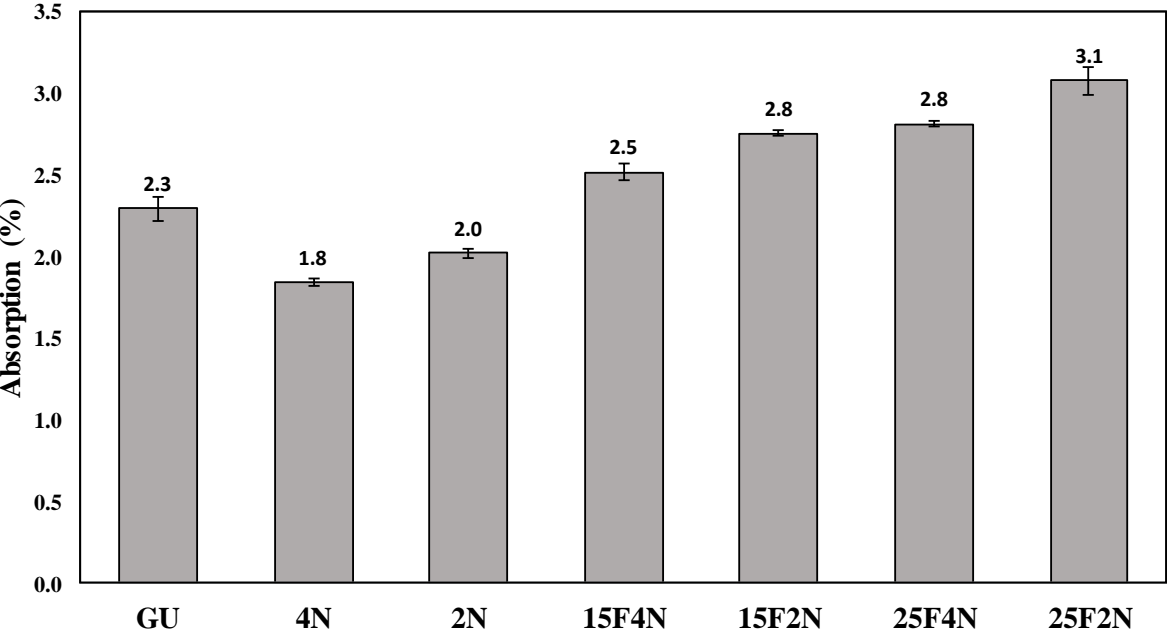


Figure 5.3 Results of fluid absorption test.

5.4. SURFACE SCALING

The joint action of de-icing salt (4% calcium chloride) and Freezing/thawing (F/T) cycles was assessed according to ASTM C672 (ASTM C672, 2014), the surface scaling results are shown in **Figure 5.4**. Aggravated surface scaling was noticed in mixtures incorporating high dosages of fly ash. Scaling in high fly ash content mixtures started after 5 F/T cycles, the mass loss rate increased dramatically after 10 cycles. Complying with the trends observed in compressive strength and fluid absorption sections, increasing fly ash content led to higher mass loss. For instance, adding extra 10% of fly ash to mixtures 15F4N and 15F2N to produce 25F4N and 25F2N resulted in increasing the cumulative mass loss by 138% and 72%, respectively. The cumulative mass loss after 50 cycles for 25F4N mixture was 1050 g/m² with visual rating of 3 to 4, whereas the cumulative mass loss for 25F2N was 1550 g/m² (the highest) with visual rating of 4 to 5. The Ministry of Transportation, Ontario (MTO) (MTO LS-412, 1997) and Bureau du normalization, Quebec (BNQ) (BNQ NQ 2621-900, 2002) stipulated scaling failure limits that are 800 g/m² and 500 g/m², respectively. Although, the deciding salt specified by MTO and BNQ is 3% Sodium chloride, which is considered a less aggressive salt when compared to the 4% calcium chloride that stipulated by ASTM C672 (ASTM C672, 2014) . As per the aforementioned failure limits, both mixtures incorporating 25% deemed to be unsatisfactory.

Previous studies (Malhotra et al, 2000; Ondova et al, 2013) have showed that increasing the fly ash content reduces concrete resistance to surface scaling. This fact, among others, led to avert the usage of high dosages of fly ash horizontal concrete elements such as pavements (Huang et al, 2013; Ondova et al, 2013). This restriction is even more highlighted in cold weather exposure regimes. Various codes and guides (ACI 306R, 2016; CSA A23.1, 2014; CW3310, 2015) strictly prohibit the use of high dosages of fly ash in cold weather. This phenomenon may be ascribed to

the coarse microstructure caused by the unhydrated, slowly reactive class f fly ash. The porous microstructure caused by the unbound fly ash particles aggravated the ingress of the chloride based de-icing salt, which impulsed higher surface scaling (Malhotra et al, 2000; Ondova et al, 2013)

In contrast, all single binder nano-modified mixtures showed a limited surface scaling with mass losses that ranged between 110 and 260 g/m² (**Figure 5.4**) and low visual rating that is between 0 to 1 (**Figure 5.5**). The addition of the ultra-fine silica particles led to a marginal decrease in surface scaling, which means an overall enhancement to the durability properties on nano-modified mixtures. For example, incorporating 2% and 4% nano-silica in GU mixture to produce 2N and 4N mixtures resulted in decreasing the mass loss by 27% and 70%, respectively. Moreover, in nano-modified fly ash mixtures, a dramatic decrease in surface scaling was seen with the increase of nano-silica dosages. For instance, increasing the nano-silica dosage from 2% in mixture 15F2N to 4% to create mixture 15F4N led to decreasing the mass losses from 910 g/m² to 450 g/m² (50% reduction), enabling the later mixture to pass both of the aforementioned failure limits.

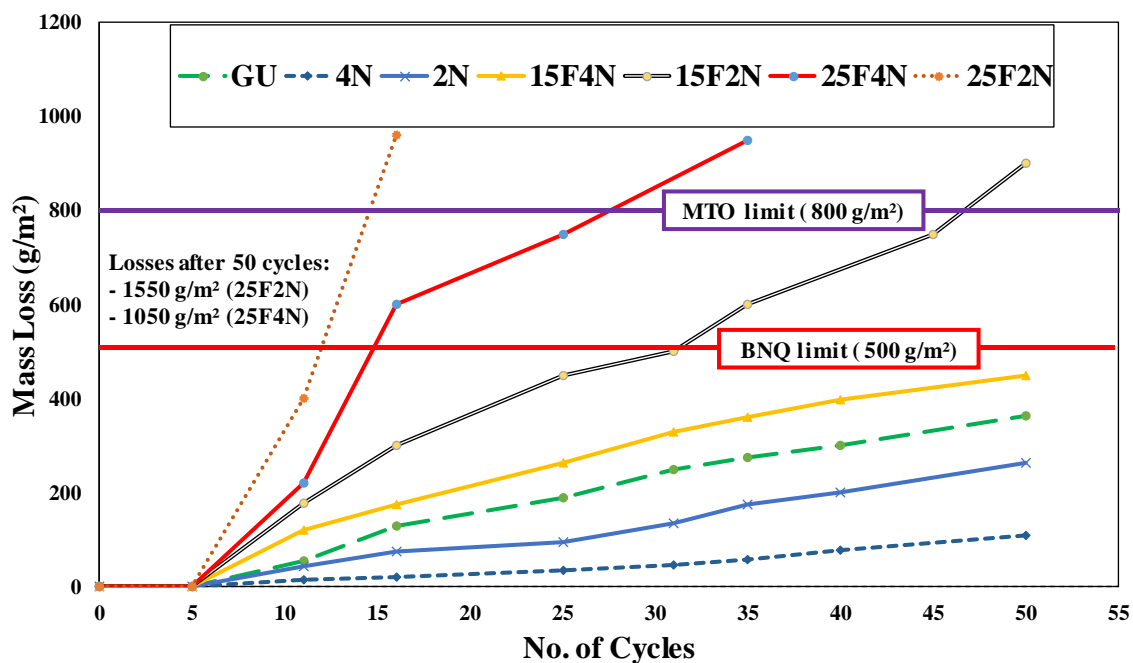


Figure 5.4 Cumulative mass loss of concrete slabs.

Complying with the trends observed in the compressive strength and absorption sections, the reduction in surface scaling may be ascribed to the effect of nano-silica particles, which improves the reactivity and hydration of concrete (Ghazy et al, 2016; said et al 2012). Salt-frost scaling occurs due to the combination of F/T cycles and the ingress of the harmful chloride-based salts, this leads to internal stresses and formation of micro-cracks that propagates into the surface and causes mass losses (Valenza et al, 2014). Two related factors fundamentally control the resistance of concrete to surface scaling; the strength and the porosity of the concrete matrix. The incorporation of nano-silica resulted in creating a dense microstructure that continued to densify over time (as depicted by compressive strength results). This led to an overall stronger matrix that limits the ingress of harmful chloride moisture and abates the propagation of cracks into the surface, thus ultimately significantly enhances concrete ability to resist scaling due to salt-frost action.

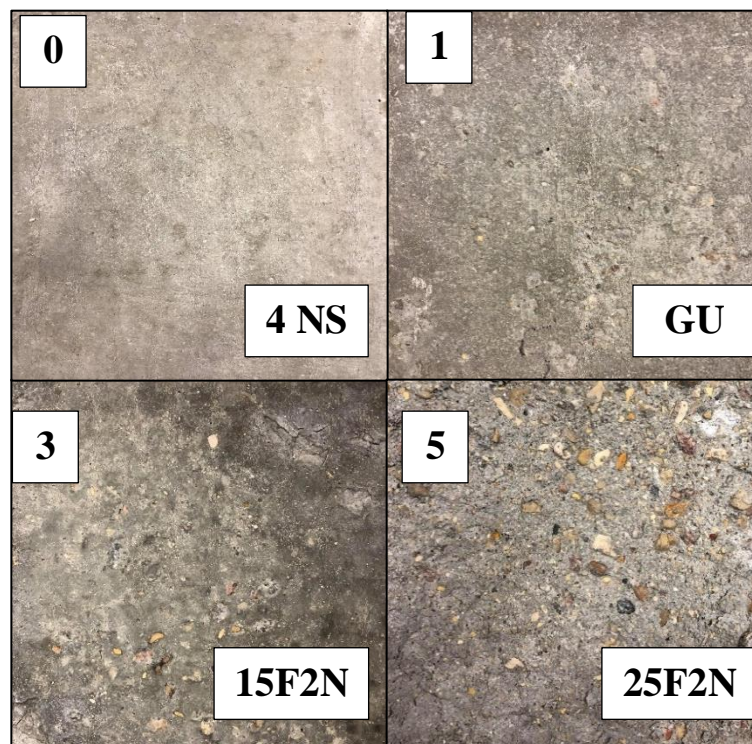


Figure 5.5 examples of visual rating after 50 F/T cycles.

5.5. RESTRAINED SHRINKAGE

Repair materials such as in concrete pavements are often restrained by a substrate or parent concrete, these layers meet at an interface surface and/or confined by a repair patch area. Thus, the adopted configuration simulates field conditions of repair concrete. **Figure 5.6** shows the results of restrained shrinkage for the investigated mixtures cured under cyclic low/freezing temperatures for 28 days, followed by drying conditions for another 28 days. This represents the alternating seasons for concrete cast and cured at cold regions. It is worth mentioning that in field conditions, concrete undergoes fluctuating relative humidity and precipitation that may depreciate the shrinkage rates. Thus, the continual hot-dry exposure adopted in this study represents an accelerated exposure, and may result in exaggerated shrinkage rates. During the first 28 days of exposure, mixtures have showed a lower shrinkage rates due to the freezing conditions that specimens encountered. However, all specimens have showed a higher shrinkage rates upon being exposed to hot-dry conditions. The loss of moisture held by capillary pores of concrete due to hot temperatures and low relative humidity resulted in increasing the levels of shrinkage during the drying exposure (Neville, 2011; Mehta et al, 2014; Soliman et al, 2011).

Generally, the trends presented herein show that mixtures incorporating fly ash exhibited lower shrinkage over the entire 56 days exposure period, which complies with previous studies performed under normal temperatures (Ghazy et al, 2017; Mehta et al, 2014; Soliman et al, 2011). When compared to the corresponding single binder mixtures, mixtures incorporating 25% fly ash showed an average of 50% and 45% less shrinkage after 28 days and 56 days, respectively. The lowest shrinkage was observed in 25F2N and 25F4N specimens which showed a shrinkage rate of approximately 2 to 2.5 microstrain/day (up to 28 days) and 2.6 to 3.25 microstrain/day afterwards (up to 56 days), the overall shrinkage in these specimens ranged between 120 and 136 microstrain

at the end of exposure. Increasing the fly ash content markedly reduced the restrained shrinkage. For instance, increasing the fly ash content from 15% to 25% resulted in decreasing the shrinkage by 28% and 25% after 28 days and 56 days, respectively. The cogent effect of fly ash in decreasing the restrained shrinkage may be ascribed to slower reactivity of fly ash, especially at early age (up to 28 days) (Ghazy et al, 2017; Mehta et al, 2014; Soliman et al, 2011).

Incorporating nano silica have augmented the reactivity of fly ash, resulting in increasing the shrinkage rates. Single binder nano-modified mixtures have showed highest restrained shrinkage with total shrinkage that ranged between 96 to 108 microstrain after 28 days and between 220 to 250 microstrain after 56 days. Previous studies (Ghazy et al, 2017; Said et al 2012) have reported that the presence of nano-silica in concrete mixtures cast and cured at normal temperatures have led to catalyzing the reactivity of fly ash and increasing various types of shrinkage. However, as depicted by the results of compressive strength (**Table 5.1**), fluid absorption (**Figure 5.3**), Surface Scaling (**Figure 5.4**), and the microstructure sections, nano-silica significantly improves the mechanical and microstructure properties of concrete mixtures, thus it is needed to produce a refined and durable concrete matrix for long-term performance.

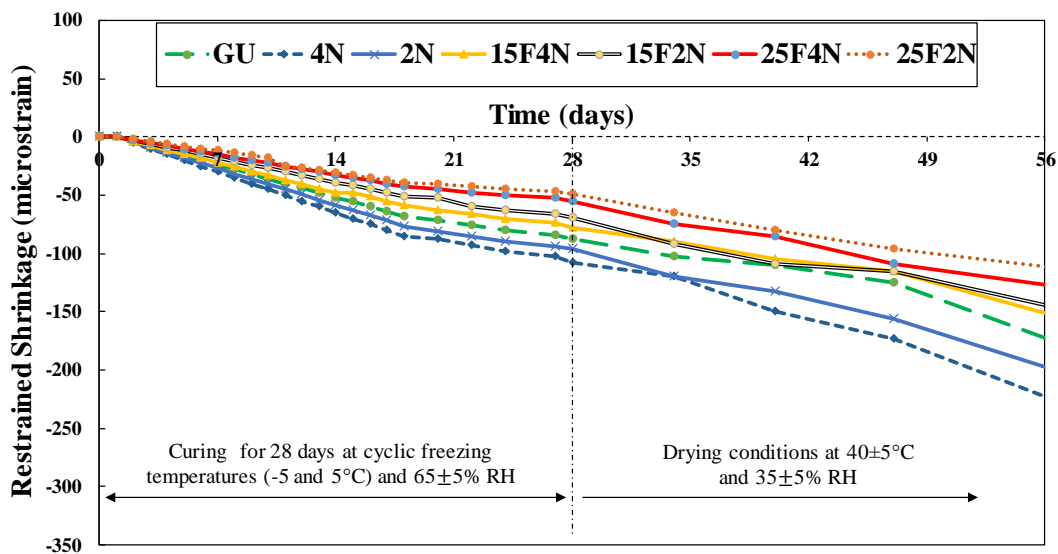


Figure 5.6 Restrained shrinkage of the repair layer in concrete slabs.

5.6. BOND STRENGTH

One of the main causes of deterioration in repaired pavements occurs due to interfacial bond failure. Thus, bond strength between the parent (substrate) concrete and repair materials was assessed according to CSA A23.2-6B (CSA A23.2 6B, 2014). The pull-off test conducted herein represents a severe scenario, as a direct, perpendicular tension force is applied on cored specimens at a rate of 50 ± 20 N/s as shown in **Figure 3.13**. The pull-off test was conducted on samples from each mixture after 28 days of curing under the aforementioned cyclic freezing/low temperature as well as after a combined cyclic exposure as it was described in **section (3.4.2)**. This exposure program was previously used (excluding the first 28 days cold temperature curing period) by other researchers (Ghazy et al, 2016; Li et al, 1999) to capture any uncertainties regarding the compatibility between the repair layer and the substrate concrete and to assess the effect of consecutive winter and summer seasons.

The average results of the bond strength before and after the combined exposure are shown in **Figure 5.7**. The average bond strength values represented by four cores from each specimen ranged from 1.18 to 2.10 MPa and from 1.49 to 2.20 MPa before and after the combined exposure, respectively. Relative to the initial values, all nano-modified and nano-modified fly ash mixtures showed an increase in bond strength after being exposed to F/T and W/D cycles. And their failure occurred at depth of at least 1 cm below the interface of the two layers, indicating the compatibility between the repair and substrate concrete layers.

The bond strength of nano-modified fly ash mixtures showed an average increase of 37% after the aforementioned combined exposure and failure that occurred in the substrate layer. Nano-modified fly ash mixtures containing 15% fly ash initially showed bond strength lower than that of the GU mixture before the combined exposure. However, these mixtures gained significant

increase in bond strength that allowed them to surpass GU mixture after the combined exposure. This shows that nano-modified fly ash mixtures can overcome the deleterious de-bonding action cause by the severe cyclic exposure, even when cured under cold weather environments. The enhanced bond strength of such mixtures can be ascribed to the pozzolanic reactivity of the blended binder system as fly ash needs more than 56 to start its pozzolanic activity (Neville, 2011; Wesche, 2014). The late-age pozzolanic reactivity was enhanced possibly due to the presence of moisture that was introduced by the combined exposure system.

Single binder nano-modified mixtures showed an increase in bond strength that ranged between 4% and 8% before and after the combined exposure, respectively. For instance, in mixture 4N the bond strength before the exposure was 2.10 MPa and increased to 2.20 MPa after the combined exposure. This may be ascribed to the vigorous reactivity of nano-silica which sped up the rate of hydration reactions and consequently improved the bond at the interface with substrate concrete.

The combination of nano-silica, fly ash, and CWAS may have created a favorable environment for the formation of secondary calcium-silicate-hydrate (C-S-H) at the interface due to the chemical reaction between them and the remainder of CH available in the substrate concrete. Therefore, it created a more binding gel (CSH) and a denser microstructure, which ultimately led to an enhanced bonding by increasing mechanical interlocking (Ghazy et al, 2016), this proved by the results from the fluid absorption and MIP results.

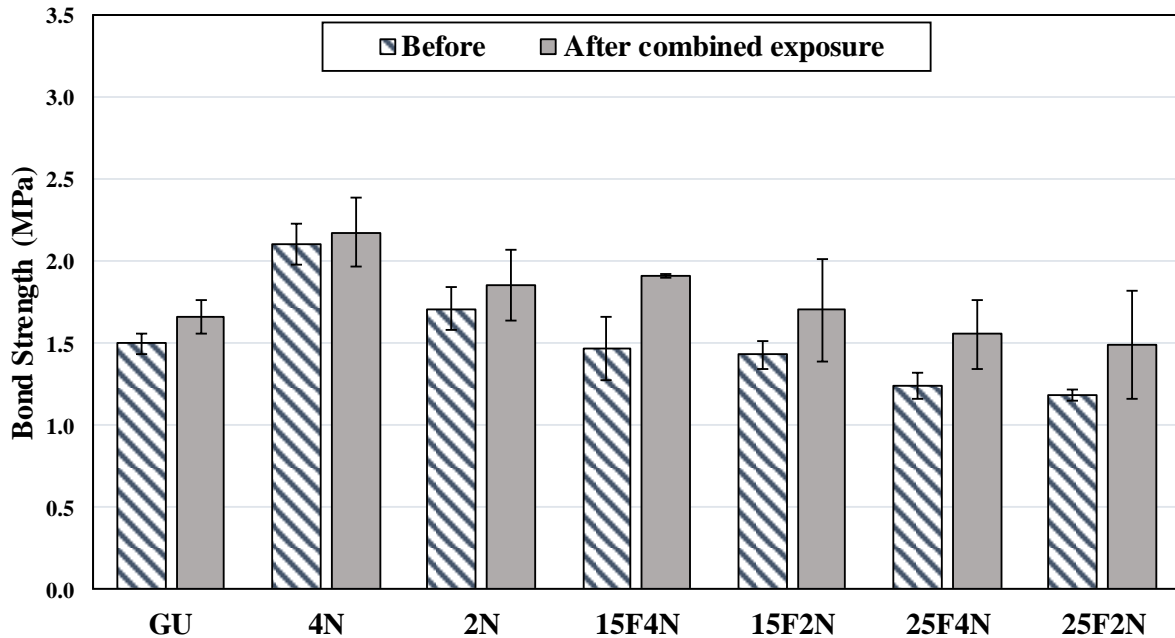


Figure 5.7 Bond Strength test results.

5.7. MERCURY INTRUSION POROSIMETRY

The Mercury Intrusion Porosimetry (MIP) test results for repair mixtures are listed in **Table 5.2**. The results include total cumulative intrusion, apparent porosity, threshold pore diameter, and proportion of micro-pores (pores that are less than 0.1 μm). The test was conducted on a pea-size concrete chunks extracted from the middle of the specimens after 28 days of curing under the aforementioned cyclic freezing/low temperatures.

The trends of MIP test results presented herein conformed to the macro-scale tests (fluid absorption and surface scaling). Generally, mixtures incorporating fly ash showed higher cumulative intrusion, apparent porosity and threshold pore diameter as well as lower proportions of micro-pores. These values have been markedly influenced by increasing the fly ash content. For instance, increasing the fly ash content from 15% in mixture 15F2N to 25% to create mixture 25F2N led to increase the total cumulative intrusion, apparent porosity and threshold pore diameter by 20%, 16% and 40%, respectively. It also resulted in decreasing the proportion of micro-pores

by 10%. Mixture 25F2N have showed the highest total cumulative intrusion (9.36×10^{-2} ml/g) and 17.7% Apparent porosity, which firmly confirms and explains the trends observed in the fluid absorption and surface scaling sections.

The relatively large porosity and high intrusion facilitated the ingress of moisture penetrating the concrete samples, this is translated in the higher absorption and surface scaling of this mixture as discussed in the previous sections. Moreover, the coarser pore structure represented by only 52% and 56% micro-pores in mixtures incorporating high fly ash content explains the reduction in compressive strength especially in early ages. mixtures 25F2N and 25F4N, comprising 25% fly ash, had the highest porosity, lowest compressive strength (up to 91 days) and yielded highest absorption among all mixtures.

The ultra-silica particles have imposed a significant improvement in nano-modified and nano-modified fly ash mixtures. This improvement is substantiated by the positive development of the nano-modified mixtures. Significant reduction in the amount of intrusion, porosity, and threshold pore diameter was noticed upon incorporating nano-silica particles. It also increased the proportion of the micro-pores in those mixtures. For instance, incorporating 4% nano-silica in mixture GU to produce mixture 4N decreased the porosity and threshold pore diameter by 8% and 67%, respectively as well as increasing the proportion of micro-pores by 19%.

Moreover, the effect of adding nano silica to blended binder fly ash mixtures led to refining the coarse microstructure of fly ash mixtures. For example, increasing the nano-silica dosage by 2% in mixture 15F2N to produce mixture 15F4N resulted in decreasing the porosity from 15.2% to 14% and threshold pore diameter from 0.2 to 0.17; correspondingly, increasing the proportion of micro-pores from 58% to 61%. By precipitating in air-filled voids and enhancing the hydration

process (Said et al 2012; Ghazy et al, 2016; Haruehansapong et al 2014), nano-silica particles blocked the harmful connected capillary voids and transformed them into a discrete micro-pore. The ultra-fine silica particles created a denser pore structure and markedly enhanced the resistance of nano-modified concrete against fluid penetration and ultimately resulted in a relatively lower absorption, surface scaling and improved compressive strength.

Table 5.2 Summary of MIP results for repair mixtures.

Sample	Total Cumulative Intrusion$\times 10^{-2}$ (ml/g)	Apparent Total Porosity (%)	Threshold Pore Diameter (μm)	Proportion of Micro- Pores ($<0.1 \mu\text{m}$) (%)
GU	7.82	14.2	0.15	58
4NS	7.22	13.0	0.05	69
2NS	7.42	13.8	0.08	67
15F4N	7.51	14.0	0.17	61
15F2N	7.76	15.2	0.2	58
25F4N	8.72	16.0	0.25	56
25F2N	9.36	17.7	0.28	52

6. Summary, Conclusions and Recommendations

6.1. Summary

The experimental program of this thesis mainly consisted of two phases, constructed to evaluate several innovative nano-modified mixtures for cold weather applications. In both phases, the mixing and casting operations were done at temperature of $-5\pm 1^\circ\text{C}$, and the curing was done under cyclic freezing/low ($5\pm 1^\circ\text{C}$) temperatures until testing. These cycles were designed based on the temperature data extracted from the City of Winnipeg weather data for the last 10 years representing weather in late fall and early spring. The mixture designs used in this study involve using three main variables that are considered to have significant impact on mixtures cast and cured in cold weather conditions. In the first phase of this thesis, mixtures designs involved using; GU cement, fly ash contents of 0 to 25%, nano-silica contents of 0 to 4% and a combination of calcium nitrite (CNI) and calcium nitrate (CNA) as Cold Weather Admixture System (CWAS). The dosage of antifreeze admixtures was kept constant at 15% by mass of mixing water, a concentration which was selected according to phase diagrams of these materials. The total binder (single or blended) content in all mixtures and the water-to-binder ratio (w/b) were kept constant at 400 kg/m^3 and 0.32, respectively. This w/b was selected to advantageously affect the properties of concrete similar to the ratios used in high-performance concrete.

In Phase I, 15 concrete mixtures were prepared to investigate the three parameters adopted, Design of Experiments (DOEs) approach was used to categorize the experimental variables and test their significance based on the Response Surface Method (RSM) and utilizing Face-Centered Composite Design (FCCD) statistical approach. Based on this approach, a statistical software was used to derive models, which have the capability of predicting five responses based on given inputs

extracted from the laboratory experiments, these responses are represented by: initial and final setting times, compressive strengths at 3 and 28 days, and fluid absorption to assess the fresh, hardened and durability properties, respectively. Analysis of Variance (ANOVA) was used to test the different factors of the models and their interactions to distinguish the significant and insignificant variables.

Furthermore, to corroborate and further understand the trends observed in the macro-scale tests, a microstructural analysis was conducted on samples from mixtures in this phases. These microstructural analysis tests included; Backscattered scanning electron microscopy (BSEM), Differential scanning calorimetry (DSC), and Mercury Intrusion Porosimetry (MIP).

In Phase II, a reduced matrix of concrete mixtures were selected based on the results from the first phase of this study. The assessment criteria of this phase focused on the suitability of the selected mixtures as a speciality repair materials for concrete in cold regions. Seven mixtures incorporating materials similar to those in phase I were prepared to evaluate the early-age as well as long-term properties of nano-modified and nano-modified fly ash concrete mixtures as well as their compatibility with substrate/parent concrete. The fresh properties in this phase were evaluated by determining the slump, setting time and internal temperature of concrete. The compressive strength test was conducted at 1, 3, 7, 14, 28, 56 and 91 days to evaluate the early-age and long-term hardened properties. Moreover, the durability properties were assessed based on fluid absorption, surface scaling, restrained shrinkage, bonding strength tests as well as MIP test was conducted to analyze the microstructure of these mixtures.

6.2. Conclusions for Phase I

The experimental and modeling studies in this phase were conducted to comprehend the effects of fly ash and nano-silica with different types of CWAS on concrete mixtures cast and cured under cyclic freezing/low temperatures (-5 and 5°C). Based on this phase of the study, the following conclusions can be drawn:

- The derived statistical models had strong association with the experimental datasets; thus, they are reliably capable of simulating various responses that represent fresh (setting time), hardened (compressive strength), and durability (fluid absorption) properties of normal and nano-modified concrete cast and cured under freezing/low temperatures.
- Increasing the CNI dosage in CWAS improved the overall performance of concrete; consequently, CNAI had balanced performance in terms of depressing the freezing point of mixing water, accelerating solidification of concrete and improving the kinetics of binder hydration compared to CNA and CNAAI.
- Increasing the fly ash content led to prolonging the setting times, decreasing the compressive strength and increasing the fluid absorption of concrete. This was ascribed to the slow reactivity of fly ash, especially under such cold temperatures, which led to producing coarse microstructure relative to the other mixtures.
- The inclusion of nano-silica enhanced the properties of concrete mixtures by shortening the setting time, increasing compressive strength and decreasing fluid absorption of concrete. Thus, the functionality of nano-silica was maintained under this freezing/low temperature curing regime, owing to the coexistence of CWAS.
- The TG results highlighted the role of nano-silica in markedly improving microstructural evolution of the cementitious matrix at very-early age (nucleation effect) and at later ages

through its pozzolanic activity after 7 days. Together with its physical filler effect, this caused the nano-modified mixtures to attain discontinuous and dense microstructure (MIP and BSEM/EDX trends) after 28 days under this cold curing regime.

- The overall outcomes of this phase suggest that incorporating nano-silica with single or blended binders, especially with CNAI, in concrete cast and cured under freezing/low temperatures, can achieve balanced and superior performance in terms of fresh, hardened and durability properties. Therefore, nano-modified concrete mixtures may present a viable option in cold regions, without the need for heating practices, and thus allowing for versatile construction schedules in late fall and early spring periods. Yet, this needs to be further augmented by field trials, which are recommended for future research.

6.3. Conclusions for phase II

Based on the results of the experiments conducted on the selected mixtures for repair applications under cold weather environments, the following conclusions can be drawn:

- The trends depicted by the results of setting time, and compressive strength, and fluid apportion tests in this phase conform to those observed in phase I. The higher dosages of fly ash (up to 25%) significantly prolonged the setting time, delayed early-age strength development, and created a porous microstructure that was vulnerable to fluid penetration. Conversely, nano-silica markedly shortened the setting time, enhanced hydration and created dense microstructure.
- Nano-modified fly ash mixtures showed enhanced workability, ample hardening times, and maintained a favorable internal temperature for the continuation of the hydration process even when exposed to cyclic freezing/low temperatures. This may provide smooth repair process,

without the need for long closure times for key infrastructure repairs such as in roads and bridges, especially under cold weather conditions.

- The synergistic effects of incorporating nano-silica, fly ash, and CWAS significantly enhanced the early-age and long term compressive and bond strengths of concrete cast and cured under the adopted cyclic freezing/low temperatures. This combination provided a balanced early-age and long-term properties and compensated for adverse effects of the slower hydration rate of class F fly ash. All investigated mixtures reached a strength of above 20 MPa and 30 MPa at 3-days and 14-day, respectively. A strength which qualifies them for most flat work applications such as concrete pavements.
- Fluid penetration and surface scaling increased with the inclusion of high dosages of fly ash (25%) due its slow reactivity that coarse microstructure, especially in early-ages. However, the later property of fly ash controlled the shrinkage of concrete.
- The incorporation of nano-silica positively contributed to reducing the ingress of fluids and surface scaling of concrete mixtures and created a dense microstructure structure (as proved by MIP tests results). However, due to its vigorous reactivity, nano-silica triggered higher rates of restrained shrinkage, but without visible cracking.
- Overall, the results showed a strong potential for nano-modified fly ash mixtures to be used as a specialty cold weather repair material. Mixtures incorporating fly ash (up 15%), nanosilica (up to 4%), and CNAI provided a balanced early-age and long-term durability performance; they present a viable option for various repair applications such as in concrete pavements. This option can replace the conventional methods, which can significantly reduce life cycle costs, and negative environmental impact associated with the current cold weather concreting practice.

6.4. Recommendations for future research work

- Based on the results of this research, the long-term performance of selected nano-modified fly ash mixtures should be assessed under deep-freeze (below -5°C) exposure conditions.
- Conduct field studies using the newly introduced materials in cold regions with temperatures similar to those adopted in this study, to confirm the results presented herein.
- Investigate the effects of different nano-materials in concrete such as nano-alumina and nano-clay at different dosages under cold exposure conditions.
- Conduct a life-cycle cost/benefit and environmental impact analyses comparing the options presented herein and the currently used conventional cold weather concreting practices.

7. References

- Abd.El.Aleem, S., Heikal, M. and Morsi, W.M., (2014), "Hydration characteristic, thermal expansion and microstructure of cement containing nano-silica" *Construction and Building Materials*, Vol. 59, pp. 151–160.
- ACI Committee 306, (2016), "Guide to Cold Weather Concreting" ACI 306R, American Concrete Institute, Farmington Hills, Michigan.
- ACI committee 318, (2002), "Building code requirements for structural concrete" ACI 318, American Concrete Institute, Farmington Hills, Michigan.
- ACI committee 201, (2016), "Guide to Durable concrete" ACI 201.2R, American Concrete Institute, Farmington Hills, Michigan.
- ACI committee 116, (2000), "Cement and concrete terminology" ACI 116R, American Concrete Institute, Farmington Hills, Michigan.
- Al-Alaily, Hossam S., and Assem A.a. Hassan (2016). "Refined Statistical Modeling for Chloride Permeability and Strength of Concrete Containing Metakaolin." *Construction and Building Materials*, vol. 114, 2016, pp. 564–579.
- Al-Ostaz, A.; Irshidat, M.; Tenkhoff, B.; and Ponnappalli, P. S., (2010), "Deterioration of Bond Integrity between Repair Material and Concrete due to Thermal and Mechanical Incompatibilities," *Journal of Materials in Civil Engineering*, ASCE, V. 22, No. 2, 2010, pp. 136-144. doi: 10.1061/(ASCE)0899-1561.
- Arslan, M., Cullu, M. and Durmus, G., (2011), "The effect of antifreeze admixtures on compressive strength of concretes subjected to frost action" *Gazi University, Journal of Science*, Vol. 24, No. 2, pp. 299-307.

ASTM C494 /C494M, (2015), “Standard Specification for Chemical Admixtures for Concrete”, ASTM International, West Conshohocken, Pennsylvania.

ASTM C260/C260M, (2016), “Standard Specification for Air-Entraining Admixtures for Concrete”, ASTM International, West Conshohocken, Pennsylvania.

ASTM C125, (2018), “Standard Terminology Relating to Concrete and Concrete Aggregates” American Society for Testing and Materials, Pennsylvania.

ASTM C403/ C403M, (2016), “Standard Test Method for Time of Setting Concrete Mixtures by Penetration Resistance” American Society for Testing and Materials, Pennsylvania.

ASTM C666/C666M, (2015), “Standard Test Method for Resistance of Concrete to Rapid Freezing and Thawing” ASTM International, West Conshohocken, Pennsylvania.

ASTM C672/C672M, (2014), “Standard Test Method for Scaling Resistance of Concrete Surfaces Exposed to De-icing Chemicals,” ASTM International, West Conshohocken, PA.

ASTM C39/C39M, (2018), “Standard Test Method for Compressive Strength of Cylindrical Concrete Specimens”, ASTM International, West Conshohocken, Pennsylvania.

Bayramov, F., Taşdemir, C. and Taşdemir, M.A., (2004), “Optimization of steel fiber reinforced concretes by means of statistical response surface method” Cement and Concrete Composites, Vol. 26, No. 6, pp. 665-675.

Behfarnia, K. and Salemi, N., (2013), “The effects of nano-silica and nano-alumina on frost resistance of normal concrete” Construction and Building Materials, Vol. 48, pp. 580-584.

Belkowitz JS, Nawrocki K and Fisher FT (2015) “Impact of nanosilica size and surface area on concrete properties”. ACI Materials Journal 112 (3): 419–428.

Barna, L.A., Seman, P.M. and Korhonen, C.J., (2011), "Energy-efficient Approach to Cold-Weather Concreting," *Journal of Materials in Civil Engineering*, Vol. 23, No. 11, 2011, pp. 1544-1551.

BNQ NQ 2621-900, (2002), "Determination of the Scaling Resistance of Concrete Surfaces Exposed to Freezing-and-Thawing Cycles in the Presence of De-icing Chemicals," Bureau de Normalisation du Québec, Annexe A, pp. 19-22.

CAN/CSA-A3001, (2013), "Cementitious Materials for Use in Concrete, Canadian Standards Association, Mississauga, ON.

Cox, D. R., & Reid, N, (2000), "The theory of the design of experiments". Boca Raton, FL: Chapman and Hall/CRC.

CSA-A23.1/A23.2, (2014), "Concrete Materials and Methods of Concrete Construction/ Test Methods and Standard Practices for Concrete" Canadian Standard Association (CSA), Mississauga, Ontario, Canada.

CSA A23.2-6B, (2014), "Determination of Bond Strength of Bonded Toppings and Overlays and of Direct Tensile Strength of Concrete, Mortar, and Grout," CSA A23.1/A23.2, Canadian Standards Association, Mississauga, ON, Canada.

CW3310-R17, (2015), "Portland Cement Concrete Pavement Works", City of Winnipeg specification, Winnipeg, Manitoba, Canada.

Damle, S.S., (2009), "Optimization of Antifreeze Admixture Formulations" Thesis draft.

Detwiler, R., Bhatta, J., and Bhattacharja, S., (1996), "Supplementary Cementing Materials for Use in Blended Cements", Portland Cement Association, Skokie, IL.

Design-Expert version 11, (2018), Software for Design of Experiments. Stat-Ease Inc., Statistics Made Easy, Minneapolis, Minnesota. www.statease.com.

Demirboğa, R., Karagöl, F., Polat, R. and Kaygusuz, M.A., (2014), “The effects of urea on strength gaining of fresh concrete under the cold weather conditions” *Construction and Building Materials*, Vol. 64, pp.114-120.

Environment and climate change Canada, (2018), “Weather Dashboard for Winnipeg,” www.winnipeg.weatherstats.ca (accessed May. 1, 2018).

European Standard BS EN 206-1, (2000), “Concrete Specification, performance, production and conformity”.

Evan, G., (2008), “Cold weather concreting” *National Precast Concrete Association Precast Magazine*, pp. 1–7.

Ghazy, A., Bassuoni, M. T. and Shalaby, A., (2016), “Nano-modified Fly Ash Concrete: A Repair Option for Concrete Pavements,” *ACI Materials Journal*, Vol. 113. No. 2, pp. 231-242.

Ghazy, A., Bassuoni, M.T., (2017), “Shrinkage of Nano-Modified Fly Ash Concrete as A Repair Material for Concrete Pavements”, *ACI Materials Journal*, Vol. 114, No. 6.

Grapp, A.A., V.B. Grapp and A.S. Kaplan. (1975) “The structure and cold resistance of concretes containing antifreeze admixtures”. In *Proceedings of the 2nd International Symposium on Winter Concreting*, 14-16 October. Vol. I. Moscow: Stroiizdat, p. 60-68.

Gonzalez, M., Tighe, S.L., Hui, K., Rahman, S. and de Oliveira Lima, A., (2016), “Evaluation of freeze/thaw and scaling response of nano concrete for Portland cement concrete (PCC) pavements” *Construction and Building Materials*, Vol. 120, pp. 465-472.

Goncharova, L.S. and F.M. Ivanov., (1975) “The properties of concretes containing antifreeze admixtures”. In *Proceedings of tile 2nd International Symposium on Winter Concreting*, 14-16 October. Vol. 1. Moscow: Stroiizdat, p. 69-71.

Haruehansapong, S., Pulngern, T. and Chucheepsakul, S., (2014), "Effect of the particle size of nanosilica on the compressive strength and the optimum replacement content of cement mortar containing nano-SiO₂", *Construction and Building Materials*, Vol. 50, pp. 471–477.

Hou, P., Kawashima, S., Kong, D., Corr, D. J., Qian, J., and Shah, S. P., (2013), "Modification Effects of Colloidal NanoSiO₂ on Cement Hydration and Its Gel Property," *Composites Part B: Engineering*, Vol. 45, No. 1, pp. 440-448.

Huang, C.; Lin, S.; Chang, C.; and Chen, H., (2013), "Mix Proportions and Mechanical Properties of Concrete Containing Very High-Volume of Class F fly ash," *Construction & Building Materials*, V. 46, pp. 71-78. doi: 10.1016/j.conbuildmat.2013.04.016

Jo, B., Kim, C., Tae, G. and Park, Jb., (2007), "Characteristics of Cement Mortar with Nano- SiO₂ Particles". *Construction and Building Materials*, Vol. 21, No. 6, pp. 1351–1355.

Karagöl, F., Demirbog, R. and Khushefati, W.H., (2015), "Behavior of fresh and hardened concretes with antifreeze admixture in deep-freeze low temperatures and exterior winter conditions" *Construction and Building Materials*, V.76, pp. 388–395.

Karagöl, F., Demirboğa, R., Kaygusuz, M.A., Yadollahi, M.M. and Polat, R., (2013), "The Influence of Calcium Nitrate as Antifreeze Admixture on the Compressive Strength of Concrete Exposed to Low Temperatures," *Cold Regions Science and Technology*, Vol. 89, pp. 30-35.

Kazempour, H., Bassuoni, M. T. and Hashemian, F., (2015), "Use of nanoparticles in cold weather masonry construction", *ASTM STP 1577: Masonry*, pp. 3-20.

Kazempour, H., Bassuoni, M.T. and Hashemian, F., (2016), "Masonry Mortar with Nanoparticles at A Low Temperature," Proceedings of the Institution of Civil Engineers- Construction Materials, Vol. 170, No. 6, pp. 297-308.

Kang, S.C., Koh, H.M. and Choo, J.F., (2010), "An efficient response surface method using moving least squares approximation for structural reliability analysis" Probabilistic Engineering Mechanics, Vol. 25, No. 4, pp. 365-371.

Krylov, B.A., A.V. Lagoida and G.P. Apostolova (1979), "Critical strength of concretes with antifreeze admixtures". Beton i Zllele (Concrete and Reinforced Concrete), no. 12, p. 27-28.

Korhonen, C. J., Cortez, E. R., Durning, T. A., and Jeknavorian, A. A., (1997), "Antifreeze admixtures for concrete." Special Report, U.S. Army Cold Regions Research and Engineering Laboratory, Hanover, NH.

Korhonen, C., Charest, B. and Romisch, K., (1997), "Developing New Low-Temperature Admixtures for Concrete: A Field Evaluation," Cold Regions Research and Engineering Lab, Hanover, NH.

Korhonen, C.J., (1990), "Antifreeze admixtures for cold regions concreting: a literature review" Cold Regions Research and Engineering Lab, Hanover, NH.

Korhonen, C. L., Cortez, E. R, and Charest, B. A., (1992), "Strength development of concrete cured at low temperature" Concrete International, Vol. 14, No. 12, pp.34-39.

Kuzmin, Y. D. (1976) "Concretes with Antifreeze Admixtures". Kiev: Budivel'nik Publishing House.

Li, M., and Victor, C. L., (2011), “High-Early-Strength Engineered Cementitious Composites for Fast, Durable Concrete Repair-Material,” *ACI Materials Journal*, V. 108, No. 1, pp. 3-12.

Li, S.; Frantz, G. C.; and Stephens, J. E., (1999), “Bond Performance of Rapid-Setting Repair Materials Subjected to De-icing Salt and Freezing-Thawing Cycles,” *ACI Materials Journal*, V. 96, No. 6, pp. 692-697.

MacGregor, J. G., Wight, J. K., Teng, S., and Irawan, P., (1997), “Reinforced Concrete: Mechanics and Design”, Third Edition, Prentice Hall, Upper Saddle River, NJ.

Malhotra, V. M.; Zhang, M. H.; Read, P. H.; and Ryell, J., (2000), “Long- Term Mechanical Properties and Durability Characteristics of High- Strength/High-Performance Concrete Incorporating Supplementary Cementing Materials Under Outdoor Exposure Conditions,” *ACI Materials Journal*, V. 97, No. 5, pp. 518-525.

Mason, R. L., Gunst, R. F., & Hess, J. L. (2003). “Statistical design and analysis of experiments with applications to engineering and science”. New York: Wiley.

Mehta, P.K., and Monteiro, P.J.M., (2014), “Concrete,” McGraw Hill Education, USA.

Mironov, S.A., O.S. Ivanova, and Yu.B.Volkov (1979), “concrete with new anti-freeze admixtures” concrete and reinforced concrete (Beton I Zhelezobeton).

Mindess, S., Young, J. F., and Darwin, D, (2003), “Concrete”, Prentice Hall, Upper Saddle River, NJ.

Montgomery, D.C., (2017), “Design and analysis of experiments” 9th Edition.

MTO LS-412, (1997), “Method of Test For Scaling Resistance of Concrete Surfaces Exposed to Deicing Chemicals,” Ontario Lab Testing Manual, Ministry of Transportation.

Mwaluwinga, S., Ayano, T. and Sakata, K., (1997), "Influence of Urea in Concrete," *Cement and Concrete Research*, Vol. 27, No. 5, pp. 733-745.

Nmai, C.K., (1998), "Cold weather concreting admixtures" *Cement and Concrete Composites*, Vol. 20, pp. 121-128.

Neville, A. M. (2012). "Properties of concrete" (5th ed.). Harlow: Pearson Education.

Ondova, M.; Stevulova, N.; and Meciarova, L., (2013), "The Potential of Higher Share of Fly Ash Cement Replacement in the Concrete Pavement," *Procedia Engineering*, V. 65, pp. 45-50. doi: 10.1016/j. proeng.2013.09.009

Ovcharov, V.I. (1972) "Effective life of corrosion inhibitor- containing concretes and mortars prepared under winter conditions". *Tsentr. Nauchno-Issled. Inst. Stroit. Konstr. im. Kucherenko*.

Prado, P.J., Balcom, B.J., Beyea, T.W., Armstrong, R.L., and Grattan-Bellew, P.E., (1998), "Concrete freeze/thaw as studied by magnetic resonance imaging" *Cement and Concrete Research*, Vol. 2, No.(28) pp. 261–70.

Powers, T. C., (1954), "Void spacing as a basis for producing air-entrained concrete", *J. Amer. Concr. Inst.*, 50, pp.

Powers, T.C. and Helmuth, R.A., (1953), "Theory of Volume Changes in Hardened Portland-Cement Paste during Freezing," *Highway Research Board Proceedings*, Vol. 32.

Polat, R., (2016), "The Effect of Antifreeze Additives on Fresh Concrete Subjected to Freezing and Thawing Cycles," *Cold Regions Science and Technology*, Vol. 127, pp. 10-17.

Ratinov, V. B., and Rozenberg, T. I., (1996), "Anti-freezing admixtures, In *Concrete Admixtures*" Handbook (Second Edition), pp. 740-799.

Said, A.M., Zeidan, M.S., Bassuoni, M.T. and Tian, Y., (2012), "Properties of Concrete Incorporating Nano-Silica" *Construction and Building Materials*, Vol. 36, p.p 838–844.

Sheikin, A.E., P.S. Kostyaev, L.M. Dobshits, V.M. Smolyanskii, N.K. Rozental, O.S. Ivanova and S.I. Pchelkin (1980) "Study of the corrosion of steel reinforcement in concretes containing certain additives". *Tr. Institute Inzh. Zheleznodorozhn. Transp.*, 662: 35.

Senff L, Hotza D, Repette WL, Ferreira VM and Labrincha JA (2010) "Mortars with nano-SiO₂ and micro-SiO₂ investigated by experimental design". *Construction and Building Materials* 24 (8): pp. 1432–1437.

Senff, L., Labrincha, J. A., Ferreira, V. M., Hotza, D., and Repette, W. L., (2009), "Effect of Nano-silica on Rheology and Fresh Properties of Cement Pastes and Mortars," *Construction and Building Materials*, Vol. 23, No. 7, pp. 2487-2491.

Soliman, A.M., and Nehdi, M.L., (2011), "Self-Accelerated Reactive Powder Concrete Using Partially Hydrated Cementitious Materials," *ACI Materials Journal*, V. 108, No. 6, pp. 596-604.

Soliman, H., and Shalaby, A., (2014), "Characterizing the Performance of Cementitious Partial-Depth Repair Materials in Cold Climates," *Construction & Building Materials*, V. 70, 2014, pp. 148-157. doi: 10.1016/j.

Sonebi, M., & Bassuoni, M. (2013). "Investigating the effect of mixture design parameters on pervious concrete by statistical modelling". *Construction and Building Materials*, 38, pp. 147-154.

Tiznobaik, M., and Bassuoni, M. T., (2018), "A Test Protocol for Evaluating Absorption of Joints in Concrete Pavements," *Journal of Testing and Evaluation*, Vol. 46, No. 4, p.p. 1636-1649.

Valenza, J. J. II, and Scherer, G. W., (2007), "A Review of Salt Scaling: II. Mechanisms,"
Cement and Concrete Research, V. 37, No. 7, pp. 1022-1034. doi: 10.1016.

Wesche, K., (2014), "Fly Ash in Concrete: Properties and Performance", CRC Press.

Xu, Q.L., Meng, T. and Huang, M.Z., (2012), "Effects of nano-CaCO₃ on the compressive strength and microstructure of high strength concrete in different curing temperature",
Applied Mechanics and Materials, Vol. 121, pp. 126-131.

Appendix A: Statistical model tests for various responses.

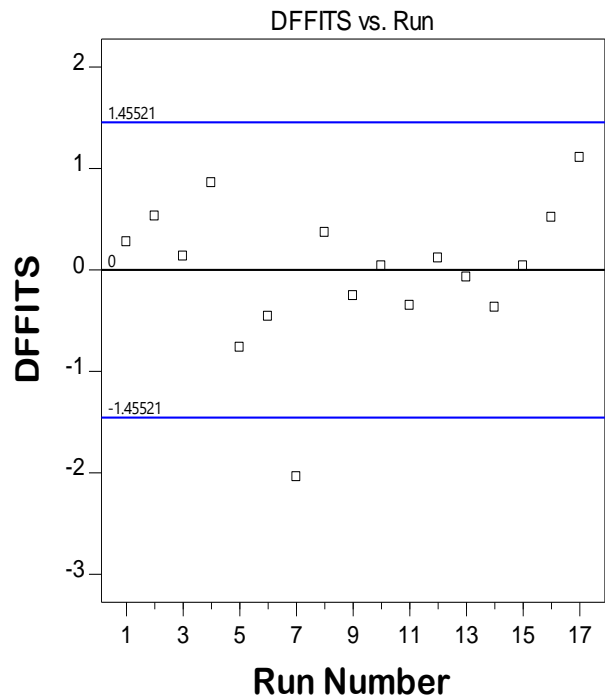
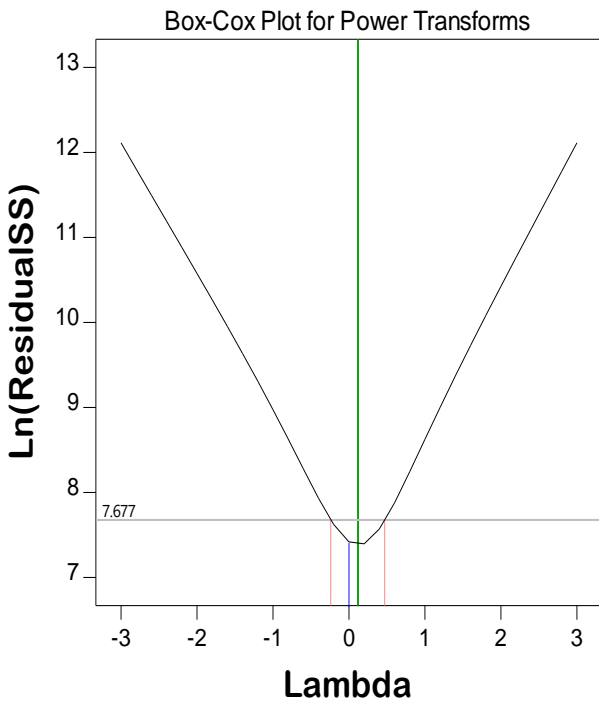
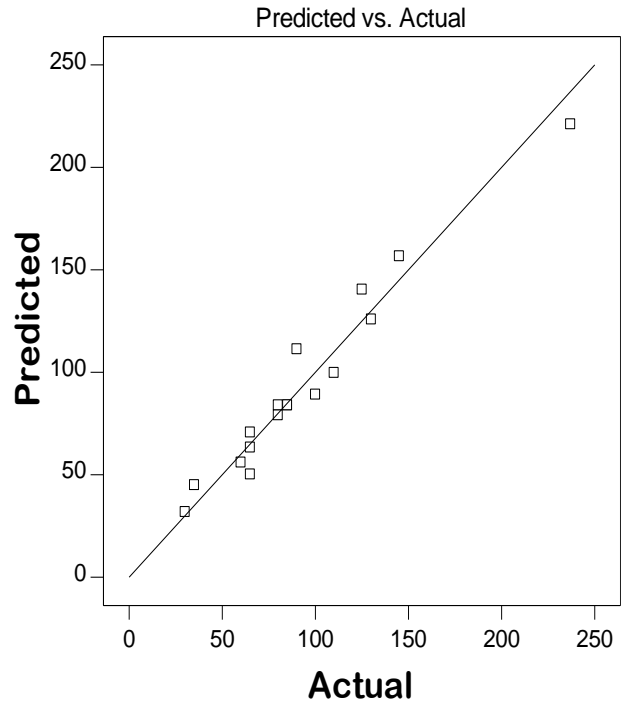
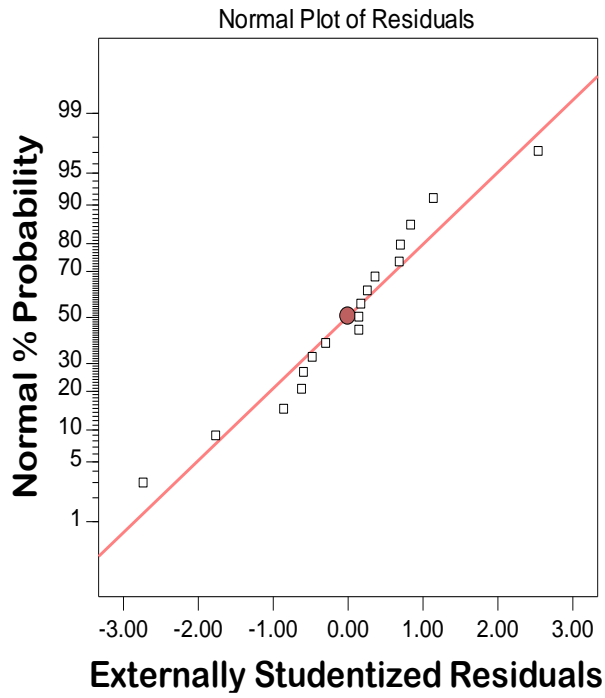


Figure A1 Log (IST) statistical model tests.

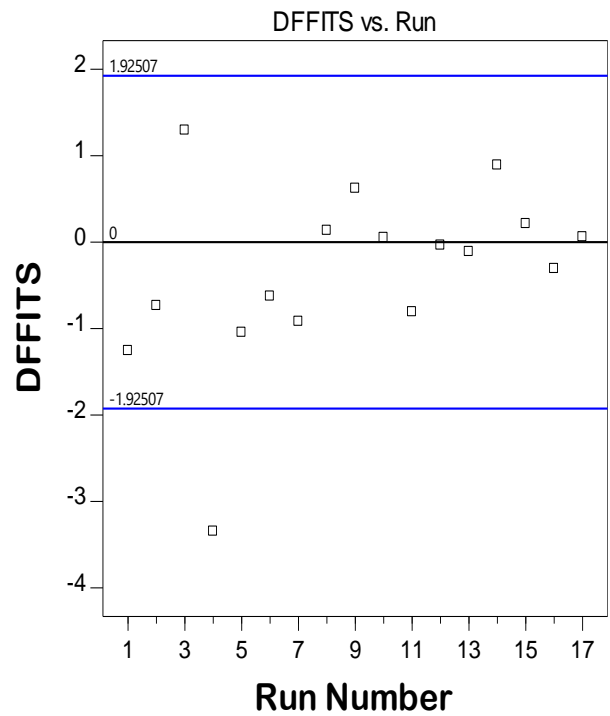
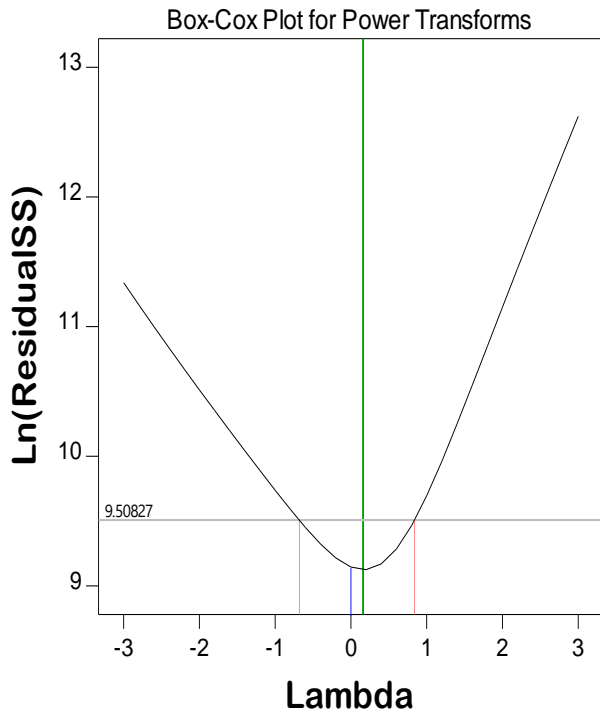
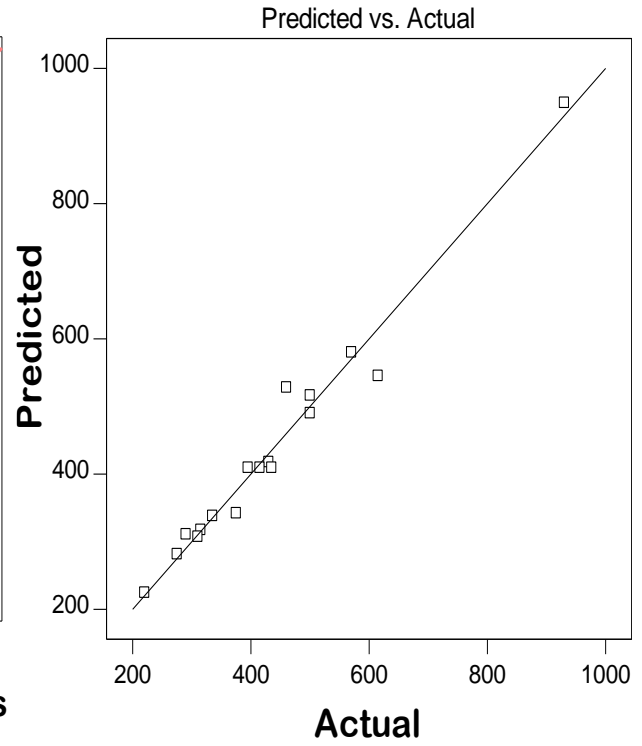
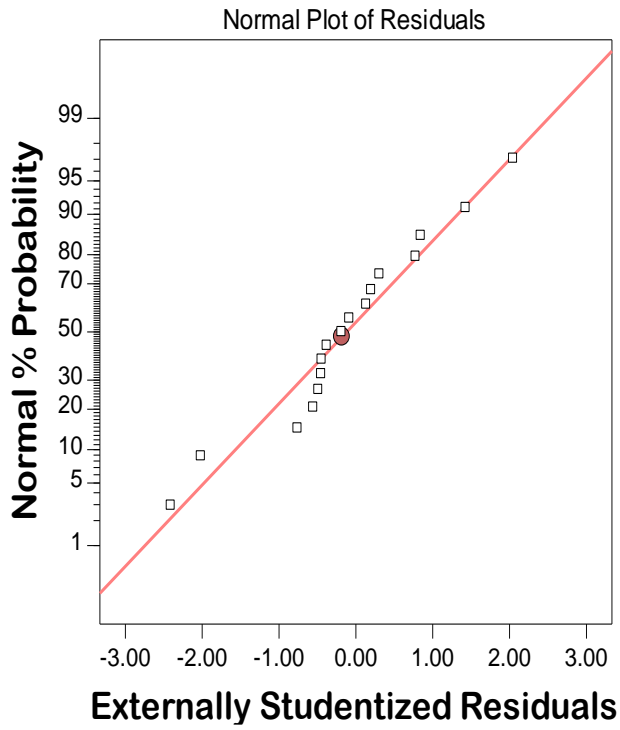


Figure A2 Log (FST) statistical model tests.

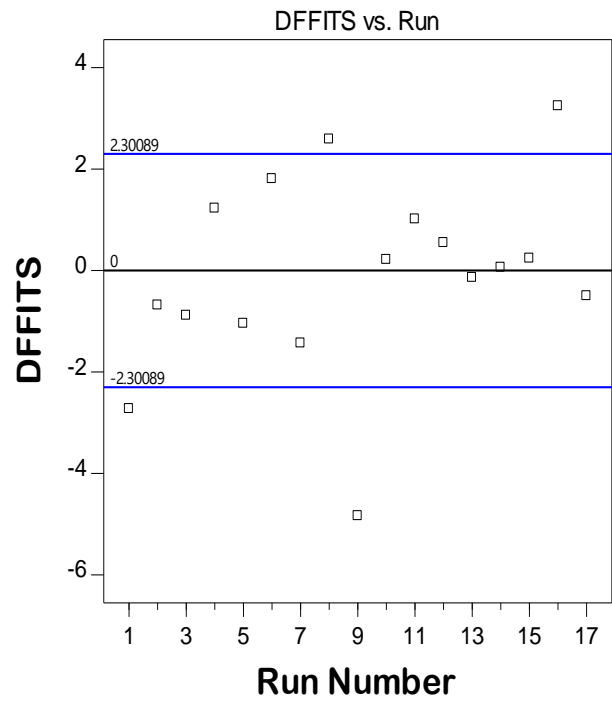
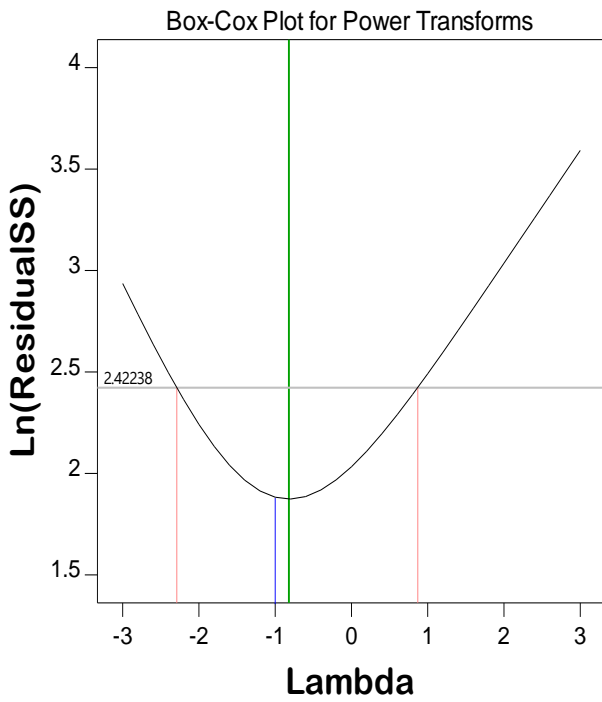
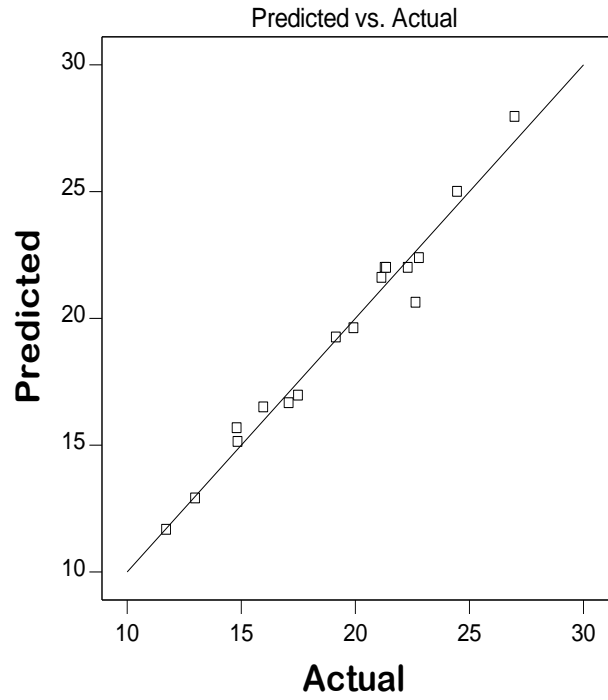
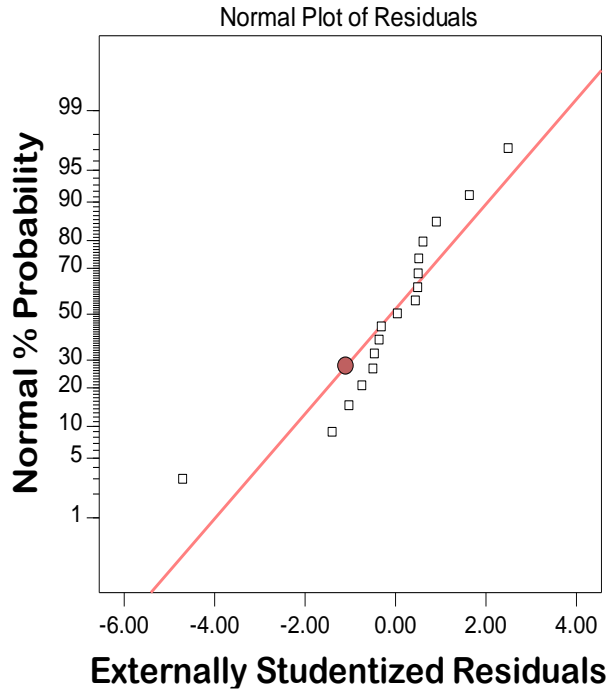


Figure A3 (1/fc3) statistical model tests.

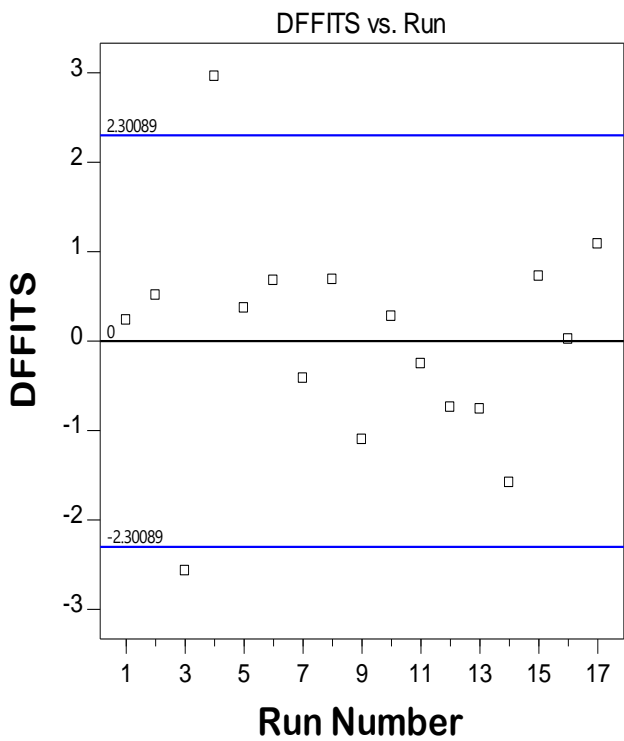
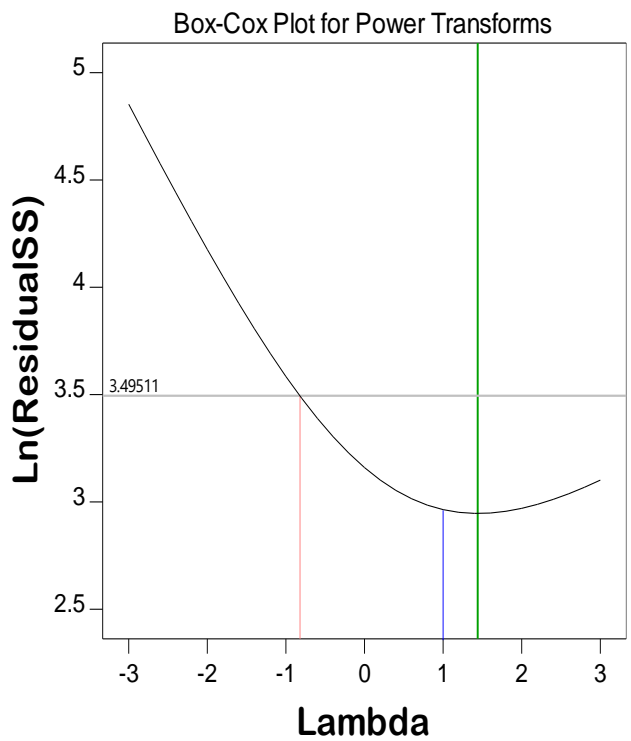
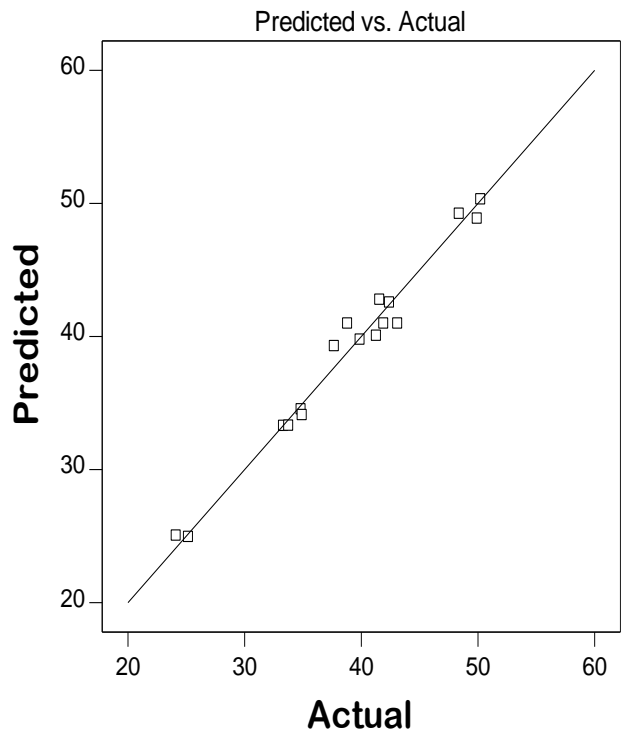
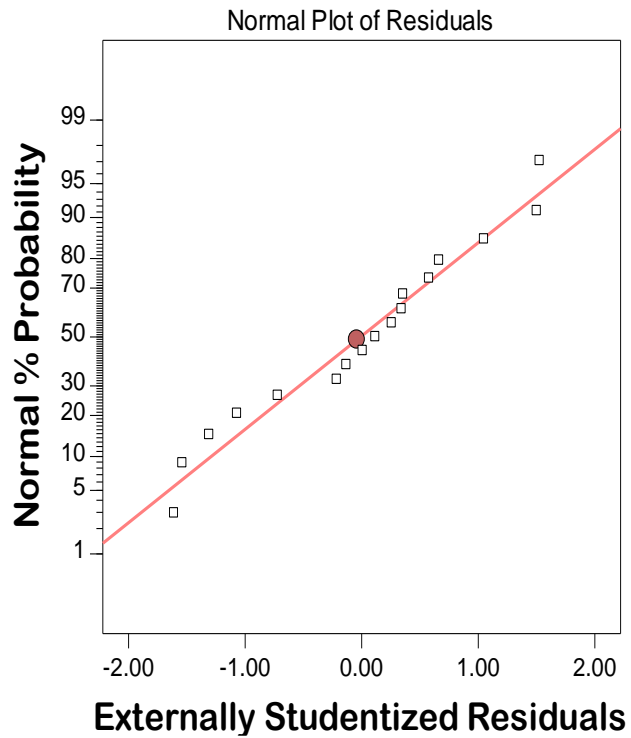


Figure A4 fc 28 statistical model tests.

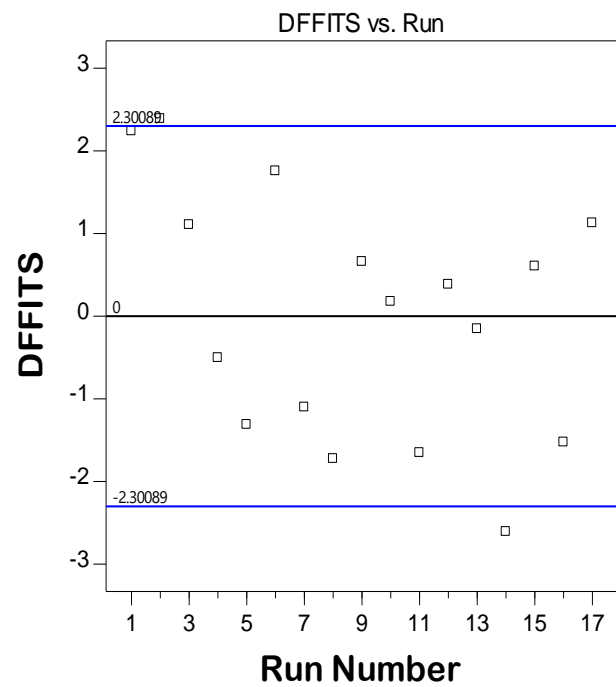
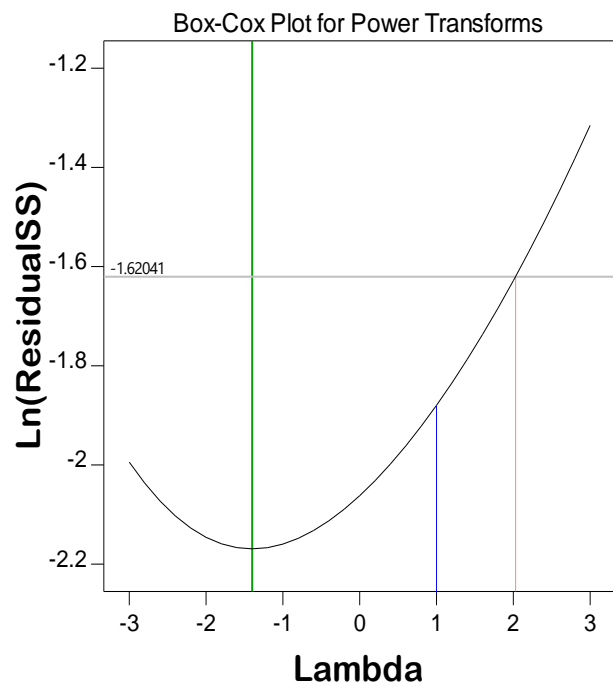
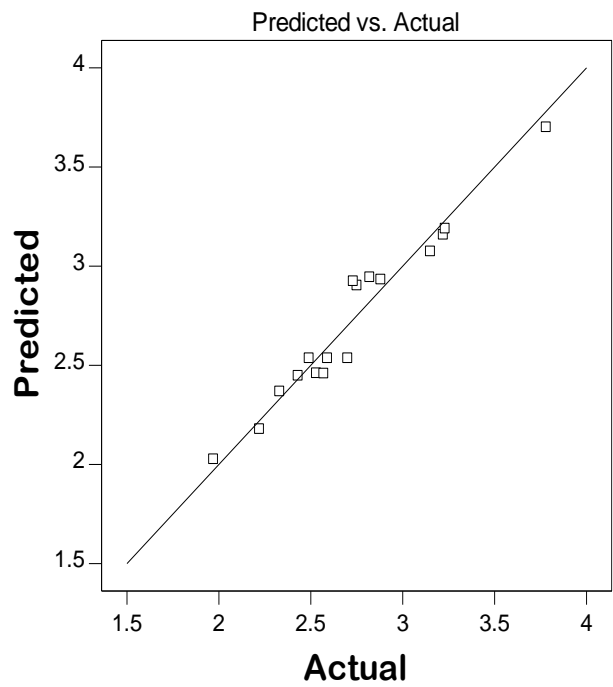
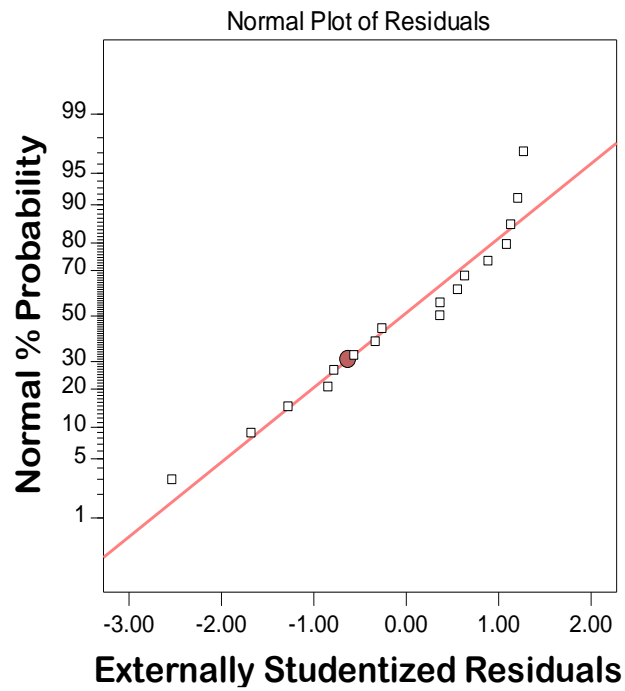


Figure A5 Absorption statistical model tests.

**Appendix B: Detailed ANOVA and Model coefficient
tables.**

TABLE B1 IST detailed ANOVA results.

Source	Sum of Squares	df	Mean sq	F-value	P-value	Significance
Model	0.7036	3	0.2345	67.1829	0.0000	significant
N	0.0559	1	0.0559	16.0132	0.0015	
F	0.1497	1	0.1497	42.8828	0.0000	
A	0.4980	1	0.4980	142.6526	0.0000	
Residual	0.0454	13	0.0035			
Lack of Fit	0.0449	11	0.0041	17.6735	0.0547	not significant
Pure Error	0.0005	2	0.0002			
Cor Total	0.7490	16				
<u>Fit statistics</u>						
Std. Dev.	0.0591					
Mean	1.9203					
C.V. %	3.0768					
R²	0.9394					
Adeq Precision	29.3284					

*N=nano-silica F=Fly ash A=anti-freeze admixture.

TABLE B2 IST model coefficients.

Factor	Coefficient Estimate	df	Standard Error	95% CI Low	95% CI High	VIF
Intercept	1.92	1	0.0143	1.89	1.95	
N	-0.0748	1	0.0187	-0.1151	-0.0344	1
F	0.1224	1	0.0187	0.082	0.1627	1
A	-0.2232	1	0.0187	-0.2635	-0.1828	1

*N=nano-silica F=Fly ash A=anti-freeze admixture.

TABLE B3 FST detailed ANOVA results.

Source	Sum of Squares	df	Mean sq	F-value	P-value	Significance
Model	0.3490	6	0.0582	54.9573	0.0000	significant
A-Nano-Silica	0.0608	1	0.0608	57.4084	0.0000	
B-Fly-ASh	0.1219	1	0.1219	115.2093	0.0000	
C-CNA:CNI	0.1545	1	0.1545	145.9882	0.0000	
AB	0.0000	1	0.0000	0.0183	0.8951	
AC	0.0074	1	0.0074	7.0233	0.0243	
BC	0.0043	1	0.0043	4.0965	0.0705	
Residual	0.0106	10	0.0011			
Lack of Fit	0.0097	8	0.0012	2.7646	0.2927	not significant
Pure Error	0.0009	2	0.0004			
Cor Total	0.3595	16				
<u>Fit statistics</u>						
Std. Dev.	0.0325					
Mean	2.6114					
C.V. %	1.2458					
R²	0.9706					
Adeq Precision	29.9556					

*N=nano-silica F=Fly ash A=anti-freeze admixture.

TABLE B4 FST model coefficients.

Factor	Coefficient Estimate	df	Standard Error	95% CI Low	95% CI High	VIF
Intercept	2.61	1	0.0079	2.59	2.63	
N	-0.0779	1	0.0103	-0.1009	-0.055	1
F	0.1104	1	0.0103	0.0875	0.1333	1
A	-0.1243	1	0.0103	-0.1472	-0.1014	1
NF	0.0016	1	0.0115	-0.0241	0.0272	1
NA	0.0305	1	0.0115	0.0049	0.0561	1
FA	-0.0233	1	0.0115	-0.0489	0.0023	1

*N=nano-silica F=Fly ash A=anti-freeze admixture.

TABLE B5 3-days compressive strength detailed ANOVA results.

Source	Sum of Squares	df	Mean Square	F-value	p-value	Significance
Model	0.0028	9	0.0003	41.5000	< 0.0001	significant
N	0.0006	1	0.0006	77.1100	< 0.0001	
F	0.0013	1	0.0013	176.6000	< 0.0001	
A	0.0001	1	0.0001	17.3200	0.0042	
NF	0.0000	1	0.0000	2.3100	0.1721	
NA	0.0000	1	0.0000	0.5052	0.5002	
FA	0.0000	1	0.0000	0.0438	0.8402	
N²	0.0003	1	0.0003	40.2300	0.0004	
F²	0.0000	1	0.0000	1.3000	0.2924	
A²	0.0000	1	0.0000	2.8600	0.1345	
Residual	0.0001	7	0.0000			
Lack of Fit	0.0001	5	0.0000	7.0600	0.1287	not significant
Pure Error	0.0000	2	0.0000			
Cor Total	0.0029	16				
Fit statistics						
Std. Dev.	0.0027					
Mean	0.0547					
C.V. %	5.0266					
R²	0.9816					
Adeq Precision	23.6274					

*N=nano-silica F=Fly ash A=anti-freeze admixture.

TABLE B6 3-days compressive strength model coefficients.

Factor	Coefficient Estimate	df	Standard Error	95% CI Low	95% CI High	VIF
Intercept	0.0456	1	0.0012	0.0428	0.0484	
N	-0.0076	1	0.0009	-0.0097	-0.0056	1
F	0.0116	1	0.0009	0.0095	0.0136	1
A	-0.0036	1	0.0009	-0.0057	-0.0016	1
NF	-0.0015	1	0.001	-0.0038	0.0008	1
NA	0.0007	1	0.001	-0.0016	0.003	1
FA	0.0002	1	0.001	-0.0021	0.0025	1
N²	0.0107	1	0.0017	0.0067	0.0146	1.54
F²	0.0019	1	0.0017	-0.0021	0.0059	1.54
A²	0.0028	1	0.0017	-0.0011	0.0068	1.54

*N=nano-silica F=Fly ash A=anti-freeze admixture.

TABLE B7 28-days compressive strength detailed ANOVA results.

Source	Sum of Squares	df	Mean Square	F-value	p-value	Significance
Model	871.36	9	96.82	34.97	< 0.0001	significant
N	187.84	1	187.84	67.85	< 0.0001	
F	633.93	1	633.93	228.99	< 0.0001	
A	1.5	1	1.5	0.541	0.4859	
NF	0.12	1	0.12	0.0434	0.841	
NA	0.8978	1	0.8978	0.3243	0.5868	
FA	3.62	1	3.62	1.31	0.2905	
N²	17.34	1	17.34	6.26	0.0408	
F²	0.2197	1	0.2197	0.0794	0.7863	
A²	4.59	1	4.59	1.66	0.2389	
Residual	19.38	7	2.77			
Lack of Fit	9.57	5	1.91	0.3901	0.8287	not significant
Pure Error	9.81	2	4.91			
Cor Total	890.74	16				
<u>Fit statistics</u>						
Std. Dev.	1.66					
Mean	38.9					
C.V. %	4.28					
R²	0.9782					
Adeq Precision	19.8777					

*N=nano-silica F=Fly ash A=anti-freeze admixture.

TABLE B8 28- days compressive strength model coefficients.

Factor	Coefficient Estimate	df	Standard Error	95% CI Low	95% CI High	VIF
Intercept	40.99	1	0.712	39.31	42.68	
N	4.33	1	0.5262	3.09	5.58	1
F	-7.96	1	0.5262	-9.21	-6.72	1
A	0.387	1	0.5262	-0.8572	1.63	1
NF	0.1225	1	0.5883	-1.27	1.51	1
NA	-0.335	1	0.5883	-1.73	1.06	1
FA	-0.6725	1	0.5883	-2.06	0.7185	1
N²	-2.54	1	1.02	-4.95	-0.14	1.54
F²	0.2863	1	1.02	-2.12	2.69	1.54
A²	-1.31	1	1.02	-3.71	1.09	1.54

*N=nano-silica F=Fly ash A=anti-freeze admixture.

TABLE B9 Fluid absorption detailed ANOVA results.

Source	Sum of Squares	df	Mean Square	F-value	p-value	
Model	2.88	9	0.3199	14.67	0.0009	significant
N	0.4884	1	0.4884	22.4	0.0021	
F	1.47	1	1.47	67.28	< 0.0001	
A	0.5429	1	0.5429	24.9	0.0016	
NF	0.0036	1	0.0036	0.1657	0.6961	
NA	0.0406	1	0.0406	1.86	0.2146	
FA	0.019	1	0.019	0.872	0.3815	
N²	0.0567	1	0.0567	2.6	0.151	
F²	0.0017	1	0.0017	0.0794	0.7862	
A²	0.0647	1	0.0647	2.97	0.1286	
Residual	0.1526	7	0.0218			
Lack of Fit	0.1306	5	0.0261	2.37	0.3232	not significant
Pure Error	0.0221	2	0.011			
Cor Total	3.03	16				
Fit Statistics						
Std. Dev.	0.1477					
Mean	2.73					
C.V. %	5.41					
R²	0.9497					
Adeq						
Precision	14.7815					

*N=nano-silica F=Fly ash A=anti-freeze admixture.

TABLE B10 Fluid absorption model coefficients.

Factor	Coefficient Estimate	df	Standard Error	95% CI Low	95% CI High	VIF
Intercept	2.54	1	0.0632	2.39	2.69	
N	-0.221	1	0.0467	-0.3314	-0.1106	1
F	0.383	1	0.0467	0.2726	0.4934	1
A	-0.233	1	0.0467	-0.3434	-0.1226	1
NF	0.0212	1	0.0522	-0.1022	0.1447	1
NA	0.0712	1	0.0522	-0.0522	0.1947	1
FA	0.0487	1	0.0522	-0.0747	0.1722	1
N²	0.1454	1	0.0902	-0.0679	0.3587	1.54
F²	0.0254	1	0.0902	-0.1879	0.2387	1.54
A²	0.1554	1	0.0902	-0.0579	0.3687	1.54

*N=nano-silica F=Fly ash A=anti-freeze admixture.